Berichte
zur Polar-
und Meeresforschung

587
2009

Reports
on Polar and Marine Research

The Expedition of the Research Vessel "Maria S. Merian" to the Davis Strait and Baffin Bay in 2008 (MSM09/3)

Edited by
Karsten Gohl, Bernd Schreckenberger, Thomas Funck
with contributions of the participants

HELMHOLTZ GEMEINSCHAFT

ALFRED-WEGENER-INSTITUT FÜR
POLAR- UND MEERESFORSCHUNG
In der Helmholtz-Gemeinschaft
D-27570 BREMERHAVEN
Bundesrepublik Deutschland

ISSN 1866-3192

Hinweis

Die Berichte zur Polar- und Meeresforschung werden vom Alfred-Wegener-Institut für Polar-und Meeresforschung in Bremerhaven* in unregelmäßiger Abfolge herausgegeben.

Sie enthalten Beschreibungen und Ergebnisse der vom Institut (AWI) oder mit seiner Unterstützung durchgeführten Forschungsarbeiten in den Polargebieten und in den Meeren.

Es werden veröffentlicht:

— Expeditionsberichte (inkl. Stationslisten und Routenkarten)
— Expeditionsergebnisse (inkl. Dissertationen)
— wissenschaftliche Ergebnisse der Antarktis-Stationen und anderer Forschungs-Stationen des AWI
— Berichte wissenschaftlicher Tagungen

Die Beiträge geben nicht notwendigerweise die Auffassung des Instituts wieder.

Notice

The Reports on Polar and Marine Research are issued by the Alfred Wegener Institute for Polar and Marine Research in Bremerhaven*, Federal Republic of Germany. They appear in irregular intervals.

They contain descriptions and results of investigations in polar regions and in the seas either conducted by the Institute (AWI) or with its support.

The following items are published:

— expedition reports (incl. station lists and route maps)
— expedition results (incl. Ph.D. theses)
— scientific results of the Antarctic stations and of other AWI research stations
— reports on scientific meetings

The papers contained in the Reports do not necessarily reflect the opinion of the Institute.

The „Berichte zur Polar- und Meeresforschung” continue the former „Berichte zur Polarforschung”

* Anschrift / Address
Alfred-Wegener-Institut
Für Polar- und Meeresforschung
D-27570 Bremerhaven
Germany
www.awi.de

Editor in charge:
Dr. Horst Bornemann

Assistant editor:
Birgit Chiaventone

Die "Berichte zur Polar- und Meeresforschung" (ISSN 1866-3192) werden ab 2008 ausschließlich elektronisch als Open-Access-Publikation herausgegeben (URL: http://epic.awi.de).

The Expedition of the Research Vessel "Maria S. Merian" to the Davis Strait and Baffin Bay in 2008 (MSM09/3)

Edited by
Karsten Gohl, Bernd Schreckenberger, Thomas Funck
with contributions of the participants

Ber. Polarforsch. Meeresforsch. 587 (2009)
ISSN 1866-3192

Contact:

Karsten Gohl
Alfred Wegener Institute for Polar and Marine Research (AWI)
Dept. of Geosciences, Section of Geophysics
Am Alten Hafen 26
D-27568 Bremerhaven
Germany

karsten.gohl@awi.de

Contents

1. Zusammenfassung / Summary

In diesem Fahrtabschnitt MSM09/3 wurden in einer Kooperation zwischen dem Alfred-Wegener-Institut für Polar- und Meeresforschung (AWI), der Bundesanstalt für Geowissenschaften und Rohstoffe (BGR), dem Geologischen Dienst von Dänemark und Grönland (GEUS) und der Dalhousie University geophysikalische Untersuchungen in der Baffinbucht und Davisstraße zwischen Grönland und dem kanadischen Baffininsel durchgeführt. Als Teilvorhaben des IPY-2007/08-Kernprojekts *Plate Tectonics and Polar Gateways in the Earth System* (PLATES & GATES) hatte das Projekt DAVIS GATE das Ziel, eine tektonische und sedimentäre Rekonstruktion des Öffnungsprozesses dieser Meeresstraße zu entwickeln. Die Baffinbucht und Davisstraße spielen eine wichtige Rolle für den Flachwasseraustausch zwischen dem arktischen und dem atlantischen Ozean. Die plattentektonische Entwicklung sowie die magmatischen Ereignisse im Laufe dieser Entwicklung sind bisher kaum bekannt und erforderten eine eindringliche geophysikalische Untersuchung, um akkurate paläobathymetrische und paläogeographische Datensätze für eine vollständige geodynamische Rekonstruktion dieses „Gateway" zu erstellen. Entlang von drei refraktions/weitwinkelseismischen Profilen unter Nutzung von Ozeanbodenseismometern auf insgesamt 62 Stationen sowie dem Einsatz der Mehrkanal-Reflexionsseismik mit einem 3000 m langen Streamer sind Daten von der sedimentären Bedeckung bis in die tiefe Kruste und teilweise vom obersten Mantel gewonnen worden. Weitere seismische Profildaten ergänzen diese Messungen und lassen Einblicke in die Strukturen des Grundgebirges sowie der dominanten Verwerfungszonen, z.B. der Ungava-Störung, zu. Eine parallel angelegte Magnetfeldvermessung ist auf die Auflösung der zeitlichen Entwicklung der ozeanischen Kruste der Baffinbucht ausgerichtet worden. Ausdünnung und Absenkung der kontinentalen Kruste und Übergangskruste in der Davisstraße und die Entwicklung der ozeanischen Kruste der Baffinbucht konnten mit diesen geophysikalischen Daten, zu der auch kontinuierlich aufgezeichnete Schwerefeld- und Sedimentechographiedaten gehören, untersucht werden. Diese Daten liefern die Informationen über die geometrischen und physikalischen Eigenschaften der Kruste und ihrer Sedimentbedeckung, die für ein realistisches tektonisches, geodynamisches und sedimentäres Modell notwendig sind, das den kontinentalen Abbruchs und der Entwicklung des Ozeanbeckens zwischen Grönland und Kanada paläo-topographisch im Detail beschreibt.

The cruise leg MSM09/3 was conducted as a cooperative project between the Alfred Wegener Institute for Polar and Marine Research (AWI), the Federal Institute for Geosciences and Resources (BGR), the Geological Survey of Denmark and Greenland (GEUS) and Dalhousie University. A geophysical survey covered areas of Baffin Bay and Davis Strait between Greenland and the Canadian Baffin Island. A component of the IPY 2007/08 Lead Project *Plate Tectonics and Polar Gateways in the Earth System* (PLATES & GATES), this project DAVIS GATE is aimed to develop a tectonic and sedimentary reconstruction of the opening process of this oceanic gateway. Baffin Bay and Davis Strait play an important role in the shallow water exchange from the Arctic to the Atlantic Ocean. The plate-tectonic evolution as well as the magmatic history of this region has been sparsely known and required a careful geophysical investigation in order to construct a set of gridded detailed paleo-topographic maps for a complete geodynamic reconstruction of this gateway. With a set of three seismic refraction/wide-angle reflection profiles, using ocean-bottom seismometers on 62 stations, as well as multi-channel reflection seismic recordings with a 3000-m long streamer, data were acquired from the sedimentary cover to the deep crust and even from parts of the uppermost mantle. Additional seismic data supplement these profiles and provide insights into the structures of the basement and dominant fault zones such as the Ungava fault

system. A parallel running magnetic survey aimed to resolve the temporal evolution of the oceanic crust of Baffin Bay. The extension and subsidence of the continental and transitional crust in the Davis Strait and the evolution of oceanic crust in the Labrador Sea and Baffin Bay could be investigated with dataset to which continuously recorded gravity anomaly data and sub-bottom profiler data also contribute. This dataset provides the basis of geometrical and physical properties of the crust required for a realistic geodynamic model which will describe the break-up and the ocean basin evolution between Greenland and Canada in terms of detailed paleo-topography.

2. Tectonic and Geological Framework

(T. Funck, K. Gohl)

2.1 General Setting

Davis Strait is a bathymetric high between Baffin Island to the west and Greenland to the east that separates Labrador Sea from Baffin Bay (Figure 2.1). The oldest undisputed sea-floor spreading magnetic anomaly in Labrador Sea is magnetic chron 27 (61.3–60.9 Ma) (Chalmers and Laursen, 1995). Other authors suggest that sea-floor spreading started during magnetic chron 33 (79.7–74.5 Ma) (Roest and Srivastava, 1989) or between chron 29 and 31 (66–64 Ma) (Chian et al., 1995a). A reorientation of the spreading axis took place during magnetochron 24r (55.9–53.3 Ma), at the same time as sea-floor spreading started between Greenland and Europe, and then ceased by magnetochron 13 (33 Ma) (Srivastava, 1978).

Baffin Bay is the northwest extension of the Labrador Sea spreading system. The transform margin in Davis Strait that links these two rift axes is characterized by the Ungava transform fault, a name that was first introduced by Kerr (1967). Later, the term Ungava fault zone (UFZ) became more commonly used. The position of the UFZ is taken to be along the SE side of a line of striking positive gravity anomalies. Davis Strait, unlike Labrador Sea and Baffin Bay, is bounded by volcanic margins. Onshore, Palaeogene volcanics crop out on either side of the strait in a short narrow belt near Cape Dyer on Baffin Island and in a wider zone in the Disko-Svartenhuk area of West Greenland. Storey et al. (1998) identified two pulses of volcanism in West Greenland: one between 60.7 and 59.4 Ma and one between 54.8 and 53.6 Ma. The first pulse is probably related to the arrival of the Greenland-Iceland plume. Larsen and Saunders (1998) explain the almost simultaneous volcanism from 62 to 60 Ma in West Greenland (Storey et al., 1998), East Greenland (Larsen and Saunders, 1998), and on the British Isles (Pearson et al., 1996) by rapid lateral flow of a small plume head that impinged on the continental lithosphere. Continental break-up of East Greenland from NW Europe occurred at 56 Ma (Larsen and Saunders, 1998) and caused a reorientation of the spreading axis in Labrador Sea (Srivastava, 1978). Storey et al. (1998) suggested that the second pulse of volcanism in West Greenland could be related to this reorientation of the spreading axis, during which remnants of the plume could have generated melts along the UFZ. Volcanics, lava flows and seaward dipping reflectors (SDR) are mapped in large areas of Davis Strait (Skaarup et al., 2006; Chalmers and Laursen, 1995; Chalmers, 1997). In addition, volcanics were drilled in the Hekja O-71 (Klose et al., 1982), Ralegh N-18 (BASIN database, Geological Survey of Canada, Dartmouth, Nova Scotia, Canada), and Gjoa G-37 (Klose et al., 1982) wells. Laser Argon dating on basaltic rocks of the Gjoa well yielded ages of 59.5 Ma (Williamson et al., 2001), which relates those rock samples to the first pulse of volcanism.

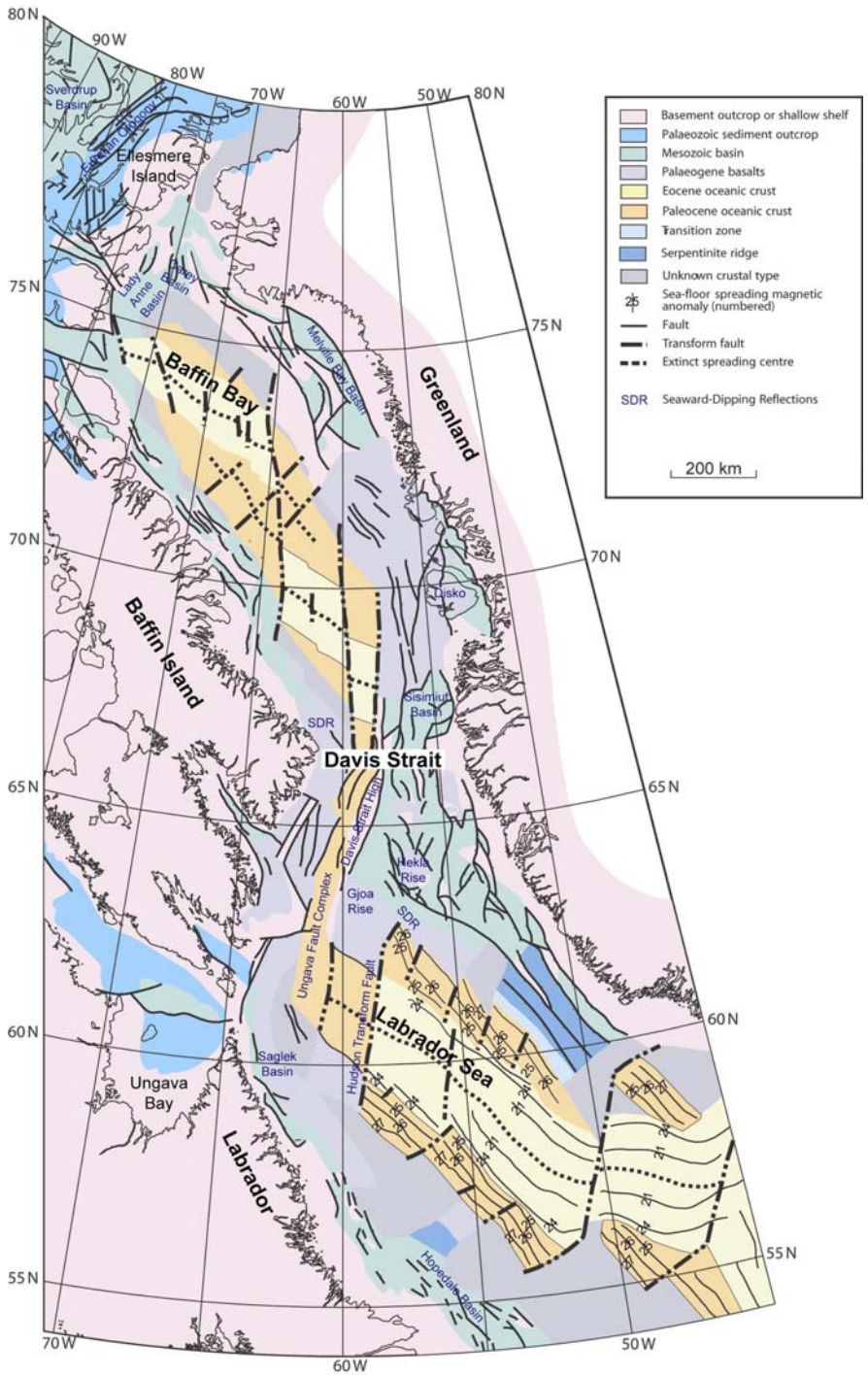

Fig. 2.1. Geological map of Labrador Sea, Davis Strait and Baffin Bay (from Chalmers and Oakey, 2007).

Baffin Bay forms a sedimentary basin that extends from Davis Strait in the south to Nares Strait in the north. The sediment thickness is up to 12 km in northern Baffin Bay (Reid and Jackson, 1997). The nature of the crust in Baffin Bay is disputed. Keen et al. (1974) provide evidence that the Baffin Bay crust was created by seafloor spreading, which is supported by refraction seismic velocity models that are compatible with oceanic crust (Keen and Barrett, 1972). In contrast, Reid and Jackson (1997) interpret their velocity model as indication for serpentinized mantle in northern Baffin Bay in support for amagmatic continental rifting and separation. Serpentinized mantle is often observed in ocean-continent transition zones of non-volcanic continental margins (e.g. Funck et al., 2003, 2004) or at ultra-slow spreading ridges (Jokat et al., 2003). Chalmers and Pulvertaft (2001) point out that there are no unequivocal

magnetic anomalies in Baffin Bay that can be related to seafloor spreading. Absence of these anomalies could be related to oblique spreading or to a blanketing effect of up to 12 km of sediments. The position of the extinct spreading axis and transform faults in Fig. 2.1 are determined from gravity and magnetic anomaly maps (Chalmers and Pulvertaft, 2001; Chalmers and Oakey, 2007).

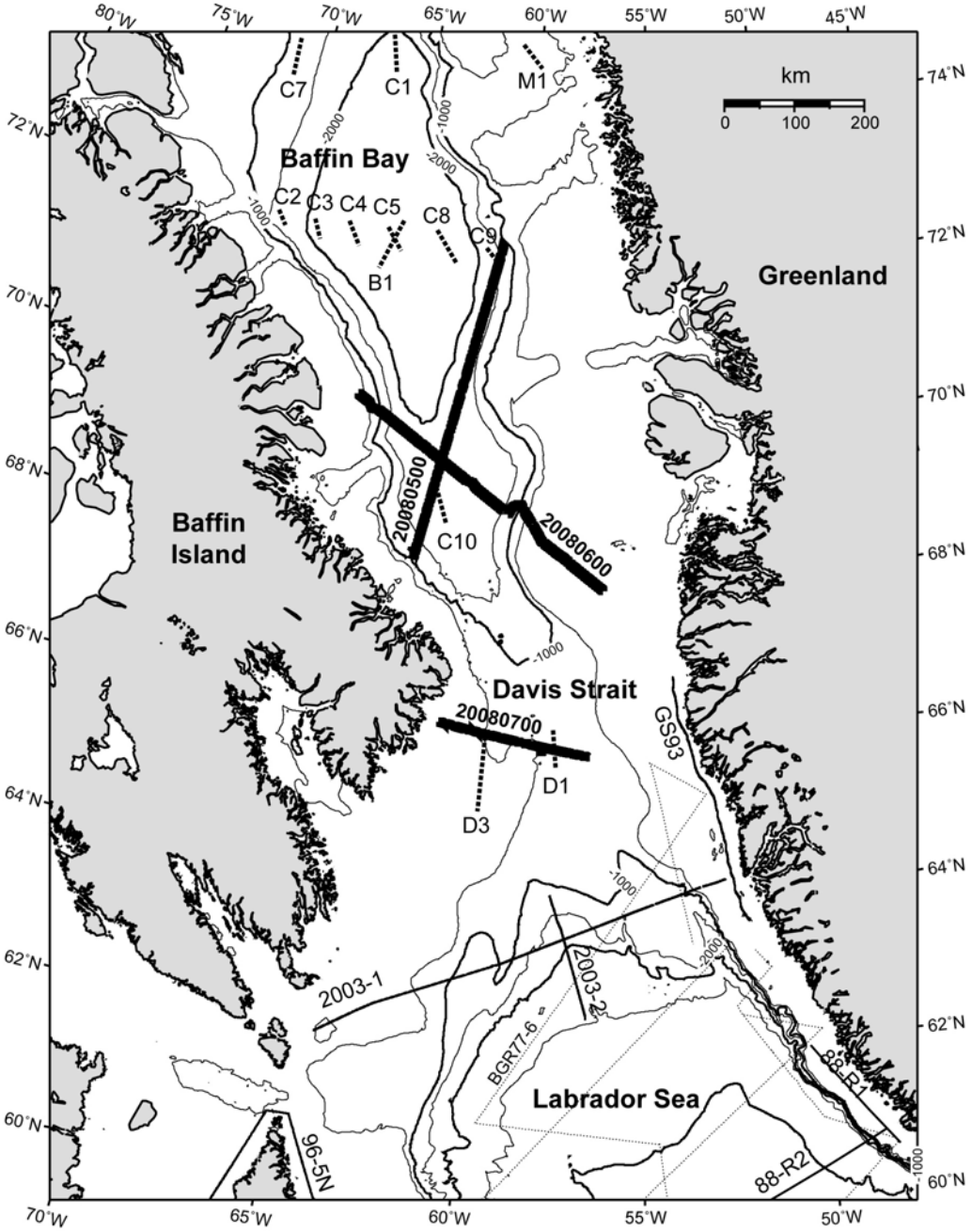

Fig. 2.2. Bathymetric map of the study area (contour interval 500 m). The seismic refraction lines of this cruise are shown as bold lines. Dashed lines indicate the locations of short reversed refraction experiments with recording buoys: lines C1 to C10, B1, D1, and M1 (Keen and Barrett, 1972); D3 (Srivastava et al., 1982). Modern refraction seismic lines with ocean-bottom seismometers or land stations are shown as thin solid lines: lines 2003-1 (Funck et al., 2007), 2003-2 (Gerlings et al., in press), GS93 (Gohl and Smithson, 1993), 96-5N (Funck et al., 2000), 88-R1 (Chian and Louden, 1992) and 88-R2 (Chian and Louden, 1994). Regional seismic reflection lines of the BGR in the northern Labrador Sea are marked with thin dotted lines.

2.2 Geophysical Data

The coverage with refraction seismic data and regional deep reflection seismic data is quite variable along the ocean basins west of Greenland. The most detailed picture is available for Labrador Sea with a number of refraction profiles defining the non-volcanic nature of the conjugate continental margins of Labrador and SW Greenland (e.g. Chian and Louden, 1994; Chian et al., 1995a). In addition, long regional reflection seismic lines were acquired by the BGR, the Geological Survey of Canada (GSC) and LITHOPROBE (e.g. Chalmers and Laursen, 1995; Chian et al., 1995b; Hall et al., 2003). A dense grid of seismic reflection data has been acquired for hydrocarbon exploration along the Davis Strait and Baffin Bay in the last years, but most of these data have short record lengths which do not cover the middle to lower crust. Due to active exploration licenses, in particular along the West Greenland margin, most of these data are not accessible.

In Baffin Bay, modern refraction seismic lines with ocean bottom seismometers are limited to the entrance of Nares Strait (Jackson and Reid, 1994; Reid and Jackson, 1997), where Reid and Jackson (1997) interpret velocities of 6.8 km/s as indication for serpentinized mantle rather than oceanic crust. The remainder of Baffin Bay is only covered by short sonobuoy profiles (Fig. 2.2) that show velocity models compatible with oceanic crust (Keen and Barrett, 1972).

In southern Davis Strait, two lines from the NUGGET experiment (Funck et al., 2007; Gerlings et al., in press) and a line along the Greenland coast (Gohl and Smithson, 1993) provide some information on the crustal structure in that region. Line 2003-1 (Figure 2.2) shows that Davis Strait is underlain by thinned continental crust with exception of the UFZ, where crust with an oceanic affinity was observed (Funck et al., 2007). The oceanic crust is associated with pronounced gravity and magnetic anomalies that can be correlated through Davis Strait, and this suggests that the UFZ acted as a leaky transform fault during phases of transtension. The 7 to 12 km thick continental crust on line 2003-1 is underlain by a ~5 km thick high-velocity zone (HVZ) that Funck et al. (2007) associated with southward flow of plume material along lithospheric thin spots, similar to a model suggested earlier by Nielsen et al. (2002).

While Funck et al. (2007) found no evidence for a HVZ beneath the thicker continental crust close to Greenland, Gohl and Smithson (1993) identified an up to 8 km thick HVZ at the base of the Greenlandic crust, where the Moho depth varies between 30 to 42 km. Gohl and Smithson (1993) interpret the HVZ to be associated with hot-spot magmatism in the Davis Strait and Baffin Bay region. This magmatism is also witnessed by line 2003-2 (Figure 2.2) extending from southern Davis Strait into northern Labrador Sea. Here, Gerlings et al. (in press) observed a 12 km thick oceanic crust that is overlain by an up to 2 km thick sequence of Palaeogene basalts. This is in the area of BGR line 77-6, where Chalmers and Laursen (1995) identified seaward-dipping reflections indicative for volcanic-style margins. However, the volcanism is limited to the northernmost part of Labrador Sea. Farther south, the continental margins have a non-volcanic character with serpentinized mantle in the continent-ocean transition zone (Chian et al., 1995b).

3. Scientific Objectives

(K. Gohl, B. Schreckenberger, T. Funck, V. Damm)

The Canadian Archipelago and the oceanic gateway to the Atlantic across the Baffin Bay, Davis Strait and Labrador Sea play an important role in the shallow water exchange between the Arctic Ocean and the North Atlantic. It is estimated that approximately 1-3 Sv (10^6 m^3s^{-1})

of ocean water flows presently southward which is about the same amount as the northward current flow in the Barents Sea. The plate-kinematic evolution as well as the magmatic history are still sparsely known and require a careful investigation in order to construct a set of gridded detailed paleo-topographic maps for a complete reconstruction of this Arctic-Atlantic gateway. A component of the International Polar Year (IPY 2007/08) Lead Project *Plate Tectonics and Polar Gateways in the Earth System* (PLATES & GATES), this project DAVIS GATE is aimed to develop a tectonic and sedimentary reconstruction of the opening process of this oceanic gateway.

One of the central questions addresses the origin of the volcanics from a suggested mantel plume in the Baffin Bay area which acted as a precursor of a plume that migrated underneath Greenland to the present Iceland hotspot. What is the age and the intensity of the magmatic phases in the Baffin Bay and Davis Strait? Of further importance for the paleo-topographic development is the knowledge about the extension and subsidence of the continental crust in the Davis Strait and the evolution of oceanic crust in the Labrador Sea and Baffin Bay. A detailed geophysical investigation can provide the required deep crustal data on geometrical and physical properties for a realistic geodynamic model which will improve our conception of the break-up and ocean basin evolution between Greenland and Canada.

The important questions include:

- How and in what times have the crustal structures and sedimentary processes evolved under the relatively shallow Davis Strait? When did extensional and subsidence processes start and for how long have they been active? When and during which episodes has a deep and shallow water exchange between Baffin Bay and Labrador Sea been possible?
- Is the crust of Baffin Bay of pure oceanic origin or did extension occur amagmatically with intensive serpentinization of mantle-derived material? Can a previously from gravity data derived spreading axis in Baffin Bay be verified and imaged? How did the apparently asymmetrically structured continental margins develop?
- How can ages of magmatic phases be estimated? How can their extrusive and intrusive volumes and possible magmatic underplating in the northern Davis Strait and along the conjugated continental margins of Baffin Bay be quantified?
- Can the reconstruction of the sedimentary depositional and transport processes in the Davis Strait and Baffin Bay reveal paleo-current conditions?
- The construction of a spacially and temporally highly resolved plate-kinematic and paleo-topographic model of the region will be tested with models from paleoceanographic and paleo-climatic proxies.

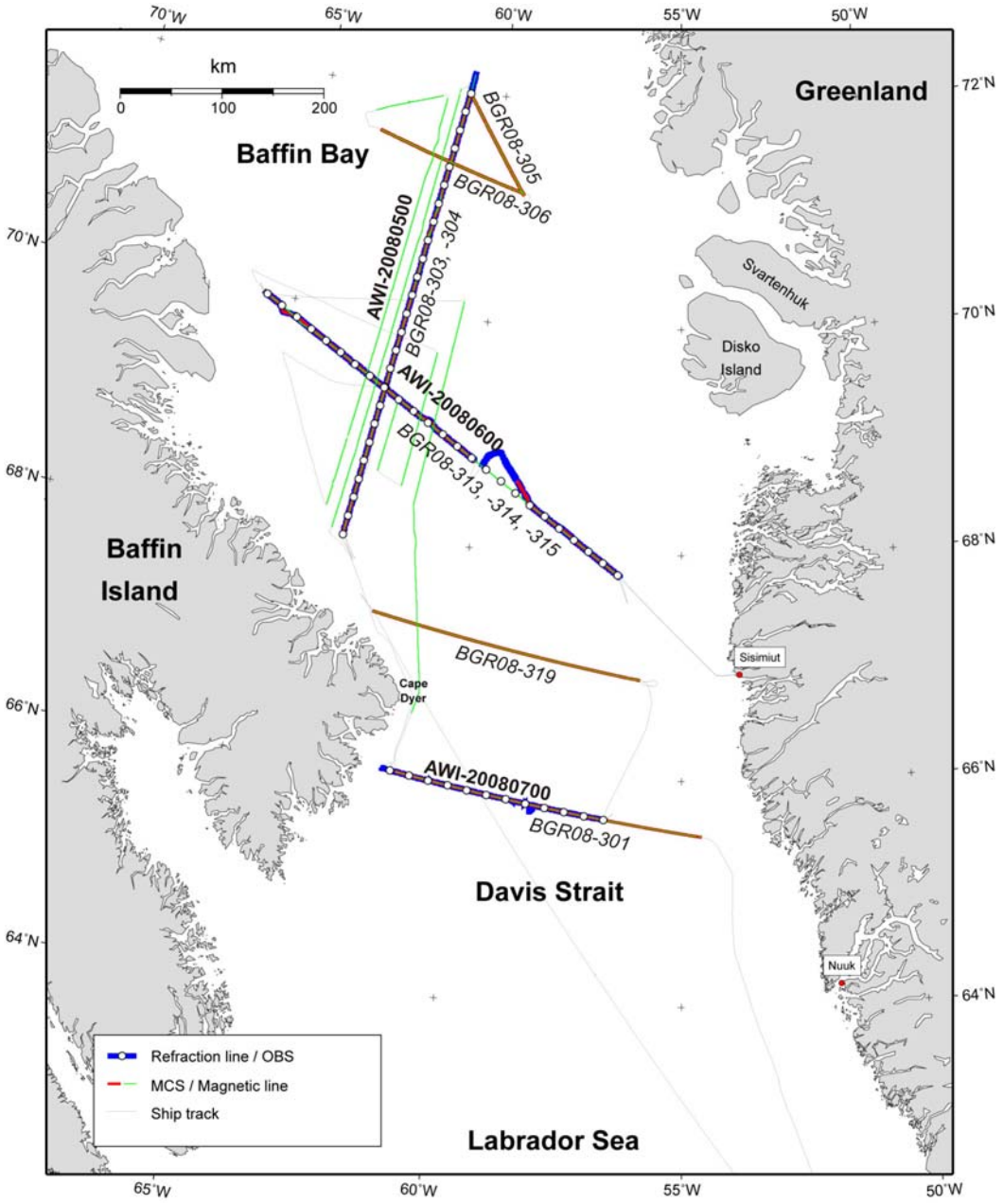

Fig. 3.1. Overview map of RV *Merian* MSM09/3 cruise track in Baffin Bay and Davis Strait with seismic and magnetic line locations. Seismic refraction lines with ocean-bottom seismometers (OBS) are annotated in bold letters; multichannel seismic reflection (MCS) reflection lines are annotated in italic letters. See Fig. 3.2 for complete line annotations.

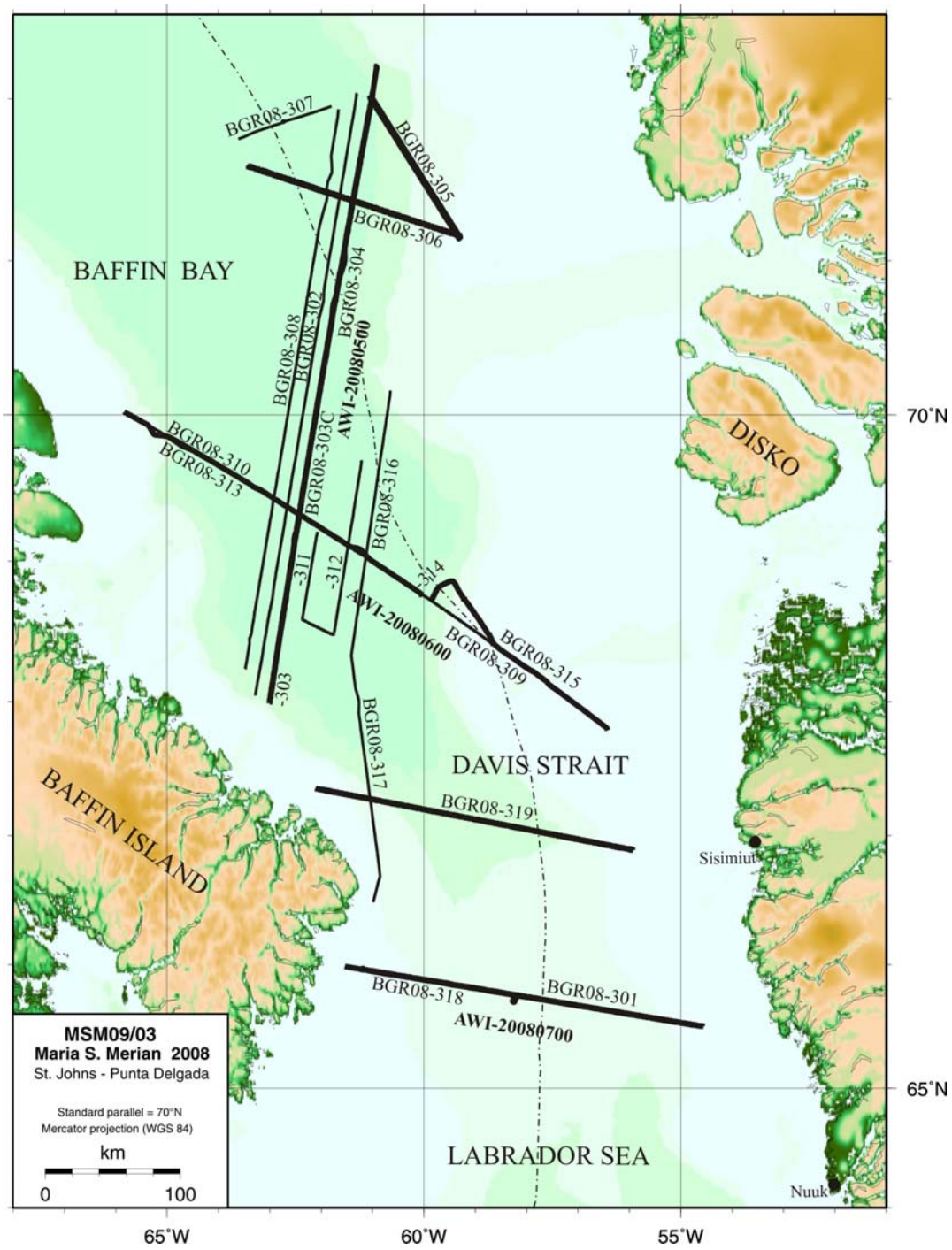

Fig. 3.2. Map with complete annotations of seismic and magnetic lines acquired during cruise MSM09/3. Seismic refraction lines with ocean-bottom seismometers (OBS) are annotated in bold letters. All other seismic and magnetic are annotated in italic letters. Refer to App. 5 for listing of all line locations and acquisition times.

4. Cruise Itinerary

(K. Gohl)

date	**approx. board time**	**hours from UTC**	**program & events**	**weather**
15.09.	08:00 13:00	-2:30	St. John's: RV *Merian* arrives; beginning container and winch loading;	fine
16.09.	 15:30	-2:30	St. John's: equipment unpacking and installation (major installation job of rented compressor containers); visit to Geophysics Group of Mem. University (Prof. Charles Hurich); gravity reference reading at outside location on campus;	fine and sunny; strong winds; later colder and cloudy
17.09.	13:00	-2:30	St. John's: arrival of participants on board; cont. equipment unpacking and installation;	cloudy
18.09.	 11:00	-2:30	St. John's: cont. equipment unpacking and installation; gravity reference reading at inside location of Memorial University;	cloudy
19.09.	00:10 15:00	 -2:00	**departure from St. John's (Canada);** cont. equipment unpacking and installation; report of sealing problem with starboard POD;	fine; later heavy winds and swell
20.09.	 11:30	-1:00	cont. equipment unpacking and installation; start continues recording of multibeam EM-120;	fine; light swell, later increasing
21.09.	09:00 – 15:30	0:00	station: releaser test in 2 steelboxes (successful for 25 of 27 releasers; use of cable transmitter and Spargel); changing course due to high swell/waves and faulty pods (sb POD has to be held fixed in forward position, port POD stops occasionally when coming out of water; best course was NW with sea from behind);	stormy conditions, high swell
22.09.		0:00	back to northward course; cont. equipment preparation; complete OBS assembly for demonstration;	sea becomes calmer
23.09.	12:30 20:00	0:00	deployment of streamer, airguns, magnetometer; start refl profile 08-301;	fine
24.09.		0:00	cont. refl profile 08-301; diesel generator for compressor failed repeatedly;	calm seas; partly cloudy
25.09.	03:20 07:00 17:00	0:00	end refl profile 08-301; recovery of seismic gear and magnetometer; transit to profile 20080500; (problem with POD control); start deploying OBS for profile 20080500 (25 OBS);	cloudy and increasing winds, later stormy
26.09.	17:30	0:00	end deploying OBS; no shot profile due to weather; start magnetic profile 08-302;	stormy
27.09.	 20:00 22:00	0:00	preparation Bolt guns; end magnetic profile 08-302; deployment streamer, Bolt guns, airgun, magnetometer;	calm seas; increasing winds in afternoon
28.09.	02:30 03:30 10:00	0:00	testing airguns; start refr/refl + mag profile 20080500/08-303; problems with Bolt airguns; magnetometer tangled in streamer; shutdown and interruption of profile operation;	medium winds and waves

	19:00		restart refr + mag profile 20080500 (no streamer);	
29.09.		0:00	cont. refr + mag profile 20080500;	fine; low swell
30.09.	16:00 17:00	0:00	end refr + mag profile 20080500; start collecting OBS of profile 20080500; problems with OBS flashers and beacons;	mostly fine; some snow showers
01.10.		0:00	cont. collecting OBS of profile 20080500; problems with OBS flashers and beacons;	fine
02.10.	02:00 06:00	0:00	end collecting OBS of profile 20080500; start refl profile 08-304;	fine
03.10.		0:00	cont. refl profile 08-304; repairing and servicing of OBS flashers & beacons;	partly sunny; increasing winds
04.10.	05:00 07:00 18:30 20:30	0:00	end refl profile 08-304; start refl profile 08-305; end refl profile 08-305; start refl profile 08-306;	cloudy; low to medium winds
05.10.	13:00 16:40 21:00 21:20	0:00	end refl profile 08-306; start mag profile 08-307; end mag profile 08-307; start mag profile 08-308;	partly cloudy; low to medium winds
06.10.	20:30	0:00	end mag profile 08-308; transit to begin of profile 20080600 slow due to stormy conditions and high swell;	strong winds and swell; stormy later
07.10.	08:00 13:30 16:30	-1:00	storm slowed down ship, therefore decision to move eastward toward the center of profile 20080600; station: sound profile and releaser & beacon/flasher test; start of magnetic profile 08-309;	stormy; winds slowed down later; less swell from midday
08.10.	09:30 16:30	-2:00	end of magnetic profile 08-309; transit to Sisimiut; **port-call Sisimiut (Greenland);** bunkering diesel fuel; gravity reference measurement;	fine, medium winds; fine and no winds
09.10.	13:00 22:00 23:30	-2:00	Schottel technician arrives to service pod problems; preparation of OBS systems; Schottel technician departs; **departing Sisimiut;** transit to profile 20080600;	fine, no winds
10.10.	06:30 14:00	-2:00	start OBS deployment profile 20080600 (25 OBS); communication with fishing vessel about possible profiling conflict;	cloudy; low to medium winds
11.10.	07:30 11:00	-2:00	end OBS deployment profile 20080600; seismic profiling impossible due to weather; start magnetic profiles 08-310, 08-311 and 08-312;	stormy
12.10.	09:00 22:00	-2:00	end magnetic surveying; transit to NW start of profile 20080600; start shooting OBS profile 20080600 with streamer;	calm seas; some swell
13.10.		-2:00	cont. profiling along profile 20080600; problems with Bolt guns; Bolt gun repair and exchange;	winds increasing
14.10.	01:00 09:00	-2:00	cont. profiling along profile 20080600; streamer recovery and detour due to fishing activity; redeployment of streamer;	medium waves/swell; later fine
15.10.	01:30	-2:00	end of OBS profile 20080600; testing Bolts guns with other trigger unit (higher voltage);	medium waves/swell;

	06:30		start collecting OBS along profile 20080600;	
16.10.	11:45 20:00	-2:00	cont. collecting OBS; end collecting OBS along profile 20080600; transit to magnetic profile; start magnetic profiles 08-316/317;	low waves/swell; fine
17.10.	18:30 21:00	-2:00	cont. magnetic profiles 08-316/317; end magnetic profiles 08-316/317; short transit to profile 20080700; start OBS deployment of profile 20080700 (12 OBS);	low to medium swell/waves
18.10.	07:00 09:00 10:00	-2:00	end OBS deployment of profile 20080700 ; start shooting OBS profile 20080700; problem with umbilical and floater entangling between SB Bolt and G-Gun array;	medium swell/waves, increasing winds
19.10.	09:45 11:45	-2:00	end shooting OBS profile 20080700; start collecting OBS along profile 20080700;	low/medium swell/waves
20.10.	00:30 08:00 16:30	-2:00	end collecting OBS along profile 20080700; transit to seismic reflection profile; leakage problem of streamer system; testing and replacement of units; OBS equipment deinstallation and packing; start refl profile 08-319;	low/medium swell/waves
21.10.	20:20 23:00	-2:00	cont. refl profile 08-319; OBS equipment deinstallation and packing; end refl profile 08-319; start transit to Ponta Delgada (Azores);	medium swell/waves; wind increasing
22.10.	16:20	-2:00	cont. transit to Ponta Delgada; magnetometer calibration loop; equipment deinstallation and packing; cont. data processing;	medium swell/waves
23.10.		-2:00	cont. transit to Ponta Delgada; equipment deinstallation and packing; cont. data processing;	medium winds
24.10.		-2:00	cont. transit to Ponta Delgada; equipment deinstallation and packing; cont. data processing;	medium winds
25.10.		-2:00	cont. transit to Ponta Delgada; equipment deinstallation and packing; cont. data processing;	medium winds
26.10.		-2:00	cont. transit to Ponta Delgada; Polartaufe & Abschlussfest;	low winds
27.10.		-2:00	cont. transit to Ponta Delgada;	low winds
28.10.	23:00	-1:00	cont. transit to Ponta Delgada; **arrival in Ponta Delgada (Azores)**	medium winds
29.10.	10:00	-1:00	participants depart ship	

5. Navigation and Data Management

(I. Heyde, B. Schreckenberger, H.-O. Bargeloh)

Several GPS receivers are installed on RV *Merian*. Following the recommendations of the ship's crew, we used the data of the SEAPATH 200 system of Kongsberg SeaTex AS. Since May 2000, GPS signals are available without the intentional degradation called 'selected availability' and since then positioning is possible with an accuracy in the order of 10-20

meters with standard GPS. This accuracy is sufficient for our survey and thus no DGPS causing additional costs was used.

A shipboard computer (PC ACP_23) in the dry lab provided the following data from the ship's navigation system once per second:

- position, speed and course from GPS
- heading from the gyro
- speed from the Doppler-sonar (DO-Log)
- water depth values from the SIMRAD EM120 multibeam echosounder (centre beam) and from PARASOUND
- Kongsberg MRU5: Roll, Pitch, Yaw
- weather data

In addition to the shipboard computers, BGR provided several desktop and laptop computers to perform the acquisition and storage of the collected reflection seismic and potential field data (Fig. 5.1). Computers were installed in the deck lab (acquisition of seismic data) and in the dry lab and the gravimeter room.

The PC (PC0440) used for the acquisition of navigation data, shotpoint data, gravity data, magnetic gradiometer data, time in UTC, depth, and water sound velocity is equipped with a large number of serial and other ports. Each of the data strings were written into the memory of the data acquisition PC by real time programs developed under LabView software. The PC is connected to a BGR-provided Meinberg GPS-clock, by which a uniform time reference to all collected data is realized.

The control of all seismic instruments (G-Guns and streamer) is managed by BGR-developed and industrial software installed on PCs, which were set up in the deck lab. All seismic data are stored intermittently on hard-disk and sequentially transferred onto tape. Shotpoint data are transferred to the data acquisition system discussed above.

The functions of the marine gravimeter are controlled by PC6536. Measured gravity values are sent to the data acquisition PC. PC6924 was used to control the operation of the SeaSpy marine gradiometer and to display the collected magnetic data. The Magson magnetometers (which were also used for experimental purposes) have no real time data transmission to the ship. Its data are stored on a flash card installed in the instrument.

A notebook computer was installed in the dry lab to provide a visual display of the ship's position in relation to the profile network by a navigation program (FUGAWI4.5). This program permanently displayed the ship's position on a nautical map on which the planned and the already finished profiles are plotted. In addition, analog recordings were produced for the magnetic total intensity, the gradient, and the raw gravity data.

The data pre-processing was performed on various computers. All data which are part of BGR's standard operations were transformed into a special data format within a procedure that checks, reformats, and collects the data items to one data set each 20 seconds on PC1420.

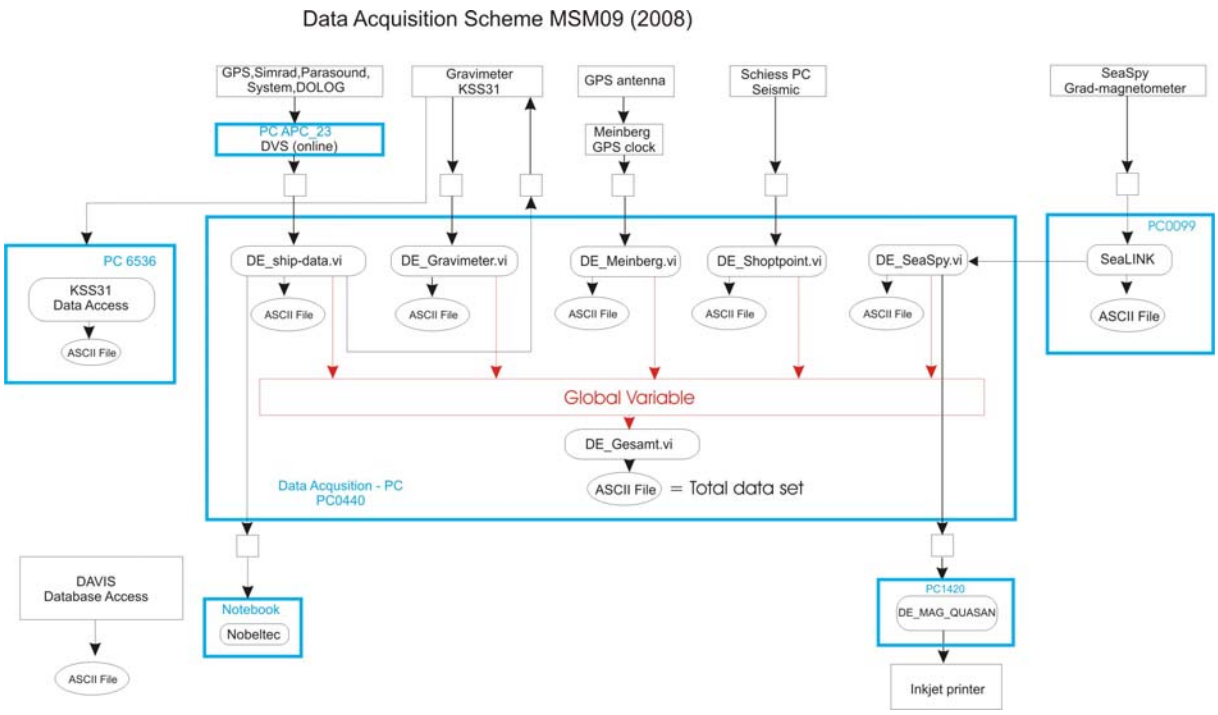

Fig. 5.1: Scheme of the data acquisition scheme installed during MSM09/3.

6. Multi-beam Bathymetry

(K. Gohl)

RV *Merian* is equipped with a Kongsberg EM-120 multi-beam echo-sounder for continuous mapping of the seafloor. This system consists of a transmitter and receiver transducer array which is installed in a mills cross below the keel of the vessel. The transceiver unit contains the transmitter and receiver electronics and processors for beam-forming and control of all parameters with respect to gain, ping rate and transmit angles. It has serial interfaces for vessel motion sensors, such as roll, pitch and heave, external clock and vessel position. The operator station processes the collected raw data, applies corrections, displays the results and logs the data to media. The EM-120 system has an interface to a sound speed sensor.

The EM-120 operates with a frequency of 12, 38 or 200 kHz and an angular coverage sector of up to 60° per port-/starboard side. If one ping is sent the receiving signal is formed into 191 beams by the transducer unit through the hydrophones in the receiver unit. The beam spacing can be defined in an equidistant or equiangular distance, or in a mix of both of them. The ping-rate depends on the water depth and the runtime of the signal through the water column. The variation of angular coverage sector and beam pointing angles was set automatically which optimizes the number of usable beams. The transmit fan is split into individual sectors with independent active steering according to vessel roll, pitch and yaw. This forces all soundings on a line perpendicular to the survey line and enables a continuous sampling with a complete coverage. Pitch and roll movements within ±10 degrees are automatically compensated by the software. Thus, the EM-120 can map the seafloor with a swath width about up to six times the water depth.

On this cruise leg, the EM-120 was operated continuously with a setting of 12 kHz frequency and an angular coverage of 60° to each side. Data are stored as native raw data and grid data format on the Kongsberg server disks.

7. Sediment Echosounding

(M. Ruhnau, K. Gohl)

7.1 Method and Instrument

The Parasound DS P-70 system of RV *Merian* is a sediment echosounder using the parametric effect to generate a narrow profiling beam with relatively low frequencies. With two high frequency signals emitted simultaneously (here 18 kHz and 22 kHz), a third signal at the difference frequency (e.g. 4 kHz) is generated in the water column. This signal is generated within the emission cone of the high frequency waves, which has an aperture angle of only 4°. Thus a signal of relatively low frequency can be emitted within a narrow aperture by use of a relatively small transducer antenna (area approx. 1 m²). This significantly improves the resolution of the system. An aperture of 4° corresponds to a footprint of about 7% of the water depth on the ocean floor.

On this cruise, Parasound recorded almost continuously in the investigations areas during all seismic, magnetic and transit tracks (Tab. 7.1). The system worked reliably with only minor problems.

Date	Time (UTC)	Parasound operation
22.09.2008	08:22	Begin of survey; Saving ASD- and PS3 format; Sounding mode: Single-Pulse
	16:42 - 17:04	Record interrupted
23.09.2008	13:13	Parasound system switched off
	15:05	Parasound system switched on; Sounding mode: Single Pulse
	23:22 - 08:36	PS3 record interrupted
24.09.2008	11:15	Sounding mode: Quasi-Equidistant-Transmission
25.09.2008	11:51 - 12:40	PS3 recording interrupted
	21:30	Parasound system switched off
26.09.2008	19:28	Parasound system switched on
27.09.2008	22:15	Sounding mode: Pulse-Train
28.09.2008	07:20 - 09:10	Record interrupted
29.09.2008	02:19 - 08:09	Record interrupted
30.09.2008	16:46	Parasound system switched off
02.10.2008	08:52	Parasound system switched on; Sounding mode: Pulse-Train
03.10.2008	05:22 - 11:01	Record interrupted
	12:00 - 12:02	Record interrupted
04.10.2008	11:32	Sounding mode: Quasi-Equidistant-Transmission
	13:18 - 13:27	Record interrupted
	18:37	Parasound system switched off; system restart
	19:23	Parasound system switched on; Sounding mode: Quasi-Equidistant-Transmission
	19:46 - 20:01	Record interrupted
06.10.2008	10:49	Sounding mode: Single-Pulse
07.10.2008	05:10 - 09:57	Record interrupted
	14:48 - 16:55	Record interrupted
08.10.2008	00:20 - 00:40	Record interrupted
	15:53	Parasound system switched off; system restart
10.10.2008	03:02	Parasound system switched on; Sounding mode: Single-Pulse
	05:36 - 07:09	Record interrupted
	13:48	Sounding mode: Quasi-Equidistant-Transmission
	17:26	Sounding mode: Single-Pulse
	19:46	Parasound system switched off; system restart
	20:02	Parasound system switched on; Sounding mode: Quasi-Equidistant-Transmission
11.10.2008	04:22 - 05:55	Record interrupted
12.10.2008	08:01 - 12:24	Record interrupted
13.10.2008	06:45 - 06:48	Record interrupted

14.10.2008	09:00	Parasound system switched off; system restart
	09:14	Parasound system switched on; Sounding mode: Quasi-Equidistant-Transmission
	09:50	Parasound system switched off; system restart
	10:07	Parasound system switched on; Sounding mode: Quasi-Equidistant-Transmission
15.10.2008	08:41	Parasound system switched off;
16.10.2008	14:36	Parasound system switched on; Sounding mode: Quasi-Equidistant-Transmission
19.10.2008	01:37 - 12:13	Record interrupted
21.10.2008	00:45 - 10:49	Record interrupted
	23:05	Parasound system switched off; system restart
	23:27	Parasound system switched on; Sounding mode: Quasi-Equidistant-Transmission
22.10.2008	14:52 - 17:19	Record interrupted
	20:14	End of survey

Tab. 7.1. Parasound operation protocol during MSM09/3.

7.2 Processing and Example Results

The DS P-70 system stores the Parasound data in PS3 format. Onboard processing of the PS3-data was performed by using ReflexW Version 5.0. After importing the PS3 data files, a static correction, based on the trace delays saved in the header-file, ensured the correct time delays for the whole section. Afterwards a plot-scale factor of 0.55 was applied to the data, resulting in stronger colour amplitudes. For some data sections, an additional automatic gain control (AGC) was applied to enhance deeper lying reflectors. All data are converted to SEG-Y data format and stored to hard-disks.

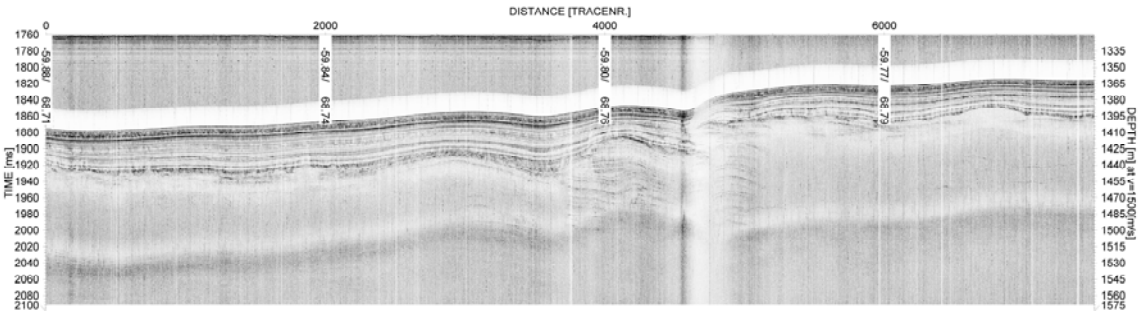

Fig. 7.1. Example of Parasound record from the Baffin Bay basin which reveals penetration down to 120 m below seafloor in parts of the record after automatic gain control (AGC) with a scaling factor of 1.1 and a window length of 25 ms was applied.

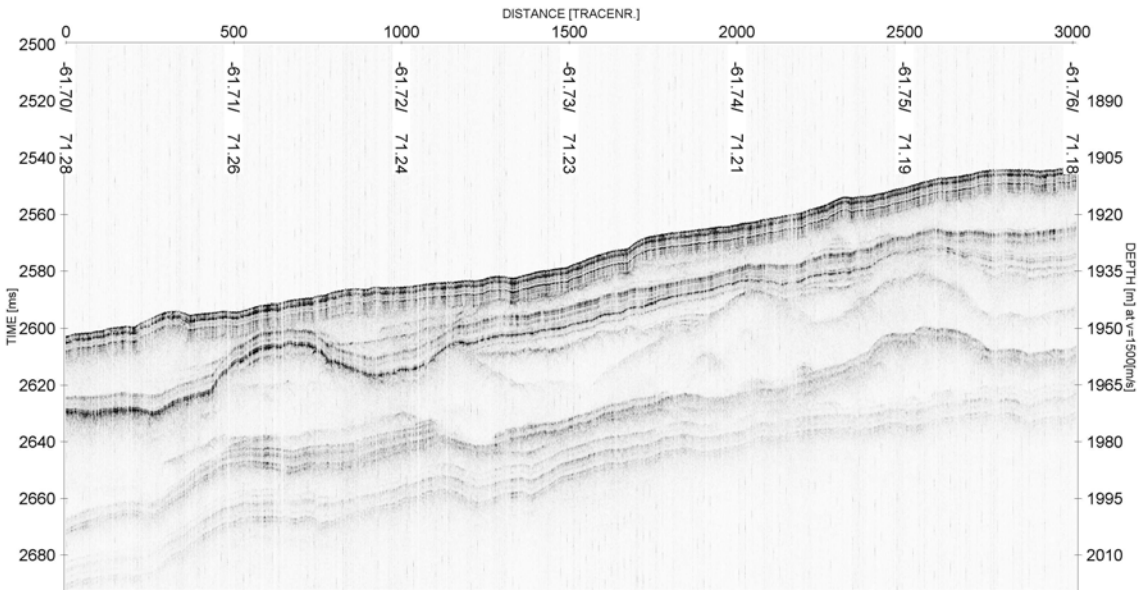

Fig. 7.2. Example of Parasound record from the Baffin Bay basin showing sedimentary sequences alternating between stratified and sediment-wave deposition character.

8. Gravimetry

(I. Heyde, B. Schreckenberger, H.-O. Bargeloh)

8.1 Method and Instruments

During the cruise MSM9/3, the BGR owned sea gravimeter system KSS31M was used. The KSS31M was installed in the gravimeter room one level below the main deck (Fig. 8.2). The sea gravimeter was located approximately 1 m above the vessel's nominal water line, 0.5 m to portside from the centerline, and 54 m forward of the stern.

The gravimeter system KSS31M is a high performance instrument for marine gravity measurements, manufactured by the Bodenseewerk Geosystem GmbH. While the sensor is based on the Askania type GSS3 sea gravimeter designed by Prof. Graf in the 60ties, the development of the horizontal platform and the corresponding electronic devices took place at the Bodenseewerk Geosystem in the second half of the 70ties. The system was modernized and modified in 2001 by the successor company Bodensee Gravitymeter Geosystem GmbH. The KSS31M system consists of two main assemblies: the gyro-stabilized platform with the gravity sensor and the data handling subsystem.

The gravity sensor (Fig. 8.3) consists of a tube-shaped mass that is suspended on a metal spring and guided frictionless by 5 threads. It is non-astatized and particularly designed to be insensitive to horizontal accelerations. This is achieved by limiting the motion of the mass to the vertical direction. Thus it is a straight line gravity meter avoiding cross coupling effects of beam type gravity meters. The main part of the total gravity acceleration is compensated by the mechanical spring, but gravity changes are compensated and detected by an electromagnetic system. A displacement of the spring-mass assembly with respect to the outer casing of the instrument is measured using a capacitance transducer.

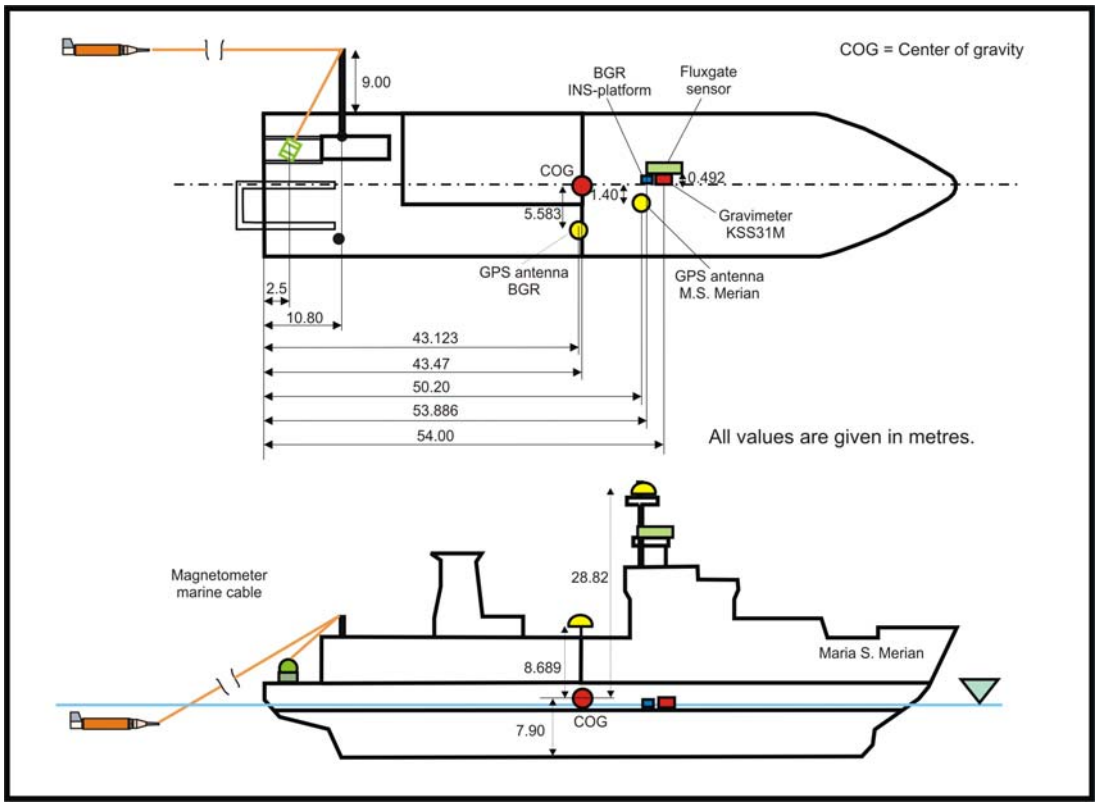

Fig. 8.1. The locations of the GPS antenna, BGR GPS and INS platform, magnetometer winch, outrigger port, fluxgate sensor and gravity meter on RV *Merian* during MSM09/3. The magnetometer towfish distances from the ship's GPS position follows from the sketch, taking cable length on the winch, cable path along the outrigger, and GPS antenna position into account.

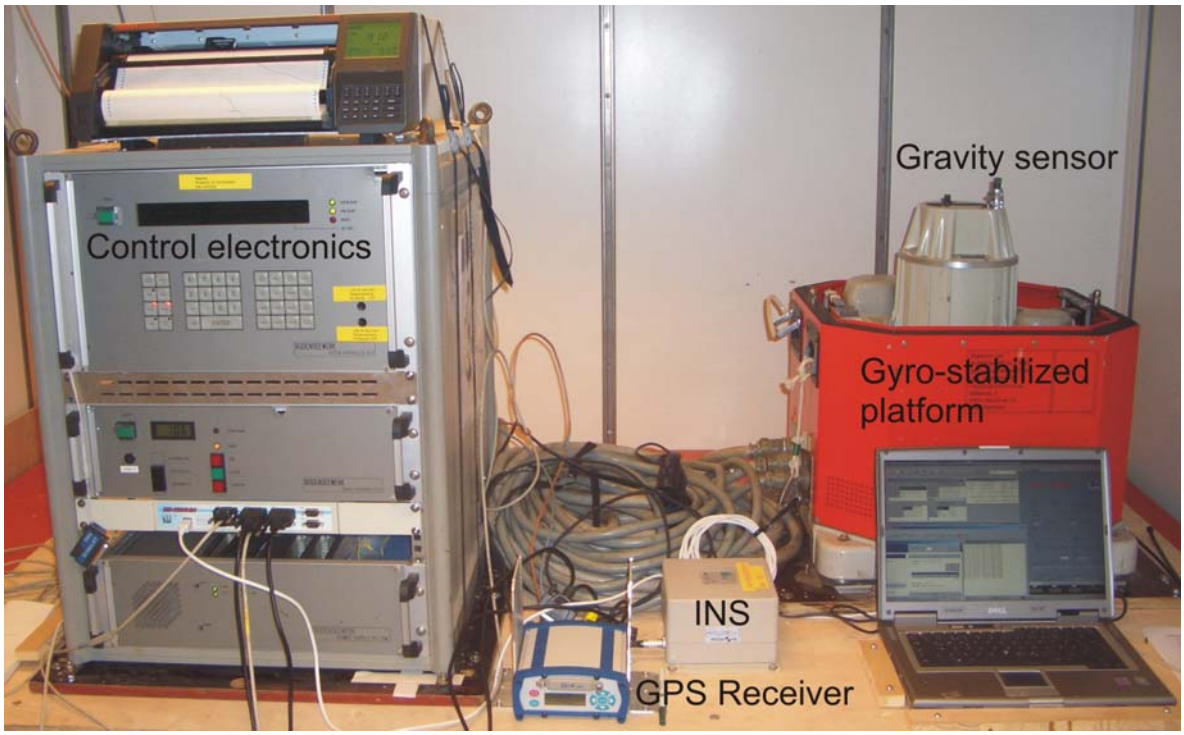

Fig. 8.2. KSS31M gravimeter system (platform with sensor and electronics rack), GPS instrumentation and INS unit in the gravimeter lab of RV *Merian*.

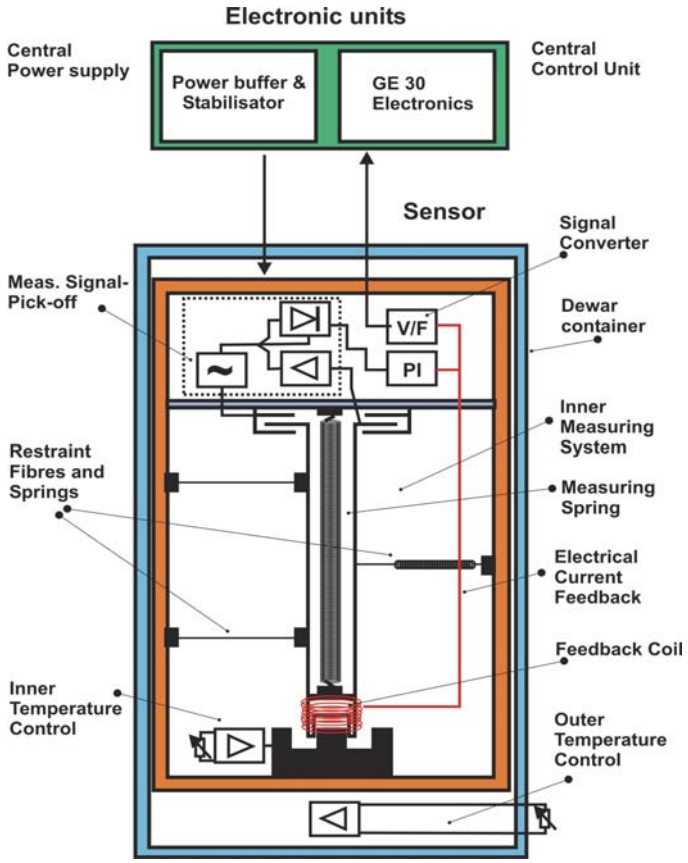

Fig. 8.3. Principle sketch of the gravity sensor GSS30 of the gravimeter system KSS31M.

The leveling subsystem consists of a platform stabilized in two axes by a vertical electrically erected gyro. The stabilization during course changes can be improved by providing the system with online navigation data. The control electronics and the power supply of the platform are located in the data handling subsystem unit. Functions like gyro run-up and -down sequences and the automatic platform caging are performed by the system controller unit located in the data handling subsystem, too. The stabilized platform will keep the sensor in an upright position with an accuracy of leveling in the order of 0.5 minutes of arc. This is particularly important as the sensor is very sensitive to tilting. Vertical acceleration, however, cannot be eliminated. Luckily on a ship the vertical acceleration oscillates periodically with a period of some seconds. This signal can be eliminated easily by means of lowpass filtering.

The data are transmitted to the BGR data acquisition and processing system in the dry lab and online navigation data from this system are sent with a rate of 1 Hz to support the stabilizing platform. The support is realized as follows: The horizontal position of the gyro-stabilized platform is controlled by two orthogonal horizontal accelerometers. The platform is leveled in such a manner that the horizontal accelerations are zero. If the ship describes a curve, the additional horizontal acceleration will cause the platform to be leveled according to the resulting apparent vertical axis. This axis may differ substantially from the true vertical axis and will result in too small gravity values and additionally in an effect of horizontal accelerations on the measured gravity. This effect is eliminated by supplying the system with online navigation data. From this input, a microprocessor calculates the leveling errors and enters them into the platform electronics which accordingly corrects the platform.

During the transits in the beginning and the end of the cruise, GPS data were supplied by a NovAtel SPAN system, which combines GPS and INS data. The GPS antenna was installed on a railing two decks above the main deck. The distance from the INS unit near the KSS31M sensor to the antenna was 6.08 m to starboard, 10.73 m to the rear and 9.56 m upwards. The INS attitude data were recorded with a sampling rate of 10 Hz and are used for the reconstruction of the magnetic component data measured by the 3-component fluxgate magnetomer fixed on top of the observation deck.

8.2 Data Processing

Processing of the gravity data consists essentially of the following steps:

- a time shift of 76 seconds due to the overcritical damping of the sensor
- conversion of the output from reading units (r.u.) to mGal by applying a conversion factor
- of 0.94542 mGal/r.u., on this cruise this was done in the system itself by hardware setting
- connection of the harbour gravity value to the world gravity net IGSN 71 (see 9.3)
- correction for Eötvös effect using the navigation data
- correction for the instrumental drift (not performed until completion of the cruise)
- subtraction of the normal gravity (WGS67)

As a result, we get the so-called free-air anomaly (FAA) which in the case of marine gravity is simply the Eötvös correceted observed absolute gravity minus the normal gravity. According to the selectable time interval of the data acquisition system, gravity values are available every 20 seconds.

Additionally the gravity anomalies, which are provided every second directly by the data handling subsystem of the KSS31M, were recorded with a separate computer. Free-air gravity anomalies are obtained when the KSS31M is supplied with the necessary navigation data (geographical latitude and longitude, speed, course over ground and heading). These data are available every second. The differences in both data sets are small. For the display and interpretation of gravity data the 20 s values were used. This interval is sufficient for ship-borne data and the 1 Hz data do not provide a higher resolution. However, outliers were removed manually in both data sets. Also the gravity data collected during the deployment and recovery of OBS were usually disregarded.

8.3 Gravity Ties to Land Stations

To compare the results of different gravity surveys the measured data have to be tied in a world-wide accepted reference system. This system is represented by the International Gravity Standardization Net IGSN71 (Morelli, 1974). The IGSN71 was established in 1971 by the International Union of Geodesy and Geophysics IUGG as a set of world-wide distributed locations with known absolute gravity values better than a few tenths of mGal. According to the recommendations of the IUGG, every gravity survey, marine or land, should be related to the datum and to the scale of the IGSN71.

Therefore, land gravity measurements have to be carried out to connect the gravity measurements at sea with the IGSN71. The marine geophysical group of BGR uses for gravity connections a LaCoste&Romberg gravity meter, model G, no. 480 (LCR G480).

The point descriptions and absolute gravity values of reference stations in St. John's (Newfoundland) were kindly provided by Natural Resources Canada. The stations belong to the Canadian Gravity Standardization Network (CGSN). Prof. Charles Hurich (Earth Science Department, Memorial University of Newfoundland) helped us to get access to the stations 01 and 03 on the campus of the Memorial University. Especially station 03 in the former seismometer room on a concrete pillar can be regarded as very reliable.

RV MARIA S. MERIAN moored at the pier No. 17 in the harbour of St. John's (Fig. 8.4). On Sept. 16 and 18, tie measurements to point A on the pier opposite the gravimeter room on MERIAN have been made. Point A is located near the third bollard 32 m from the western corner of the pier. The connection measurements resulted in an average absolute gravity value of 980828.62 mGal (with water level –2.3 m, IGSN71) for point A at the water level. That results in an absolute gravity value of 980828.3 mGal for the location of the gravity sensor. The reading of the KSSM31 at the leaving time (Sept. 19, 2008, 01:00 UTC) from the pier was 899.59 mGal.

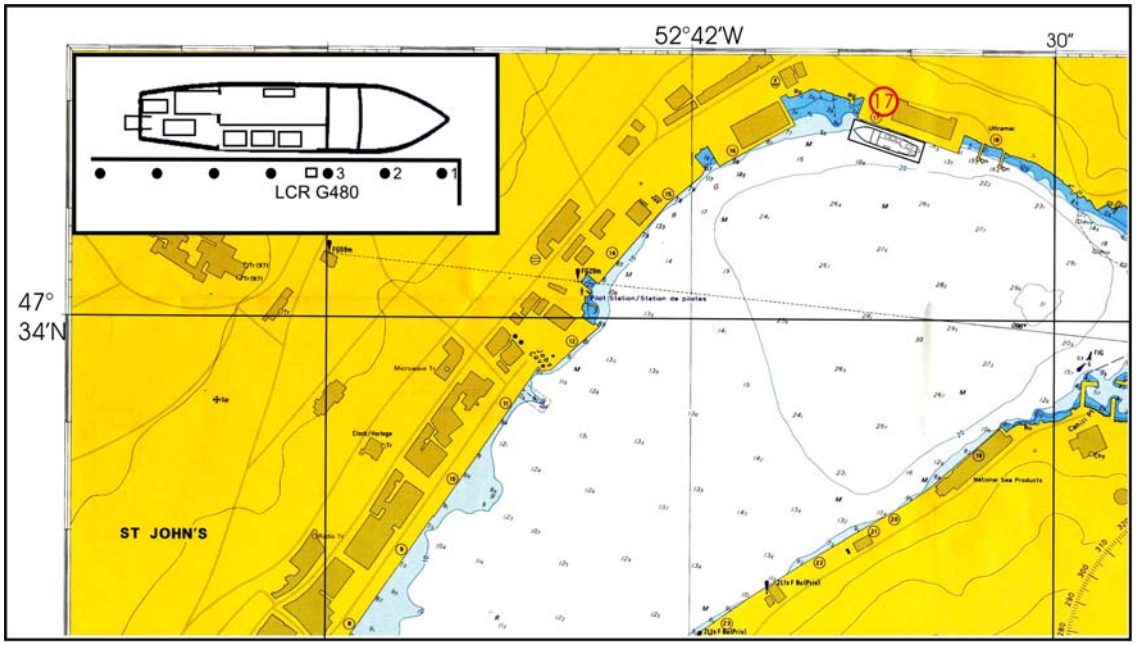

Fig. 8.4. Location of the docking site of RV MARIA S. MERIAN at pier no. 17 in St. John's harbour with site of dock-side gravity tie point.

Station	Observer	Date	Time UTC	Reading units	Gravity value [mGal]
A	H	16.09.08	17:10	4383.26	4455.744
01	H	16.09.08	17:45	4376.09	4448.435
02	H	16.09.08	18:40	4383.61	4456.101
A	H	16.09.08	18:50	4383.27	4455.755
A	H	18.09.08	12:30	4383.25	4455.734
03	H	18.09.08	13:10	4375.25	4447.578

A	H	18.09.08	13:50	4383.26	4455.744
04	H	08.10.08	12:20	5934.31	6038.081
B	H	08.10.08	12:28	5934.11	6037.877
05	H	29.10.08	09:35	3682.68	3741.769
C	H	29.10.08	10:00	3683.07	3742.156

Tab. 8.1. Observation summary of the gravity tie measurements in St. John's (Newfoundland), Sisimiut (Greenland) and Ponta Delgada (Azores) during MSM09/3. Gravity in mGal was calculated using LCR G 480 scaling table. H = I. Heyde (observer).

Reference Stations:

01: Memorial University St. John's, Rear of the Physics-Chemistry Building (47°34.4'N, 52°44.0'W, 60 m a.s.l.) 980820.620 mGal (IGSN71)

02: St. John's, seawall of Harbour Drive opposite Atlantic Place (47°33.78'E, 52°42.45'W, 3 m a.s.l.) 980828.340 mGal (IGSN71)

03: Memorial University, St. John's, Seismology Vault in Science Building (47°34.38'N, 52°44.03'W, 61 m a.s.l.) 980819.850 mGal (IGSN71)

04: Atlantkaj, Sisimiut, Greenland Station No. 67705 of KMS Gravity Net 982411.400 mGal (IGSN71)

05: Igreja de S. José, Ponta Delgada, Station NP-370 Inst. Geográfico Português (37°44.25'N, 25°40.43'W, 9.52 m a.s.l.) 980114.240 mGal (IGSN71)

Gravity stations:

A: St. John's harbour, pier no. 17, 32 m from the western corner of the pier

B: Sisimiut, Atlantkaj, 15 m from the eastern corner of the pier

C: Ponta Delgada, pier no. 12

Differences between reference and gravity stations:

01 – A = - 7.309 mGal
02 – A = +0.346 mGal
03 – A = - 8.161 mGal

Absolute gravity at A (from 01): 980827.929 mGal
Absolute gravity at A (from 02): 980827.994 mGal
Absolute gravity at A (from 03): 980828.011 mGal

Absolute gravity for A (reduced to water level –2.3 m) 980828.62 mGal (IGSN71 system).

Absolute gravity at gravity sensor (1 m above water level) 980828.3 mGal used for the gravity tie on 19.09.2008 (01:30 UTC).

Reading of sea gravimeter KSS31 at that time: 899.59 mGal.

04 – B = - +0.204 mGal

Absolute gravity at B (from 04): 982411.196 mGal

Absolute gravity for B (reduced to water level –2.3 m) 982411.81 mGal (IGSN71 system).

Absolute gravity at gravity sensor (1 m above water level) 982411.5 mGal used for the gravity tie on 08.10.2008 (22:00 UTC).

Reading of sea gravimeter KSS31 at that time: 2480.33 mGal.

On Oct. 8, R/V MARIA S. MERIAN docked at the Atlantkaj in Sisimiut, Greenland (Fig. 8.5). Tie measurements to reference station 04, which is located only about 50 m from the mooring site B, have been made. The point description and absolute gravity value of the reference station was kindly provided by Kort- og Matrikelstyrelesen (KMS, Copenhagen, Denmark). Point B is located near the first bollard 15 m from the eastern corner of the pier. The connection measurements resulted in an average absolute gravity value of 982411.81 mGal (with water level –2.3 m, IGSN71) for point B at the water level. That results in an absolute gravity value of 982411.5 mGal for the location of the gravity sensor. The reading of the KSSM31 on Oct. 8 (22:00 UTC) was 2480.33 mGal.

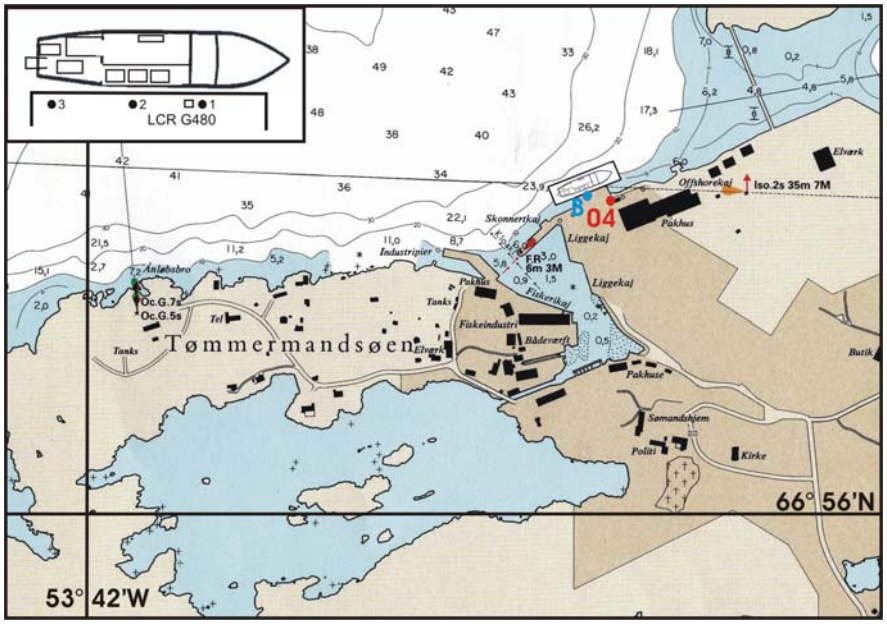

Fig. 8.5. Location of the docking site of R/V MARIA S. MERIAN in Sisimiut (Greenland) and gravity tie points.

The instrumental drift for the first part of cruise MSM09/3 can be derived from the readings in St. John's and Sisimiut to +2.46 mGal in19.9 days or +0.123 mGal/day. This drift rate is rather high and can be explained probably by the fact that the sensor was not completely temperature stabilized when St. John's was left. The sensor, however, was heated already from Sept. 14, 17:30 UTC with an interruption of less than 1 hour during transportation on Sept. 16. Obviously it takes more than 4 days before the sensor is temperature stabilized and does show its normal drift rates of 1-2 mGal/month only. This behavior has to be tested back in Hannover.

At the end of the cruise R/V MARIA S. MERIAN moored at pier No. 12 in the harbour of Ponta Delgada harbor (Fig. 8.6). On Oct. 29, tie measurements to point C on the pier opposite the gravimeter room of MERIAN were made. The tie measurements were done about 50 cm to the south-east of bollard No. 24. The point description and absolute gravity value of the reference IGSN71 station in Ponta Delgada was kindly provided by the Instituto Geográfico Português (Lisboa, Portugal).

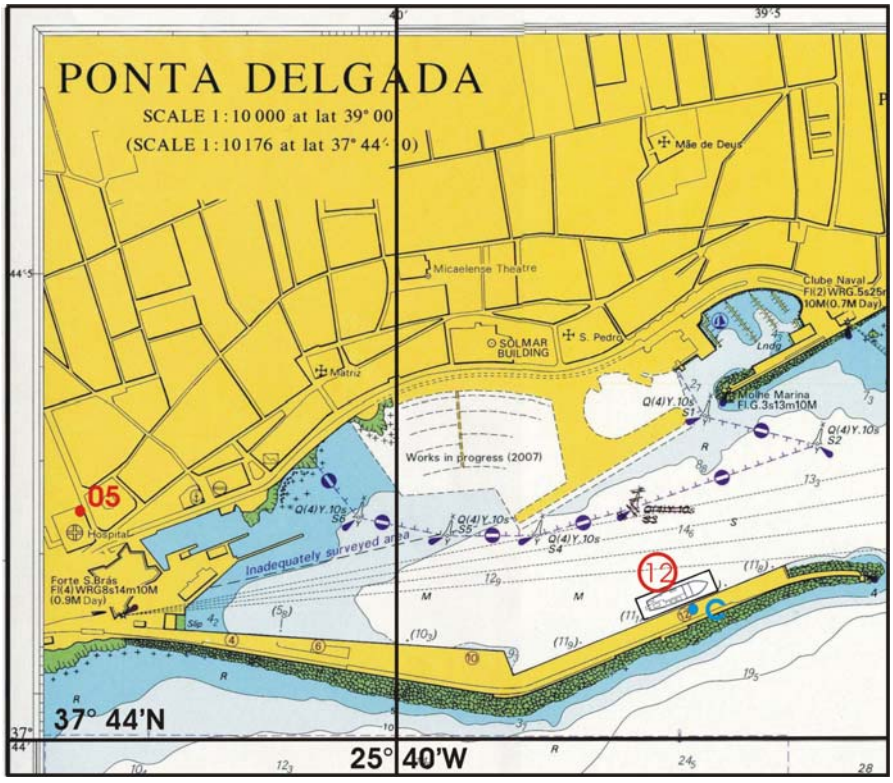

Fig. 8.6. Location of the docking site of RV MARIA S. MERIAN at pier no. 12 in Ponta Delgada (Sao Miguel, Azores) and gravity tie points.

Differences between reference/gravity stations:

05 – B = - 0.39 mGal

Absolute gravity at B: 980114.63 mGal

The connection measurements resulted in an average absolute gravity value of 980115.19 mGal (reduced to water level –2.1 m, IGSN71) for point B. This results in an absolute gravity value of 980114.88 mGal for the location of the gravity sensor (1 m above sea level). The reading of the KSS31 at the same time (Oct. 29, 2008, 08:30 UTC) was 185.25 mGal.

The instrumental drift for the second part of cruise MSM09/3 can be derived from the readings in Sisimiut and Ponta Delgada to +1.54 mGal / 20.45 days or 0.0075 mGal/day. This drift rate is normal for the instrument. The drift correction will be applied to the data.

8.4 Data Quality and Preliminary Results

Data Quality

In order to check the accuracy of the data quantitatively, the values at crossovers of gravity profiles are compared. Fig. 8.7 shows a map of the MSM09/3 profiles together with the crossover errors (COE). The average COE in the KSS31M data for the 35 crossovers along the track is 0.85 mGal (1σ = 0.74 mGal). The biggest difference found was 2.6 mGal. The general accuracy, however, is better than 1 mGal. Possibly the COE will become smaller applying the drift correction for the second part of the cruise after the tie measurements in

Ponta Delgada. The lower accuracy compared to previous cruises reflects the at times rough sea conditions during MSM09/3

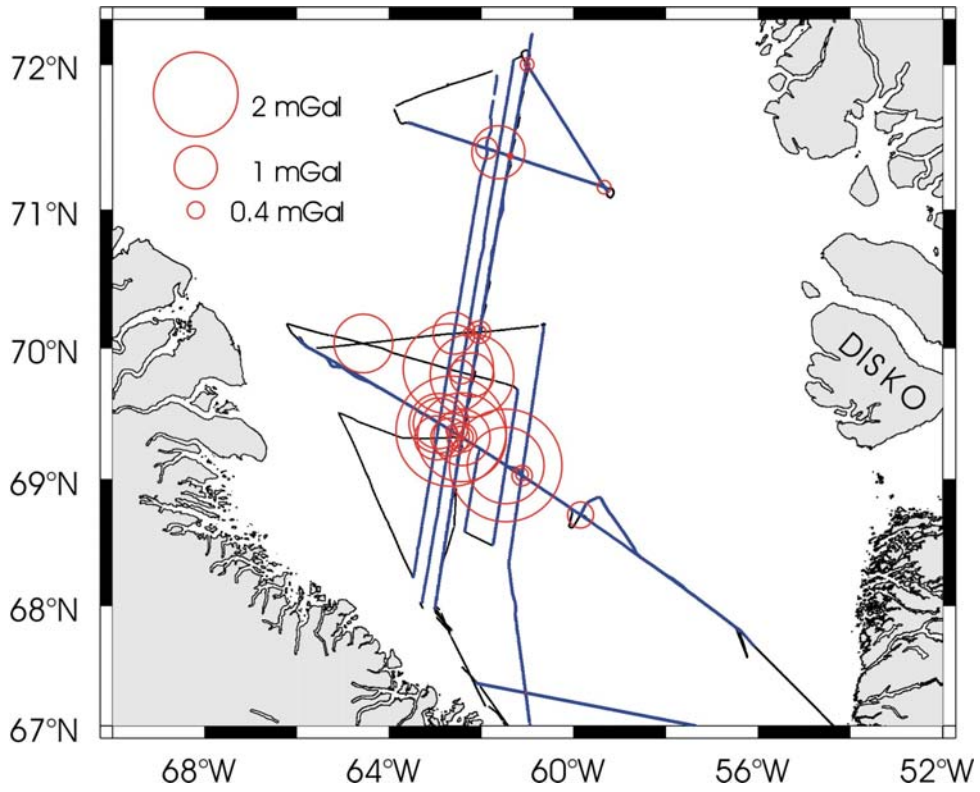

Fig. 8.7. Crossover errors (COE) of the KSS31M free-air gravity anomalies.

Gravity Database

Gravity measurements were carried out continuously from St. John's to Ponta Delgada. Therefore gravity data along all19 profiles with a total length of 4472 km were measured. In addition about 1200 km were measured along transits in the survey area. The distribution of the survey profiles can be seen in the track charts of Figs. 3.1 and 3.2.

Despite the coverage of the survey area is rather sparsely, a map of the free-air gravity anomalies was prepared. Fig. 8.8 shows the map based on a 1 x 1 (arc-)minutes grid together with the survey tracks. The map is drawn up to a distance of 15 kilometres from the survey track.

Comparison with Gravity Anomalies Derived from Satellite Altimetry

The analysis of the crossover errors shows that our gravity measurements have an accuracy of better than 1 mGal. This is far more precise than alternate methods to measure the marine gravity field as for example the calculation of free-air gravity anomalies from satellite altimeter measurements. A satellite altimeter uses pulse-limited radar to measure the altitude of the satellite above the closest point to the sea surface. Global precise tracking coupled with orbit dynamic calculations provide an independent measurement of the height of the satellite above the ellipsoid. The difference between these two measurements is equal to the geoid height. In marine areas the free-air anomaly can be calculated from the slope of the geoid. Closely spaced satellite altimeter profiles collected during the GEOSAT Geodetic Mission (~

6 km) and the ERS 1 Geodetic phase (~ 8 km) were used by different groups to calculate grids of the free-air gravity anomalies.

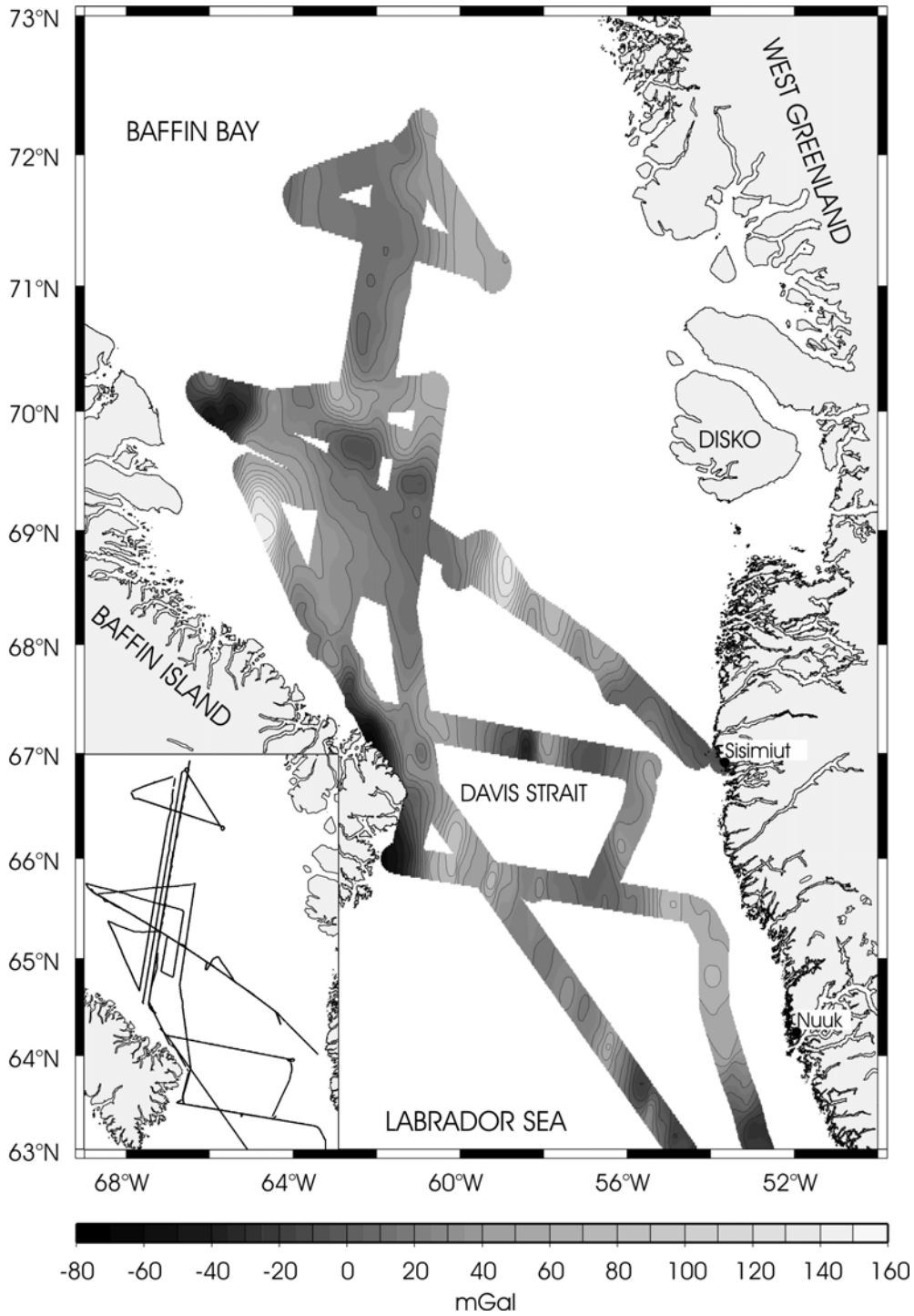

Fig. 8.8. Map of the free-air gravity anomalies in the survey area of cruise MSM09/3. The map and isolines are drawn up to a distance of 15 km from the tracks.

Our data set can serve as a reference for the comparison of two different satellite gravity data compilations. The first is the one from Sandwell and Smith (1997), version 16.1, referred to as SDW16.1 in the following. The second data set is the data set from DTU Space Center, Copenhagen (Andersen et al., 2008) here referred to as DNSC08 data set. They implemented a new technique for the interpolation of the gravity field: it is called an adaptive interpolation

where the parameters for the covariance function have been determined empirically from the altimetry and subsequently interpolated to the position of interpolation. This has shown to be effective in removing track like structures in areas of high ocean variability as the variance is much better determined.

Subtracting the 1 x 1 minute grid of the SDW16.1 and DNSC08 data from the 1 x 1 minute grid of the shipboard data one obtains the maps of the differences shown in Fig. 8.9. The maps are masked beyond a distance of 3 kilometres from the MSM09/3 profiles. The differences of both datasets range between +20 and -20 mGal, whereby along most tracks the differences are below ±4 mGal. High positive differences with the DNSC08 data are found in the NW and high negative values with both datasets near the coast of Baffin Island.

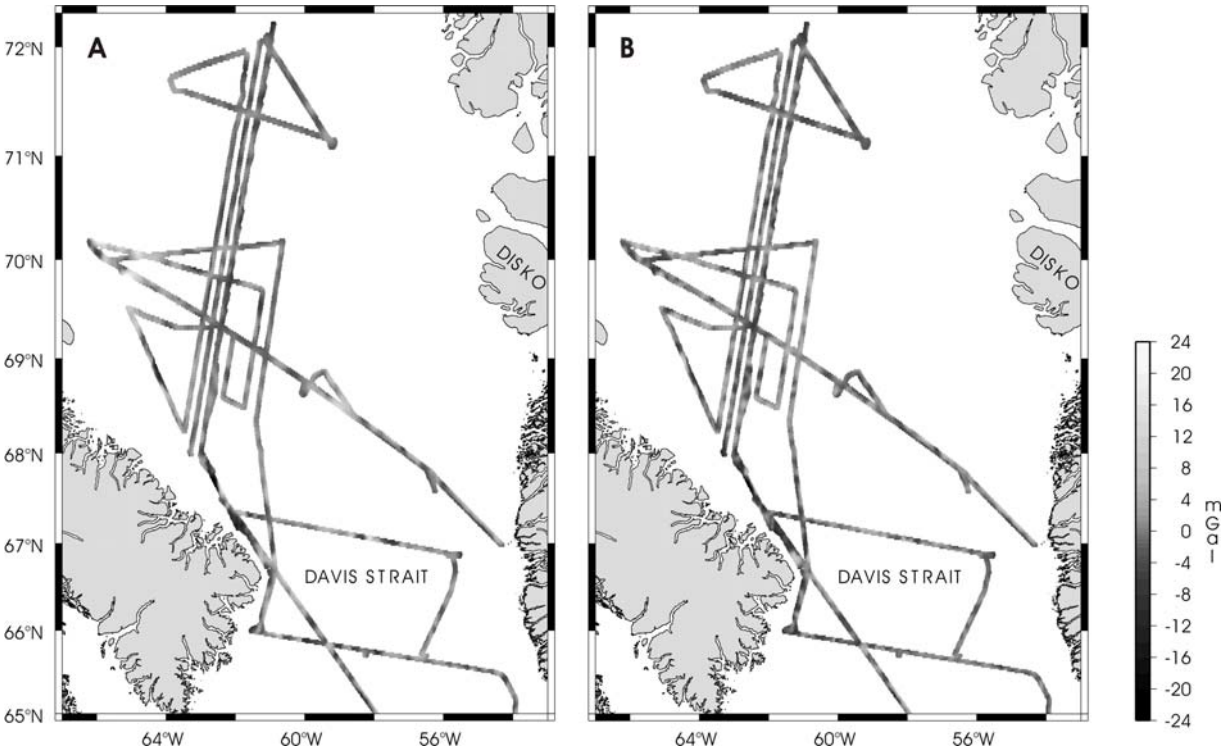

Fig. 8.9. Differences of the shipboard free-air gravity data and the gravity datasets derived from satellite altimetry (A: DNSC08, Andersen et al. (2008); B: Sandwell and Smith (1997), version 16.1).

Additionally the satellite gravity anomalies along the complete track were calculated with bicubic interpolation out of the 1 x 1 minute grids and subtracted from the shipboard data. The analysis of 116262 gravity differences along the track in the survey area between the KSS31M free-air anomalies and the satellite derived anomalies resulted in the histogram shown in Fig. 8.10. The mean differences are nearly the same, but with opposite signs (DNSC08: +0.33 mGal; SDW16.1: -0.33 mGal). However, the standard deviation is lower for the SDW16.1 data (2.55 mGal vs. 3.25 mGal). Considering the standard deviation as the main criteria, the above statistical results helped us to decide on the usage of the SDW16.1 data set for further gravity map compilations in areas where no MSM09/3 shipboard data have been measured. This result is a little bit surprising as a map using the DNSC08 data alone looks smoother and less noisy than the corresponding map using the SDW16.1 data.

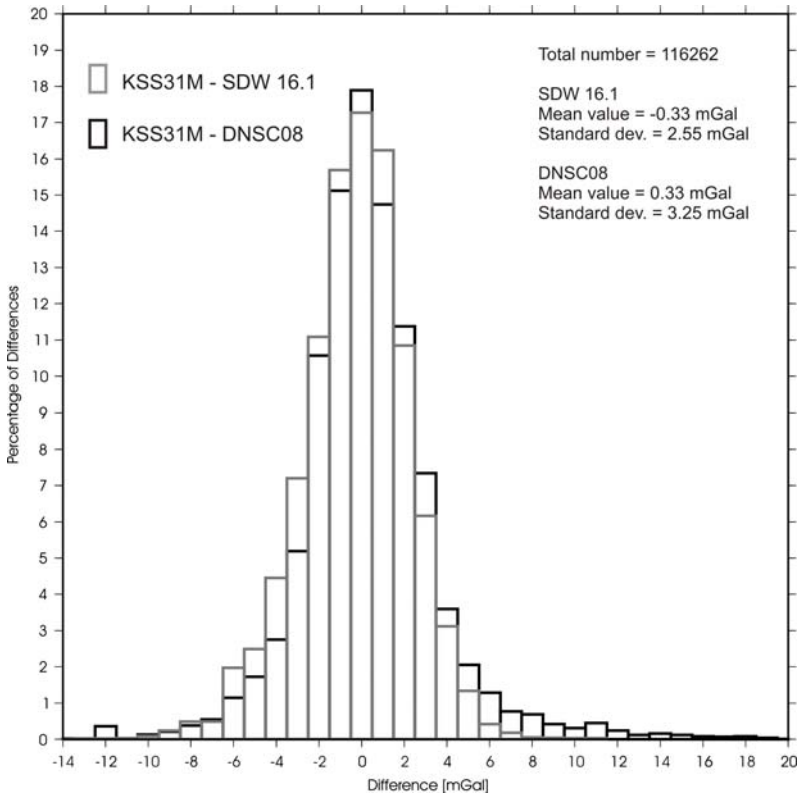

Fig. 8.10. Histogram of differences between shipboard free-air gravity data and the corresponding data from satellite altimetry data sets.

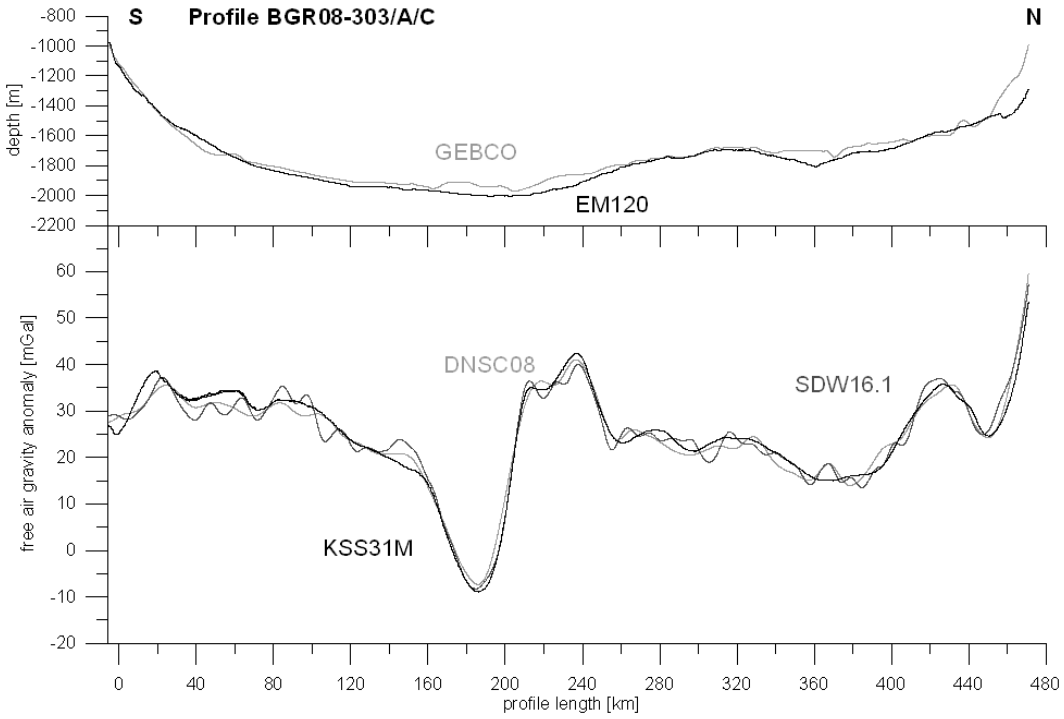

Fig. 8.11. Comparison of the ship-based KSS31M and satellite free-air gravity anomalies along profile BGR08-303/A/C (below) together with the corresponding bathymetry measured with the SIMRAD EM120 multibeam system and from the worldwide GEBCO dataset (above).

To illustrate the differences between the data sets in detail, Fig. 8.11 shows exemplary a comparison along profile BGR08-303/A/C. The wavelength range of satellite and shipboard anomalies is comparable. Approaching the coast the divergence of the data sets increases considerably. In the area of deep water the satellite data show oscillations with a wavelength of about 25 km and amplitudes of ± 3 to 5 mGal which do not correlate with anomalies in the shipboard data. We consider these differences to represent the error in the satellite data. Also the bathymetry of a worldwide data set (GEBCO by IOC, IHO, and BODC, 2003) differs considerably from the true bathymetry measured with the ship's EM120.

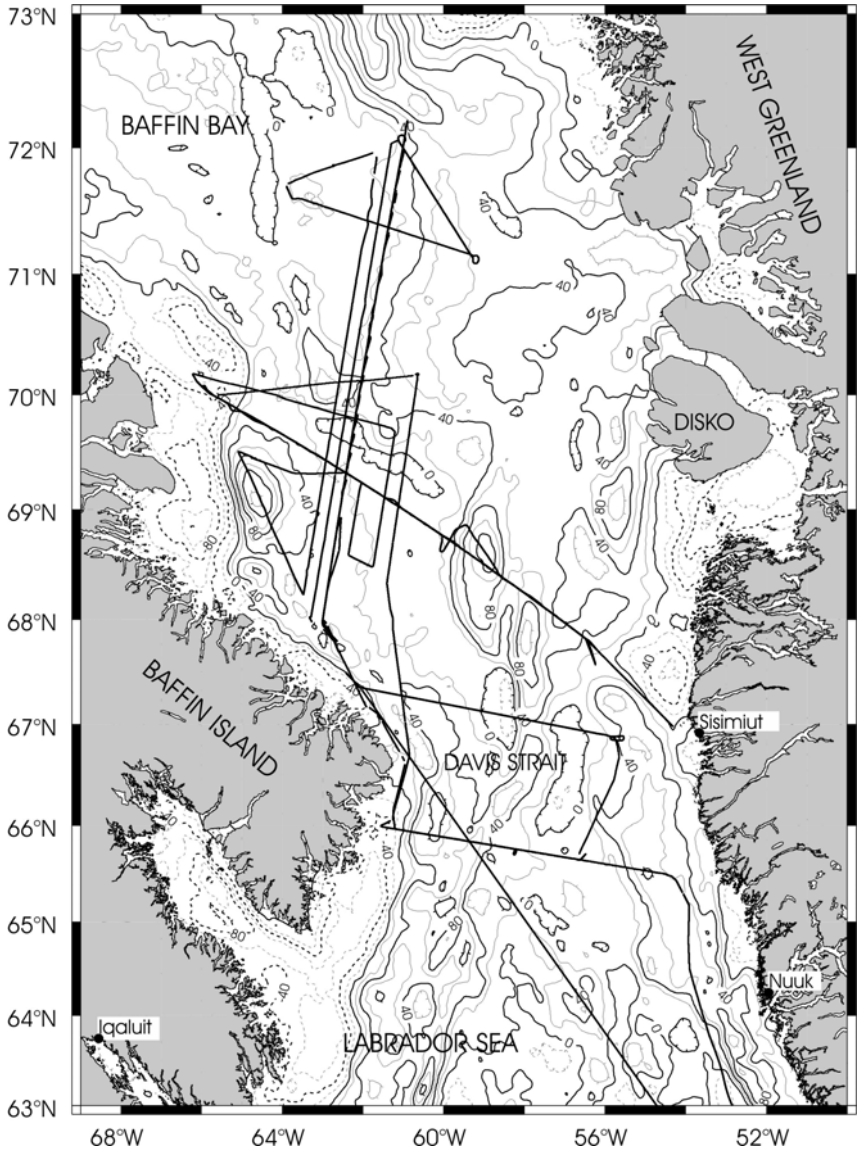

Fig. 8.12. Free-air gravity anomaly map. The underlying grid of gravity was compiled by merging MSM09/3 gravity observations and SDW16.1 gravity data derived from satellite altimetry.

To conclude the free-air gravity anomalies derived from satellite altimetry are of great importance to get an overview of the gravity field in an oceanic area. For detailed investigations, however, shipboard gravity measurements are indispensable.

Combined Free-air Gravity Map

In order to get a complete idea of the gravity field in the survey area SDW16.1 gravity data were included in areas with no MSM09/3 shipboard data for the compilation of the free-air gravity map shown in Fig. 8.12. Shipboard data of other cruises were not considered yet. The map is based on a 1 x 1 (arc-)minutes grid. The anomalies range from +180 mGal in the N on the Eastern slope of the Baffin Bay to several minima with less than -100 mGal close to both the Greenland and Baffin Island coast.

In order to correlate the gravity anomalies with topographic features in the survey area, Fig. 8.13 shows the free-air gravity anomalies underlain by the bathymetry. The oceanic crust in the Baffin Bay in the NW and the Labrador Sea in the S is characterized by free-air gravity anomalies from about -20 and to +15 mGal. In this area water depths of more than 2000 m are reached. Higher gravity values can be correlated partly with topographic highs on the oceanic crust.The southern Baffin Bay shows similar anomalies. It is connected to its northern continuation by a narrow gateway. To the South it is terminated by the topographic high of the Davis Strait. Landward the gravity anomaly values increase considerably. The map reveals prominent positive anomalies parallel to the shelf break (up to +180 mGal) both on the western and the eastern side. In the Labrador region these maxima are rather symmetrically. North of the Davis Strait these anomalies are much broader offshore Greenland than offshore Baffin Island. These anomalies are typical for rifted continental margins which are characterized by prominent free-air gravity anomalies elongated parallel to the ocean-continent transition. For example, these features could be observed along large portions of the Atlantic margins (Watts and Fairhead, 1999). Sleep and Fuyita (1997) demonstrated that a simplified ocean-continent transition (oceanic crust bordering directly on continental crust, both of uniform thickness and isostatically compensated) produces an antisymmetric free-air anomaly located at this boundary with a high on the outer shelf and a low on the oceanic crustal edge. Landward the gravity anomaly values decrease considerably. Prominent minima are reached near the south- and the northwestern coast of the Cumberland Peninsula and southeast of Disko Island. Another less pronounced minimum on the Greenland side can be found northwest of Sisimiut. These areas with increased water depths of about 500 m correspond probably to sediment basins filled with thick sediments of relatively low density.

Bouguer Gravity Anomaly Map

The underlying grid of gravity was compiled by merging MSM09/3 gravity observations and SDW16.1 satellite gravity data. The water depth values were taken from the ship's echo sounding system and from the GEBCO bathymetry data when no echo sounder depths were available. The reduction density was 1.64 g/cm³ and an infinite horizontal slab was assumed. A topographic reduction was not performed. Fig. 8.14 shows the map of the Bouguer gravity anomalies together with the bathymetry. On the oceanic crust the anomalies are positive (up to +220 mGal in the NW) with a clear north-south trending decrease of values towards the Davis Strait. Landward the values decrease rapidly. The lowest Bouguer gravity values (-80 mGal) are reached in the area of the basins southeast of Disko Island and northwest off the Cumberland peninsula on the continental shelf.

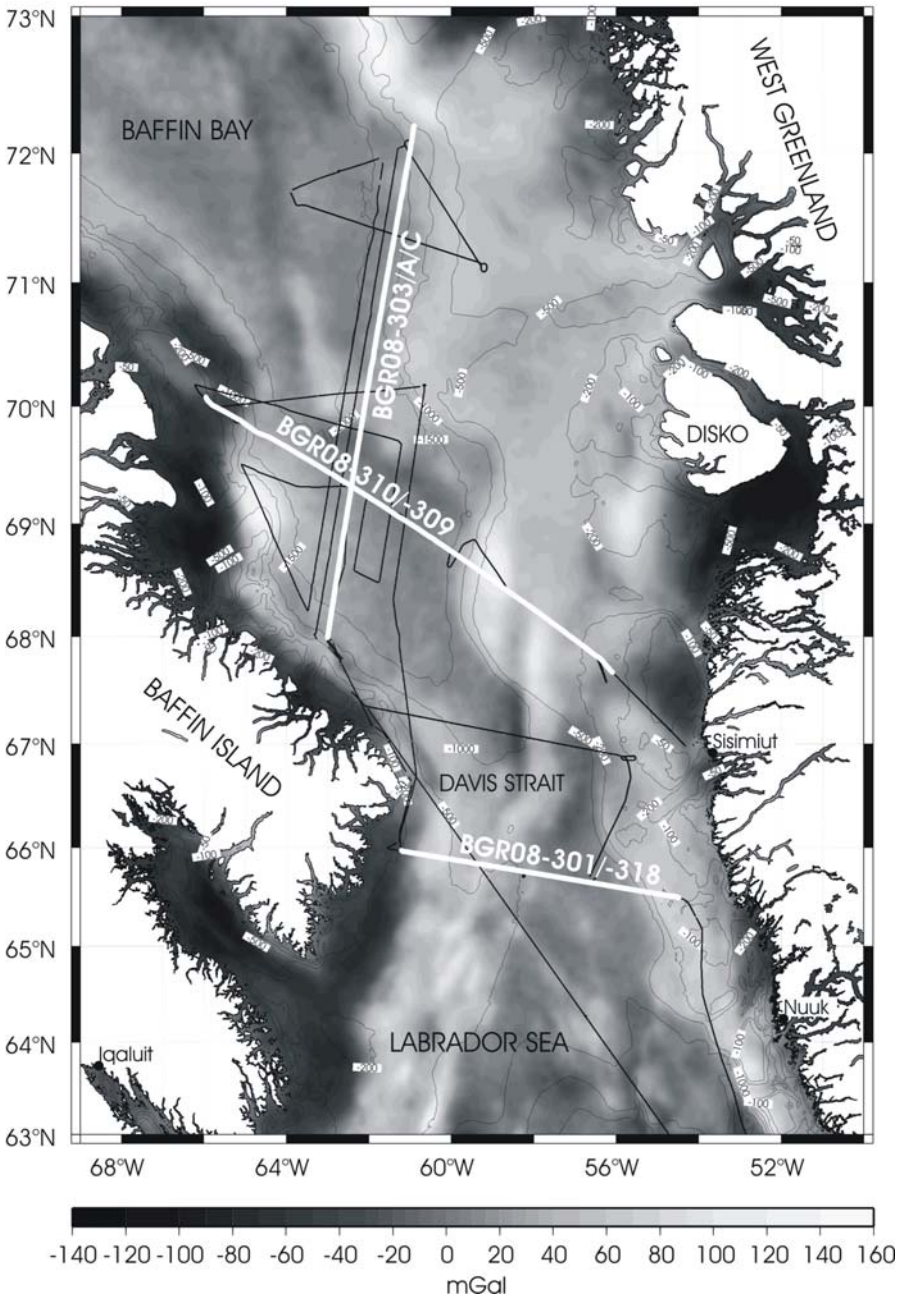

Fig. 8.13. Free-air gravity anomaly map underlain by the GEBCO bathymetry (IOC, IHO, and BODC, 2003). In addition the profiles discussed in chapter 9.5.4 are marked.

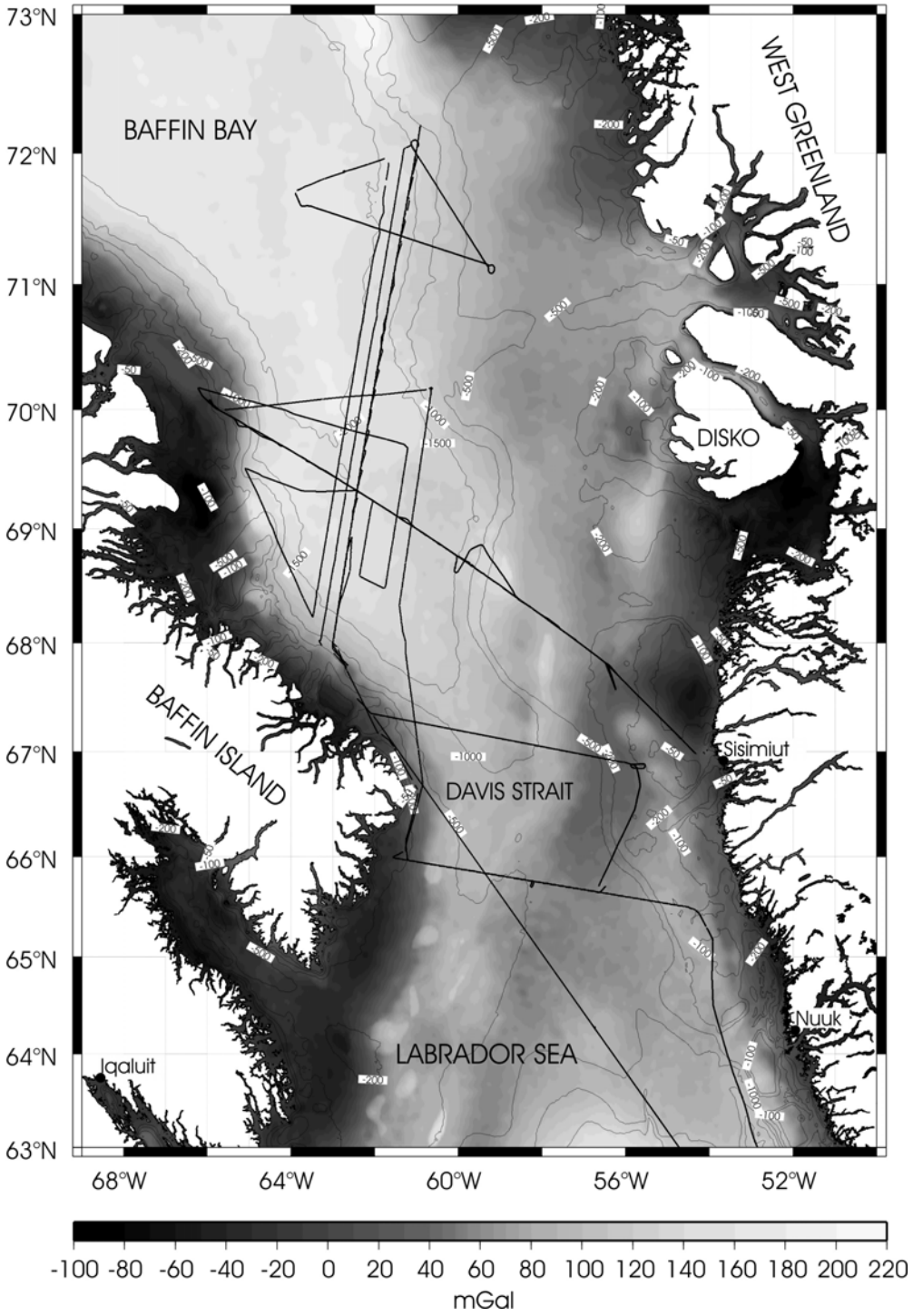

Fig. 8.14. Map of Bouguer gravity anomalies with no terrain corrections applied. The reduction density was 1.64 g/cm³. The map is underlain by the GEBCO bathymetry (IOC, IHO, and BODC, 2003).

Gravity Data Along Selected Profiles

Three representative profiles are discussed in the following. The preliminary results of the seismic reflection and magnetic profiling are taken into account. The interpretation by 2D and 3D density forward modeling will follow after the cruise when more results especially from refraction seismics are available.

BGR08-301/-318

The southernmost profile across the Davis Strait has a length of 328 km combining the data collected along MCS profile BGR08-301/318 (along seismic refraction profile AWI-20080700) (Fig. 8.15). Starting in the East the steep shelf break off Greenland is associated with a positive anomaly typical for continental margins. Westward the anomalies decrease as expected with increasing water depth. Further to the West three distinct positive anomalies can be correlated with basement highs bordering sediment basin structures. Landward the anomalies decrease considerably with decreasing depth. This can be only explained by a thick unit of low density. The MCS data in that part are strongly disturbed by multiples and give little hint to thick sediments. Also the high magnetic anomalies imply volcanic/basaltic material of normally high density. Without the results of the refraction seismics it is difficult to explain these negative gravity values at the moment. Skaarup et al. (2006) found on a MCS profile to the north a similar result. Interpretation of high-resolution seismic data shows that submarine debris flows have modified the continental slope in the Quaternary (Hiscott and Aksu, 1994). This process has produced similar anomalies on the southeastern margin of Canada (Courtney and Piper, 1992).

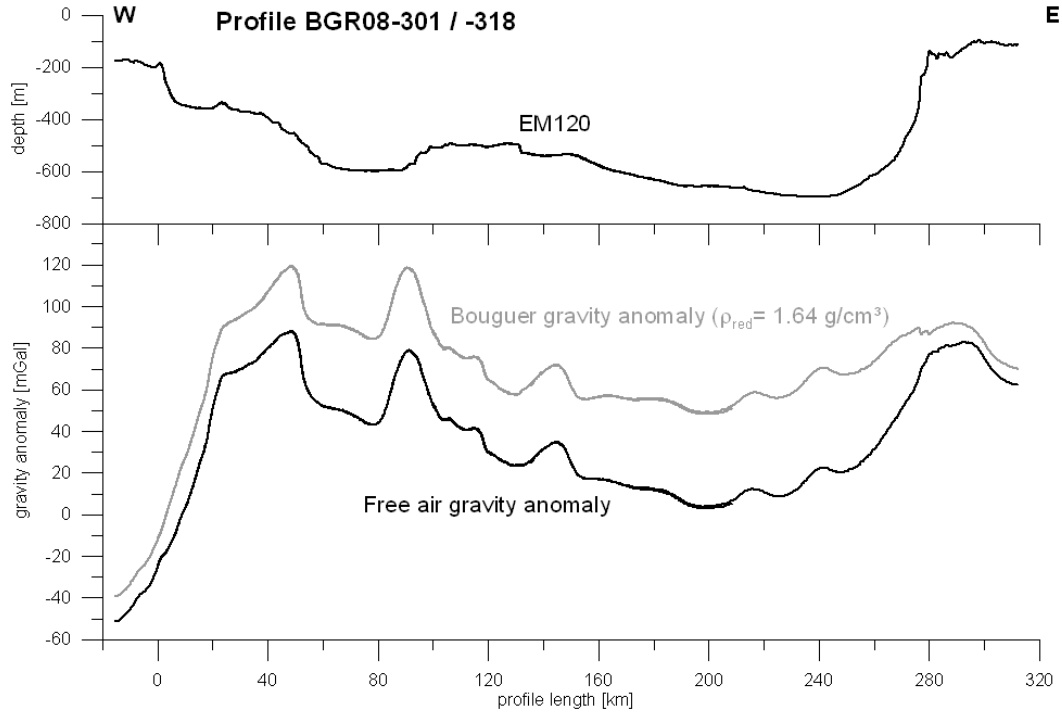

Fig. 8.15. Bathymetry (above) and gravity anomalies (below) along profile BGR08-301/-318 and AWI-20080700.

BGR08-303/A/C

The SSW-NNE running profile across the Baffin Bay has a length of 486 km (Fig. 8.16). Starting in the South the continental slope is not associated with distinct free-air gravity anomalies. Unfortunately the profile did not cross the shelf break farther South. Between profile kilometers 160 and 260 km a gravity minimum is followed by a maximum of comparable width. This feature marks the southern border of a broad bathymetry high. The MCS results show the transition from thicker sediments to a basement high. In how far this anomaly can be correlated with an extinct spreading center has to be investigated in detail taking the magnetic results into account. The free-air gravity anomalies run smoothly

northward with a maximum correlating with a basement high in the MCS data. Towards the northern profile end the gravity values increase with decreasing water depth. Unfortunately again the shelf break is not reached.

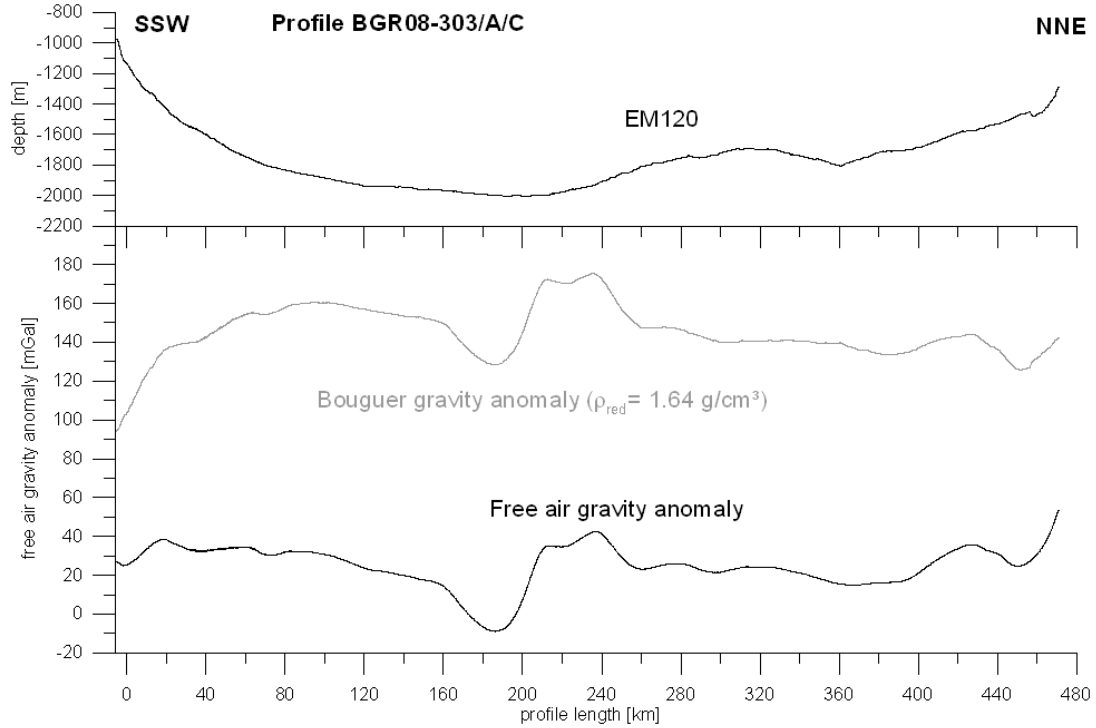

Fig. 8.16. Bathymetry (above) and gravity anomalies (below) along profile BGR08-303/A/C and AWI-20080500.

BGR08-309/-310

The NW-SE running profile (Fig. 8.17) across the Baffin Bay has a length of 478 km and was again measured with all geophysical methods used during the cruise. Starting in the West on the shelf with low values the gravity increases sharply with the steep continental slope. The gravity low correlates with the eastern flank of the Scott Graben which was crossed in the area by a profile in Skaarup et al. (2006). The gravity decreases eastward with smoothly decreasing water depth. This can be explained with increasing sediment thickness in that direction in the MCS data. Further to the East the shelf break correlates with a pronounced gravity high. On the shelf the anomalies reflect the sequence of basement highs and sediment basins. Approaching the end of the profile the gravity values decrease towards the Sisimiut Basin situated in the prolongation of the profile.

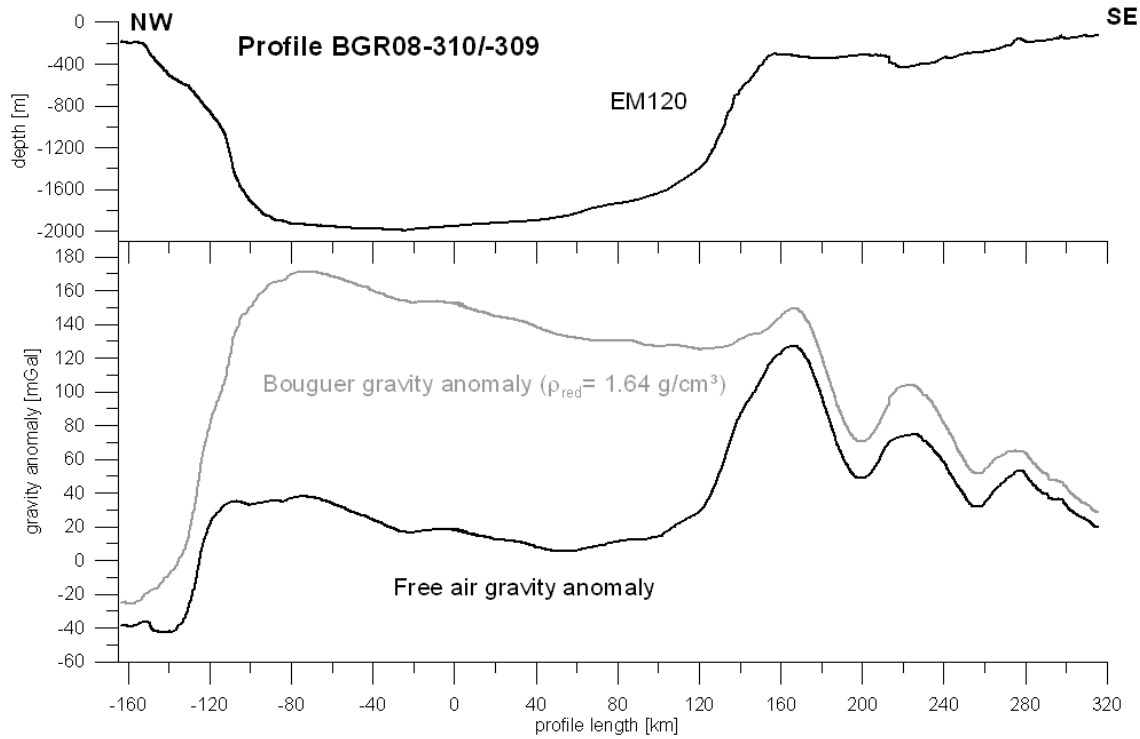

Fig. 8.17. Bathymetry (above) and gravity anomalies (below) along profile BGR08-310/-309 and AWI-20080600.

9. Magnetics

(B. Schreckenberger, I. Heyde, H.-O. Bargeloh)

9.1 Method, Instruments and Operation

The BGR magnetometer systems used during cruise MSM09/3 consisted of two independent magnetometer types which were partly operated simultaneously on one cable:

(1) the SeaSpy system with one or two Overhauser magnetometer sensors and

(2) an oriented Magson fluxgate sensor.

Overhauser sensors measure the scalar absolute value of the total magnetic field while fluxgate magnetometers measure the magnetic field vector in its three components.

Marine Magnetics SeaSpy™ Gradiometer

The SeaSpy™ Marine Gradiometer System manufactured by Marine Magnetics Corp. normally consists of two proton precession magnetometers, enhanced with the Overhauser effect. In its original configuration two exactly equivalent magnetometers are towed 150 meters apart as a longitudinal array 600 meters astern of the ship (Fig. 9.1). Both sensors measure the total intensity of the magnetic field simultaneously. The difference between the two measurements is an approximation for the longitudinal gradient of the field in the direction of the profile line. Provided that the time variations are spatially constant over the sensor spacing, the differences are free from temporal variations and their integration restores the variation-free total intensity or magnetic anomaly (apart from a constant value).

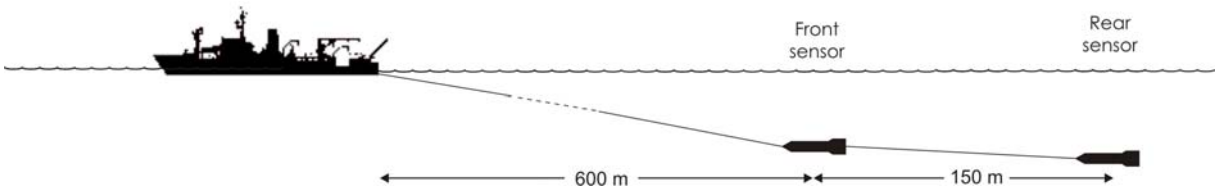

Fig. 9.1. Schematic sketch of the towed gradiometer system setup.

A standard proton precession magnetometer uses a strong DC magnetic field to polarize itself before a reading can be taken. Overhauser sensors work similar to proton magnetometers with the exception that the excitement of the proton spin (polarization) is done by radio waves which excite the spin of the electrons in an organic fluid within the sensors. The electrons then transfer their spin to the protons in the fluid via a quantum mechanical process called Overhauser effect. Similar to every other proton magnetometer the relaxation frequency of the protons is a measure for the magnitude of the ambient magnetic field. The polarization power required is much smaller than that needed by normal proton magnetometer systems and the AC field may be left active while the sensor is producing a valid output signal. This allows the sensor to cycle much faster and to produce more precise results than a standard proton magnetometer. The signal is digitized by the electronics assembly within the tow fishes which then transmit digital data strings via a two conductor tow cable to the vessel. The tow cable is connected to a deck leader which is in turn connected to the power supply and the logging computer. As configured for this survey, the Overhauser sensors had a cycle time of one second. The sensors are specified with a noise level of 0.01 nT/√Hz, a resolution of 0.001 nT, and an absolute accuracy of 0.2 nT.

Magson™ Fluxgate Magnetometer

The Magson fluxgate towfishes were designed by the BGR marine geophysics group and built by the Magson company in Berlin. The system consists of i) a digital 3-axis Magson fluxgate magnetometer yielding excellent precision, ii) a two-axis tilt-meter, type 900H made by Applied Geomechanics Ltd., iii) a two-axis and single axis accelerometer, types ADXL203 and ADXL103 made by Analog Devices, iv) sensors for temperature, pressure, and humidity, and v) a data acquisition microprocessor built by Magson as well. Fluxgate and inclinometers are mounted on a common platform. All components, shown in Fig. 9.2, are placed inside a pressurized glass-fibre tube of the same brand as the sensors of our standard SeaSpy™ gradiometer.

Fig. 9.2: Components inside the fluxgate magnetometer towfish.

The Magson fluxgate uses the principle of vector-compensating all three ring-core-sensors by means of three independent Helmholtz-coils. The internal feedback circuit, using digitally controlled DC-currents fed into the Helmholtz-coils maintains precise nulling of the field inside the ring-core. Thus the amplitude of this current can be used as a signal to measure the

vector components of the magnetic field. A factory calibration is required to provide offset, scale factor and non-orthogonality angle for each axis. All electronic components are integrated on the board of the data acquisition microprocessor. The Magson fluxgate sensor is specified with a noise level of 0.02 nT/√Hz, a resolution of 0.008 nT and a long term stability < 10 nT/year.

Inside the tow fish a special platform is used to mount the fluxgate and both tilt-sensors. The first tilt-sensor by Applied Geomechanics (900H) measures pitch and roll angles by a conductive liquid in a half filled glass vial. The tilt angle is derived by the height of liquid covering five electrodes. This inclinometer covers an angular range of ± 25°/± 40° (first/second Magson towfish) with an accuracy of about 0.01° of arc (noise level 0.005°).

The second tilt-sensors are dual axis accelerometers by Analog Devices (ADXL203), measuring pitch and roll angles over a span of ± 50°/± 20° (first/second Magson towfish) resolving 0.05° of arc (noise level 0.095°). A third accelerometer for the vertical axis (ADXL103) allows to detect an unintended upside down position of the towfish.

The accuracy of the Applied Geomechanics sensor is significantly higher, but the calibration function is non-linear and temperature dependent. The Analog Devices sensor has a faster response (cross correlation results in 0.1 s difference), the calibration function is linear and almost temperature independent, but it suffers the noise level increased by factor 2. Both tiltmeters measure not only the static acceleration, which would provide the needed true roll and pitch angles. Instead, they measure also the dynamic acceleration due to the angular accelerations of the continuously moving towfishes. This source of error can partly be reduced by filtering but remains a limiting factor of tilt estimation.

A high precision of angle measurement is necessary to rotate the field components measured in the sensors coordinate system of the moving fluxgate towfish into the horizontal geomagnetic coordinate system. By Euler rotation it is possible to separate the vertical from the horizontal field vector components. The accuracy of the vector data is limited by the accuracy of the rotation angles. For example, a 0.01° tilt deviation may result in up to 10 nT component error in the survey area. Without any yaw angle estimation, the orientation of the horizontal field vector (i.e. the north and east component) remains unknown. A crude approximation might be ship's course. Utilising magnetic heading from the fluxgates themselves removes seafloor anomalies by default, however, a numerical yaw approximation has been introduced by Engels et al. (2006), demonstrating the advantages of vector component data analysis.

An embedded microprocessor with a flash disc is used to store all fluxgate and tilt-meter readings. The storage capacity of 1 GB is sufficient to allow for 11 days of continuous operation at a sampling rate of 10 Hz.

Magnetometer Array Configurations

All magnetometer array configurations which have been applied during cruise MSM09/3 are listed in Table 9.1 together with the details of all deployments. Sensor type is identified by a serial number. S/N 13139 and S/N 13335 are Oberhauser sensors while S/N13142 denotes the Magson sensor. Usually BGR has four Overhauser sensors and two Magson sensors available. Due to two other cruises that overlap with the MSM09/3 cruise only the three sensors mentioned above were available. That proved to be a disadvantage because on the first line (BGR08-301) one of the Overhauser instruments (S/N 13335) started to develop an electronic defect that turned out to be irreparable with onboard means. Therefore, for all other lines only one Overhauser sensor (S/N 13139) and one Magson sensor (S/N 13142) were available. For technical reasons and due to adverse weather conditions on several lines

(BGR08-303 to -306 and -310 to -312) only the Overhauser sensor could be deployed. On profiles BGR08-302, -307 to -309, -316, -317, -319 and –Cal one Overhauser and one Magson sensor were deployed according to Table 9.1. Data from line BGR08-303 will most probably not be usable because the magnetometer sensor got caught by the streamer close to the vessel and the record is extremly noisy.

The calculation of gradients and the respective reconstruction of the magnetic field from the gradient will also be possible using the mixed sensor configurations. However, fluxgate sensors are by far not as stable as (Overhauser-) proton magnetometers and require calibrations. Therefore, two calibration loops (circles) were performed during the cruise. The first one belongs to line BGR08-307 in the northern part of the survey area and the second loop (BGR08-Cal) is located south of line BGR08-301 and was surveyed at the end of the magnetic operations.

During nearly all times when the fluxgate sensor was not used in the towed array it was mounted on the observation deck. Table 9.2 shows the times and data file names for all towed and onboard deployments of the fluxgate sensors. Using the motion reference unit from the ship as well as the data from the INS connected to the gravimeter it will later be attempted to compensate for the ships magnetic field by estimating the compensation matrix during turns. A comparison with the towed magnetometer shall test the accuracy limits of total magnetic field values for a ship borne fluxgate during post cruise processing. It will also be attempted to apply methods that were used by e.g. Seama et al. (1993), Korenaga (1995), Parker and O'Brian (1997) and Engels et al. (2008) to utilize the vector components for the determination of magnetic strike directions.

		(UTC)		(UTC)	(m)			(BGR08-)	
msm09_sl_data_002	267 (23.09.) 267 (23.09.) 268 (24.09.)	19:29:54 20:48:17 ca. 06:16	269 (25.09.)	03:48:26	ca. 200 600	13139 13139	13335 (none)	301	Reduced tow cable length Tow cable fully deployed Complete failure of rear sensor
msm09_sl_data_003	270 (26.09.) 272 (28.09.)	19:04:02 01:36:24	272 (28.09.)	12:24:06	600	13139	none	302 303	 Data not usable
msm09_sl_data_004	272 (28.09.)	18:52:42	274 (30.09.)	15:33:00	600	13139	none	303A, 303C	
msm09_sl_data_005	276 (02.10.)	05:17:05	278 (04.10.)	06:00:09	600	13139	none	304, 305, 306	
msm09_sl_data_006	278 (04.10.)	06:00:10	280 (06.10.)	19:45:35	600	13139	13142	307/308	Including calibration 1
msm09_sl_data_008	281 (07.10.)	17:35:02	282 (08.10.)	09:23:23	600	13139	13142	309	
msm09_sl_data_009	285 (11.10.)	12:10:27	286 (12.10.)	11:11:24	600	13139	none	310, 311, 312	
msm09_sl_data_010	290 (16.10.)	22:21:14	291 (17.10.)	20:30:23	600	13142	13139	316, 317	
msm09_sl_data_012	294 (20.10.)	18:28:23	295 (21.10.)	22:35:59	600	13139	13142	319	
msm09_sl_data_013	296 (22.10.)	18:26:27	296 (22.10.)	19:00:33	600	13139	13142	Cal	Calibration 2

Tab. 9.1. SeaSPY data files and details of sensor configurations for all towed magnetometer deployments of cruise MSM09/3.

Start date	Start time	End date	End time	Sensor id	First data file	Last data file	Read out date	Remarks
19.09.	22:23:09	20.09.	15:15:26	13142	09192223.d01	09201500.d01	20.09.08	Salinometer room
20.09.	20:13:56	23.09.	08:14:40	13142	09202013.d01	09230800.d01	23.09.08	Salinometer room
23.09.	10:26:24	25.09.	19:03:51	13142	09231026.d01	09251900.d01	25.09.08	Observation deck
25.09.	19:10:24	30.09.	16:19:14	13142	09251910.d01	09301600.d01	30.09.08	Observation deck
30.09.	16:30:47	05.10.	13:07:43	13142	09301630.d01	10051300.d01	05.10.08	Observation deck
10.10.	20:15:05	11.10.	10:24:47	13142	10102015.d01	10111000.d01	16.10.08	Observation deck
18.10.	11:10:04	19.10.	20:16:23	13142	10181110.d01	10192000.d01	19.10.08	Observation deck
23.10.	10:40:52	28.10.	09:44:44	13142	10231040.d01	10280900.d01	28.10.08	Observation deck

Tab. 9.2. Fluxgate sensor data files for all towed and onboard deployments of cruise MSM09/3.

9.2 Data Processing and Calibration

Processing

The magnetic raw data recorded by the Overhauser and fluxgate magnetometers were processed in time domain in order to obtain high quality magnetic data which are essential for further data analyses. Processing of total magnetic field gradients results in reconstructed variation free total field values. Single sensor fluxgate data provide anomalies in vector components which may still contain a variation contribution. Further processing of the vector component data with time and spectral domain methods will be part of the post-cruise work.

We use two standard processing sequences for total field magnetic data. The first one contains of a simple algorithm for cleaning erroneous data of one Overhauser sensor before the magnetic reference field (IGRF 2005) is removed. The resulting magnetic anomalies are stored using a 20 second sampling rate. Later in this chapter these values are used to display preliminary anomaly curves in several figures.

The second processing sequence is more sophisticated and uses the records of two Overhauser sensors and one towed Magson sensor. The philosophy is to pre-process raw data in the time domain in a comprehensive straight-forward and transparent way before gradiometer anomaly reconstruction and further component analysis. In the following the current status of the processing codes (version 8) is summarized briefly:

1. Code READMAG reads all data formats from the individual sensors and the ship's GPS recordings. Gaps, erroneous data records and unphysical data exceeding certain thresholds are replaced by dummy values. From GPS positions which are smoothed by a running mean, control parameters like waypath kilometers, velocity, and azimuth are derived for each sample which is accepted as having reasonable values. The time delay of each sensor according to its position behind the vessel and the ship's velocity is taken into account. Clock deviations (shift and drift) of the individual instruments are being corrected. Fluxgate raw data are calibrated firstly by the factory scalar calibration parameters (including temperature calibration) and secondly by the results from the calibration circle (Fig. 9.3). Tiltmeter angles are calibrated as well. Vector component data are obtained by applying roll, pitch and yaw angles in an Euler rotation prior to rotation into the geographic coordinate system. The magnetic heading of the fluxgates is used as a first approximation of the yaw angles.

2. Code INTERMAG interpolates all data gaps marked by dummy values either linear or by cubic splines. In order to despike and resample the scattered raw data, a median filter provides a robust mean. All data which were recorded at different sampling rates are decimated to equidistant 50 m samples, which is the window length of the median filter. For gradiometer data, the median applies to the differences in order to preserve simultaneous measurements of rear and front sensors.
3. Code IGRFMAG subtracts the ambient main field using IGRF model 2005 up to degree and order 13 (195 coefficients) with secular variation prediction (80 coefficients). From the dot product projection of the measured total field into the IGRF direction the absolute value of the IGRF is subtracted. This IGRF subtraction is done for each gradiometer sensor individually in order to remove the main field gradient. From the vector components the IGRF components are subtracted directly. Optionally a band pass filtered yaw angle can be subtracted from the fluxgates' magnetic headings before IGRF subtraction in order to eliminate yaw angles due to water currents from yaw angles due to magnetic anomalies.
4. Code FILTMAG applies a band pass filter in the time domain in order to limit purely on wavelengths related to realistic anomalies originating from crustal sources in some cases. Routinely, wavelengths shorter 6 km are removed by the lowpass filter (LP) and eliminate the high frequency scattering due to orientation errors, e.g. misleading tilts by towfish dynamics. The highpass filter (HP) gently cuts longer wavelengths and removes long period trends, fluxgate baseline instabilities, and even partly external daily geomagnetic variations. In order to avoid a loss of data at the beginning and end of each profile until all recursive filter coefficients are defined, profile boundaries are wrapped at both ends.
5. Code GRADMAG sums up total field differences between both Overhauser sensors or other arbitrary sensor pairs. The differences can be obtained either from the LP or band pass filtered data. For two sensors which are operating simultaneously in gradiometer mode, temporal external variations are constant over a horizontal spacing of 150 m. Consequently, taking differences of simultaneous readings approximates the small gradient of crustal anomalies with values often below one nT per 150 m. Summing up these small differences ('integrating the gradient') and correcting for the off-axis gradient reconstructs the stationary internal anomaly – free of external geomagnetic variations. Any constant offset between both sensors and any linear trend of the anomalous field is removed by subtracting the mean of all gradiometer differences. Consequently, anomaly profiles start and end centred at the baseline. Subtracting the trend obtained by linear regression of the reconstructed anomaly and adding the trend obtained by linear regression of the LP filtered curve helps to preserve a true anomaly trend.

The failure of one of the Overhauser sensors and the lack of spare sensors on this cruise caused problems with the procedures mentioned above because one Overhauser sensor had to be replaced by the Magson sensor. Reasonable results were obtained during the cruise but must be checked later and are therefore not reproduced here. Furthermore, it will be necessary to obtain magnetic observatory data from Greenland and/or Canada to identify times with magnetic variations and to correct our measuremants.

From visual inspection, most of the lines shown in Fig. 9.4 are disturbed by magnetic variations only to a lesser amount. Profiles BGR08-305, -310, -311 and -312 are an exception, they contain high frequency anomaly components that we attribute to variations. Also line

BGR08-304, which has the same location as line BGR08-303C is highly disturbed and is not shown in Fig. 9.4.

Fluxgate sensor calibration

A fluxgate magnetometer has to be calibrated regularly against a known reference field in order to estimate the calibration parameters. These parameters are offset, scale factor, and non-orthogonality angle for each axis, thus a total of nine parameters for a three-axis vector magnetometer. During a scalar calibration, the fluxgate sensor is rotated around all axes and the resulting total field is adjusted to the reference field. This optimization of calibration parameters is done by a least square fit (downhill simplex method, code by Jeff Gee, SIO) of the measurements. By this procedure, a combination of calibration parameters is obtained which minimizes the deviation from the reference field for all attitudes of the sensor. Calibration parameters drift slowly with time. Changes may also occur after long-distance transportation to different latitudes. Furthermore they are temperature dependent which means that factory calibrations have to be repeated at different temperatures.

In addition to a factory calibration where the sensor is rotated around all axes at different temperatures, calibration figure cruises in the survey area are necessary. Calibration parameters should be estimated at the beginning and end of each survey in order to account for the drift.

The first of such cruises was performed on October 5, 2008. The Overhauser sensor in the front position provides the reference field for the fluxgate sensor in the rear position. A simple circle was sailed at 5 knots at 10 deg/min turn rate in order to vary the azimuth, roll and pitch angles. However, the range of sensor rotation is limited, lacking tilts of the vertical axis which results in a less well defined reference level of the vertical component. On the other hand, all possible azimuth angles are present in the circle (Fig. 9.3) and therefore provide a reasonable basis for the calibration.

The convincing effect of the calibration is demonstrated in Fig. 9.3. Without any calibration, the total field of the fluxgate sensor would be far off the Overhauser reference field. The upper panel shows the result for the calibration circle using the factory calibration by Magson (and BGR test site calibration). The deviation from the Overhauser reference curve is more than 20 nT. The success of the calibration cruise in the survey area is presented in the middle panel where the Fluxgate sensor matches the Overhauser reference very well (rms error 0.6 nT).

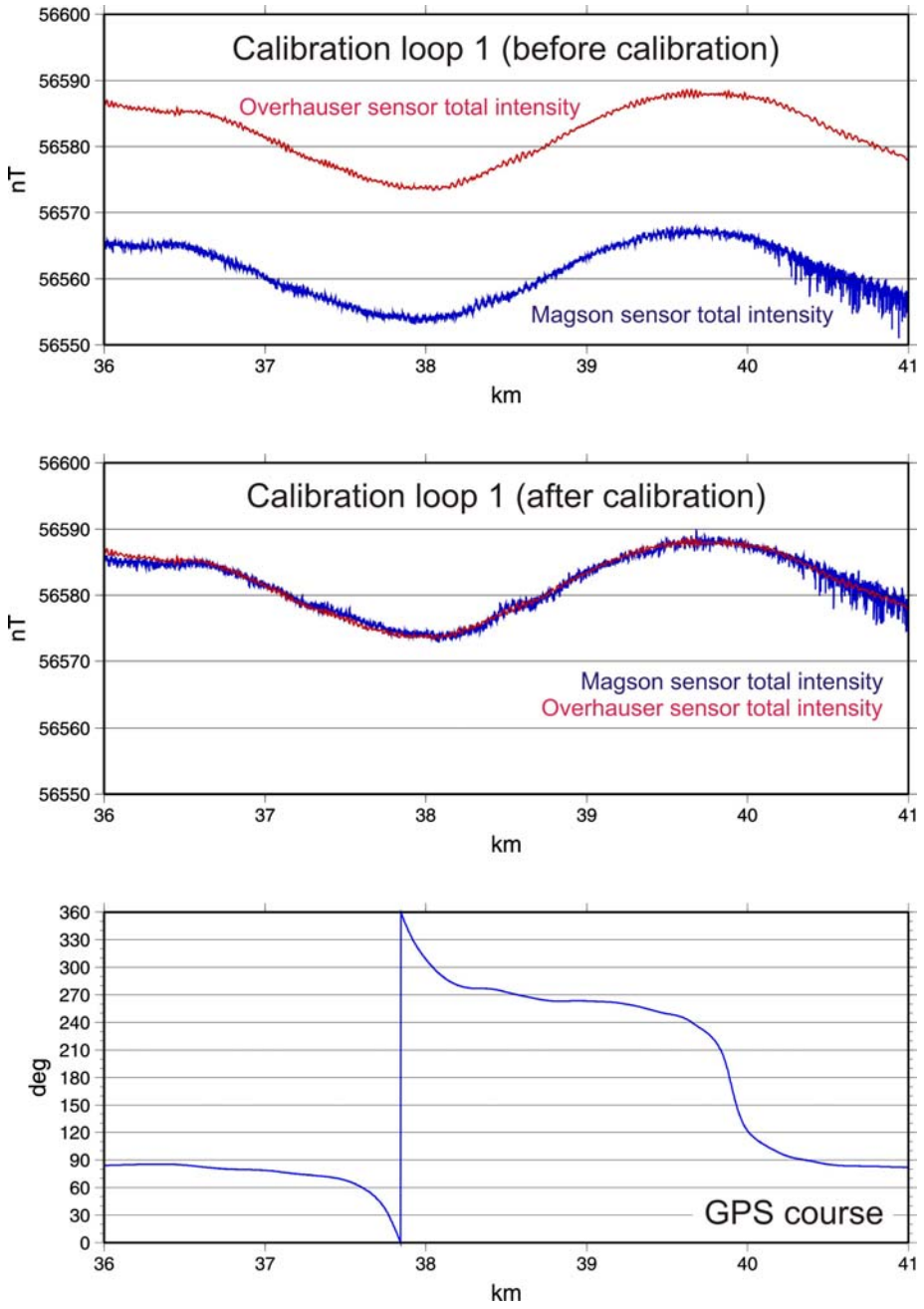

Fig. 9.3: Success of calibration for the fluxgate sensors against the Overhauser reference, demonstrated for a nearly circular loop. From top to bottom: i) only factory calibration applied, ii) additional loop calibration applied, iii) GPS course.

9.3 Preliminary Results

Fig. 9.4 shows the magnetic anomalies for all relevant lines of cruise MSM09/3 as wiggle traces along the profile lines. We have surveyed about 1800 km along all seismic lines and additionally 1300 km with magnetics only. When the data are compared with the magnetic map for the North Atlantic (Fig. 9.5; Verhoef et al., 1996) we see that the general features of the former map are still valid but that the new lines add considerably more detail to the picture, e.g. low amplitude linear features on the N-S-Lines between 68°N and 72 °N.

The measurements and the magnetic investigations concentrated on the deep water parts of the Baffin Bay (profiles BGR08-302, -303C, -308, -311, -312, -316 and -317). Here the question was to identify magnetic lineations (seafloor-spreading anomalies) over the

presumed oceanic crust. Large parts of the southernmost deeper areas of the Baffin Bay between 67°N and 70°N may be underlain by Eocene oceanic crust (Chalmers and Oakey, 2007). The inferred extinct spreading center (broken NW-SE line between 69° and 70°N in Fig. 9.4) for this phase was supposed to be represented by a distinct linear gravity minimum (see chapter 9) about 40 km north of and parallel to line BGR08-309/310 between 60°W and 64°W. North of this spreading segment (north of 70°N) the crust was inferred to belong to an older spreading regime with a different more NW-SE strike direction (broken line between 71° and 72°N). The same might be true for the area at about 68°N.

First interpretation attempts of the magnetic data failed due to a lack of symmetry around the inferred extinct Eocene spreading center. A slightly better indication for symmetry in the magnetic anomaly pattern would be obtained with a spreading center roughly at the location of lines BGR08-309/310. It will be necessary to interpret the magnetic anomalies together with the reflection seismic sections and refraction data in order to identify possible basement features that might be helpful to distinguish between different crustal types and to indentify fracture and fault zones between different spreading regimes. Other features on selected seismic lines and their relation to the magnetic anomalies are discussed only briefly in the following:

BGR08-301: The line crosses the Davis Strait in E-W direction at its most narrow and most shallow location where the water depth is well below one kilometer. The seismic section shows a deep sediment basin below the eastern half of the line and two basement highs separated by a smaller sediment basin under the western part. These features are also reflected in the magnetic anomalies (Fig. 9.4). The eastern part shows distinct but smooth anomalies while in the West high amplitudes of up to 1000 nT exist. This requires that the basement highs contain significant amounts of (basic) volcanic rocks (see also Skaarup et el., 2006). Whether the same rocks also exist below the deep (> 2 km) sediment basin in the East is not clear from the magnetic anomalies. The short smooth interval in the magnetic anomaly at 59.5° to 60°W that seems to correlate to the smaller sediment basin demonstrates the influence of magnetic source layer depth if it is assumed that the basement below this basin is also of volcanic origin. On the other hand, the more shallow areas at the Greenland shelf do not show these extreme amplitudes. According to the reconstructions for the opening time of the Labrador Sea and the Baffin Bay by Skaarup et al. (2006) this might reflect the large northward movement of Greenland since this time. In this model the Cape Dyer volcanics are an equivalent of the Disco volcanic province that now lies app. 300 km further north.

BGR08-319: This line crosses the northern Davis Strait where the water depth is greater. The shallow water areas at the western Baffin Island margin are again marked by high amplitude short wavelength magnetic anomalies. Some basement features seem to correlate to magnetic anomalies, e.g. a distinct (volcanic?) feature that penetrates the seafloor (at 58° W, see also Skaarup et al., 2006) and that might also be an expression of the Ungava fault that separates volcanic North American crust from non-volcanic Greenland crust.

BGR08-310/309 (Reflection seismic profile BGR08-313/315): The western part of this line is obviously oceanic (see discussion above) and the suspected seafloor-spreading anomalies in the middle of the basin are crossed in their strike direction. The western margin close to the Baffin Island shelf again shows large amplitude high frequency magnetic anomalies indicating that the margin still has a volcanic nature.

BGR08-306: This line starts on the oceanic crust of presumed Paleocene age and crosses the wide Greenland margin in the East. Sediments are thick (3 sec TWT) and a step like

feature seems to offset the basement at the western end of the line. It is conceivable that this step represents the boundary between two different oceanic crustal regimes if the fault zone at 64°W would be located a little bit more to the East. The magnetic anomalies including the easternmost part of the line under the continental slope resemble seafloor-spreading anomalies (e.g. C27 to C29) but this might be a pure chance.

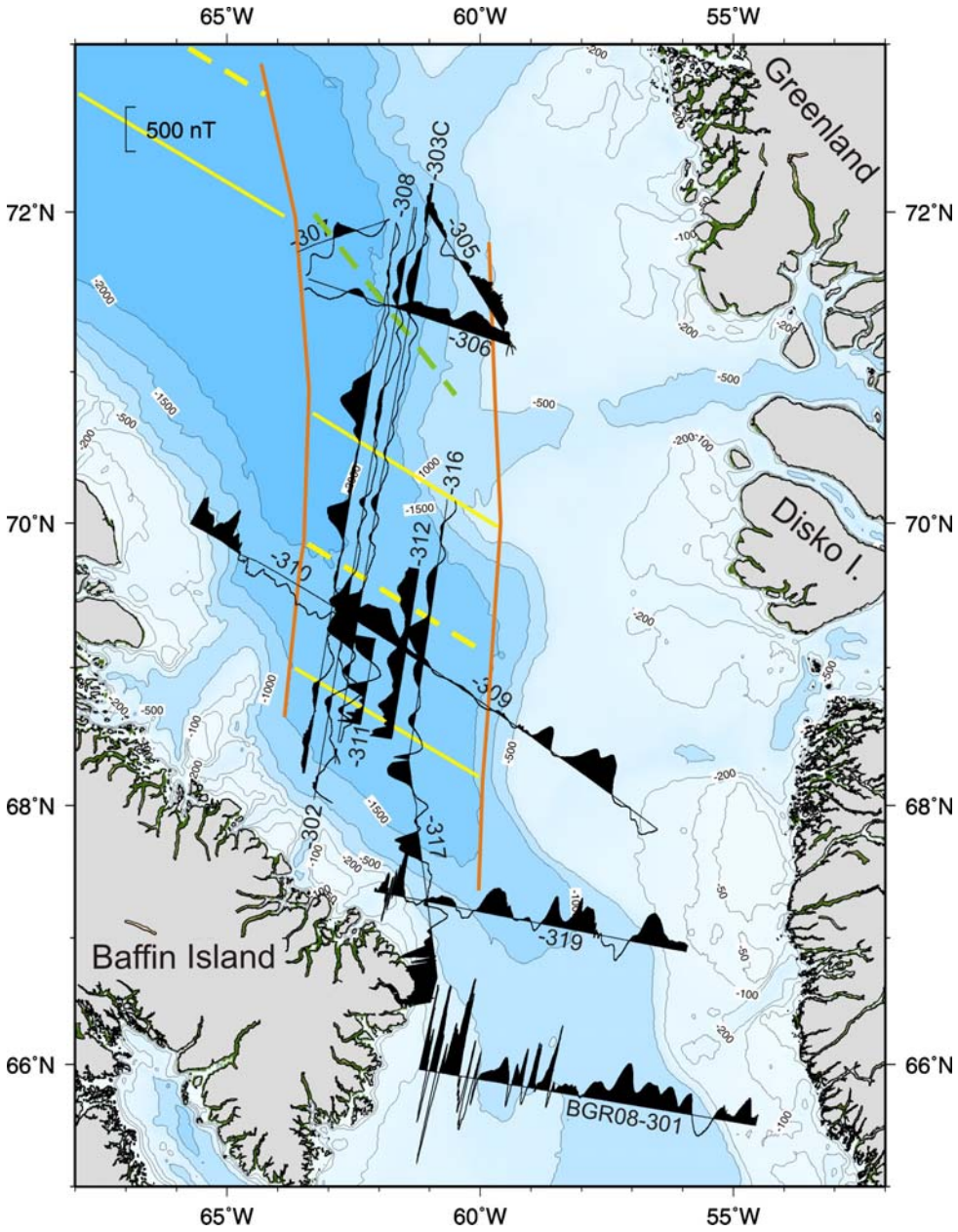

Fig. 9.4. Magnetic anomalies shown as wiggle traces for MSM09/3 profiles in the Davis Strait and the southern Baffin Bay. Positive anomalies filled black, negative anomalies blank. Structural features are from Chalmers and Oakey (2007). Southern broken line: inferred extinct Eocene spreading center and location of a gravity minimum. Northern broken line: possible Paleocene spreading center.

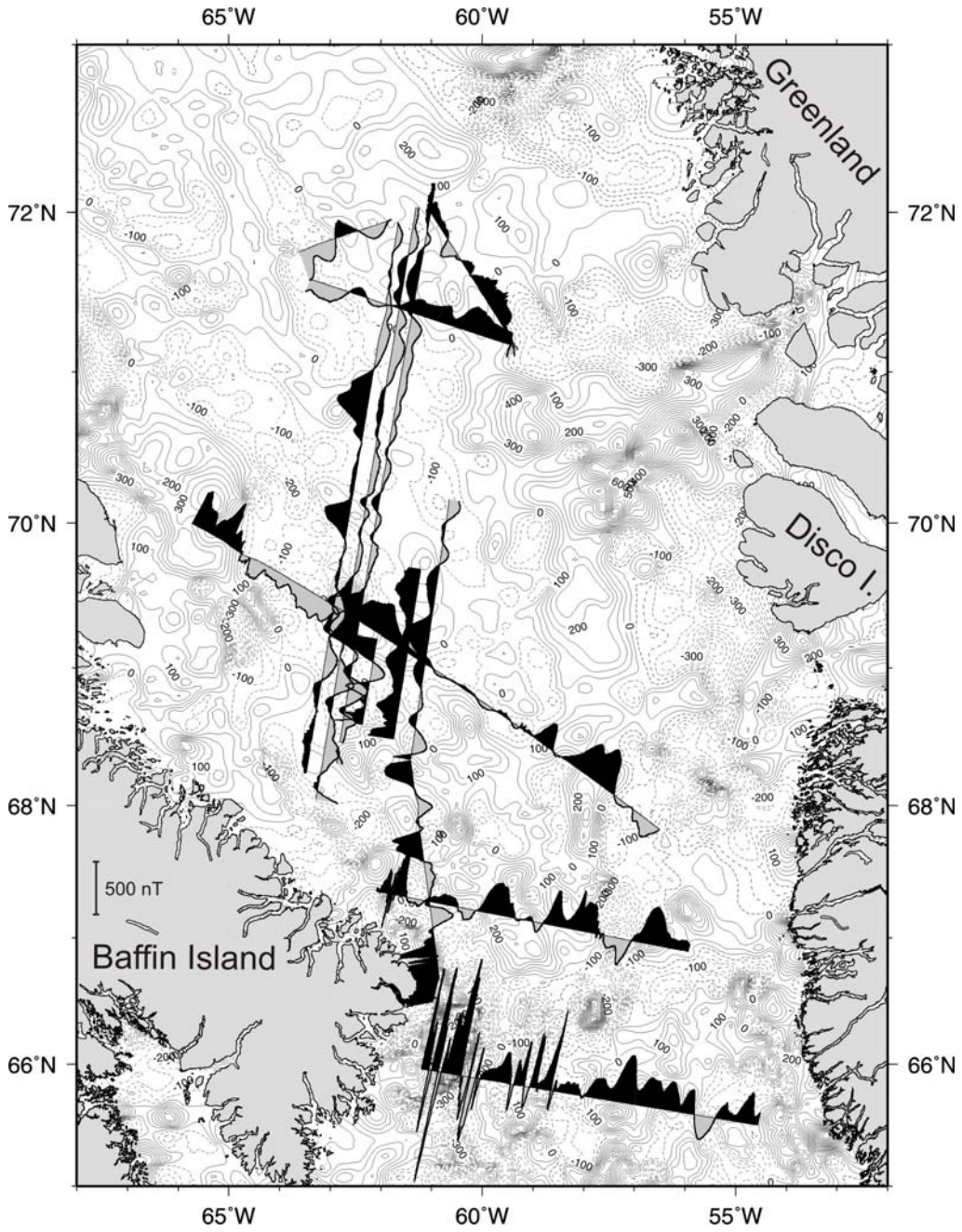

Fig. 9.5. Magnetic anomalies shown as wiggle traces for MSM09/3 profiles in the Davis Strait and the southern Baffin Bay. Positive anomalies filled black, negative anomalies blank. Magnetic contour map is after Verhoef et al. (1996). Positive anomalies continuous contour lines, negative anomalies broken contour lines.

10. Seismics

10.1 Methods

The application of seismic methods was the primary operational objective of MSM09/3 in order to obtain information of the deep structure and the seismic velocity distribution of the crust and the crust-mantle boundaries of Davis Strait and Baffin Bay. (a) We used a standard multi-channel seismic reflection (MCS) technique to image the outline and reflectivity

characteristics of the sedimentary layers and the structure of the sub-sedimentary basement and lower crust by recording the returning near-vertical wavefield. (b) Seismic refraction and wide-angle reflection techniques were used to obtain the distribution of seismic P- and S-wave velocity fields from recordings of large-offset and deeply penetrating refracted and reflected waves using ocean-bottom seismographs (OBS). Figure 10.1 illustrates the principles of both techniques.

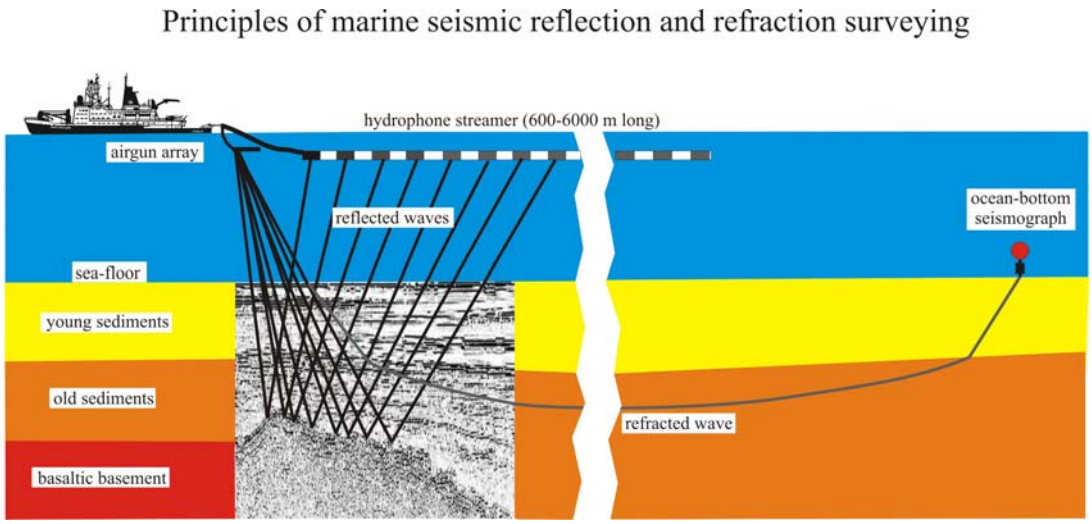

Fig. 10.1 Principles of marine seismic reflection and refraction surveying.

10.2 Seismic Equipment

10.2.1 Air Compressors

(K. Gohl, I. Miller, R. Griffin, U. Schrader)

The required large volumes of highly compressed air must be supplied by seismic air compressors. As a permanent seismic compressor is not installed on RV *Merian*, it was planned to transport the DFG-owned LMF-31 compressor from RV *Meteor* to RV *Merian*. However, due to a major damage of that compressor, the *Meteor/Merian-Leitstelle* rented three compressor containers for MSM09/3: One from the Geological Survey of Denmark and Greenland (GEUS), and two from Airbridge Ltd, a subsiderary of Exploration Electronics Ltd (EEL) in the UK. The technical specifications of the electrically powered compressors are:

EEL: 1 x Hamworthy 425E, air-intake 400 scfm = 11.3 m^3/min, up to 200 bar output, housed in 1 x 20'standard container.
1 x Hamworthy 225E, air-intake 225 scfm = 6.2 m^3/min, up to 200 bar output, housed in 1 x 20' standard container.

GEUS: 2 x Hamworthy 185E, air-intake combined 354 scfm = 10.0 m^3/min, up to 200 bar output, both compressors are housed in 1 x 20' standard container.

All three compressors were installed and serviced by the technicians R. Griffin and I. Miller of EEL. It took considerable additional installation effort on the ship's side to connect the three compressor containers to seawater cooling system, the ship's electric power and the high-pressure output to the airgun stations. Manifolds and other piping/hosing gear had to be fitted in St. John's which caused a departure delay of 16 hours.

In order to supply the full electrical power to all compressors, a containerized diesel generator was hired in St. John's. However, this generator proved to be unreliable. Despite the machine crew's major efforts to make it run, the problem remained which forced the airgun operation pressure to be reduced for most seismic reflection profiles. The generator was discharged from the ship in Sisimiut to be sent back to St. John's.

Fig. 10.2. Manifold for high-pressure air supply from compressors to airgun stations.

10.2.2 Seismic Sources, Triggering and Timing

(U. Schrader, V. Damm, G. Kallaus, Ü. Demir, T. Behrens, D. Pitschmann, A. Schwenk, K. Gohl)

The BGR's G-Gun airgun array was used during MSM09/3. The G-Gun array is subdivided into two sub-arrays with eight guns each (Fig. 10.3). Each sub-array consists of four two-gun clusters. The volumes of the individual guns of the port array are 380 in^3, 250 in^3, 180 in^3 and 100 in^3 whereas in the starboard array volumes of 250 in^3, 200 in^3 120 in^3 and 70 in^3 are used. Each sub-array is equipped with two near field hydrophones. The maximum total volume used was 3,100 in^3 (50.8 l) and the towing depth was 6 m throughout the survey. Each sub-array has a total length of 15 m. The nominal working pressure of the G-Guns is 2,100 psi (145 bar). Triggering and synchronisation was controlled by a SYNTRON GSC-90 system. It is capable to control up to 32 airguns. A detailed description of the shot triggering is given below. The far-field signatures of the G-Gun array and the frequency spectrum are shown in Neben et al. (2003; Cruise report of the BGR03 survey). During the measurements the G-Guns proved to be very reliable. Minor maintenance had to be done on the guns during the cruise. Maintenance was done exclusively during turns.

Along the OBS refraction/wide-angle reflection profiles, two large-volume Bolt 800CT airguns were used in addition to the G-Gun array in order to boost the low frequencies. For geometry of the combined G-Gun and Bolt airgun array, refer to Fig. 10.4 which shows the configuration of the array with respect to the GPS antenna used for the shooting of the

seismic refraction lines. Both Bolt airguns, having a volume of 1953 in^3 (32 l) each, increased the total airgun volume to 7006 in^3 (114.8 l). For synchronization of the G-Guns and Bolt airguns, an external hydrophone was positioned 50 m behind the ship's stern. The optimum firing point was adjusted by displaying the first-break signal of the hydrophone on an oscilloscope. On lines where the streamer was towed, we adjusted the delays by displaying the first-break signals of streamer channel no. 25-30 on the QC system. The fire delays of the Bolt airguns were adjusted to 28 ms to receive the maximum signal from the external hydrophone. Along the OBS profiles AWI-20080500 and 20080600, the Bolt airguns operated only with a maximum working pressure of 80 bars due to an insufficient signal level of 50 V for the shot trigger provided by the GCS90 G-Gun controller. During the data acquisition along OBS line AWI-20080700, an external trigger box Par Air-Gun Firing Circuit FC300 supplying a 300-V trigger level allowed to operate the Bolt airguns with a pressure of 120 bar.

Increasing technical problems with the external power diesel generator caused an unstable supply of high-pressured air for the seismic sources from all four installed external compressors. Thus, the number of operating compressors had to be reduced. Depending on the available compressor capacity, individual guns of the G-Gun array had to be switched off temporarily.

Tab. 10.1 summarises all operation parameters during the MCS and refraction/wide-angle seismic data acquisition. For detail refer to the operation protocols of the MCS data acquisition.

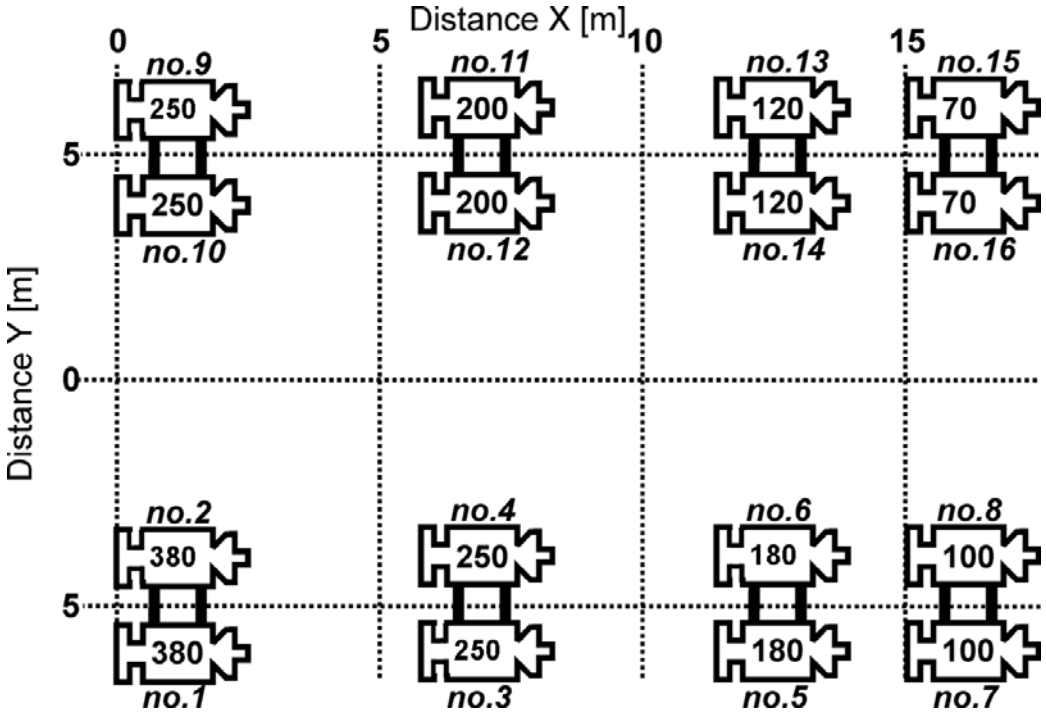

Fig. 10.3. Configuration layout of BGR's port and starboard G-Gun sub-arrays with individual gun volumes indicated in in^3.

MCS profile	Refraction profile	Shot interval [s]	G-Gun array pressure [bar]	Bolt airguns [bar]	Streamer	OBS
BGR08-301		18	100-125		**X**	
BGR08-303	AWI-20080500	60	135	Pt / 70 Sb / out	**X**	**X**
BGR08-303a, -c	AWI-20080500	60	135	Pt / 60 Sb / 75		**X**
BGR08-304		18	100-135		**X**	
BGR08-305		18	125 (without guns 15+16)		**X**	
BGR08-306		18	125 (without guns 15+16)		**X**	
BGR08-313	AWI-20080600	60	145	Pt / 60 (temp.) Sb / 75 (temp.)	**X**	**X**
	AWI-20080600	60	145	Pt / 85 Sb / 80		**X**
BGR08-315	AWI-20080600	60	145	Pt / 85 Sb / 80	**X**	**X**
	AWI-20080700	60	145	Pt / 120 Sb / 120		**X**
BGR08-319		18	130 (without guns 15+16)		**X**	

Tab. 10.1. Airgun operation parameters. Pt and Sb abbreviate Bolt airgun port and starboard deployment sides.

Shot Triggering

The shots were triggered in time intervals of 18 seconds for regular MCS profiling. Thus, the nominal shot distance of 50 m was achieved at a speed of 5.4 knots. In general, the distances were very constant (normally less than 5 m deviation). A constant shot-time interval caused by time or distance triggering at constant speed may result in problems of multiples from previous shots, which prevail CDP sorting and in most severe cases cannot be attenuated through processing procedures such as predictive deconvolution and dynamic correction before stacking. In order to avoid this problem, the time trigger interval was superposed with a random time function of ± 0.3 s. This time span is negligible for the shot distance because a scattering of only about 1 m is generated. As a result, the multiples from previous shots are not aligned after CDP sorting and will be attenuate through stacking.

The shot-time interval with the random function, representing an even distribution, was generated on the Master PC (Fig. 10.2) with an interface card for triggering the airgun array via the SEAL408XL system and the Syntron GCS90 shot trigger device. During shooting along the seismic refraction/wide-angle lines, a shot interval of 60 s was used with randomizing of the time trigger switched off.

Time triggering involves that CDP sorting has to be done by coordinates. To correlate between shot numbers and position, the FFID (Field File Identification) numbers written to cartridge were transmitted to the positioning system.

Soft-start procedure

We applied a soft-start procedure for airgun operation as common best-practise procedure for conducting seismic survey as a measure to mitigate marine mammals. In compliance with the requirements set out by the Bureau of Minerals and Petroleum of Greenland, we applied the following procedure:

1) The ship's surroundings are observed at least 10 minutes before the start of an airgun operation by using binoculars. If whales or seals are observed within a range of 200 m to the ship, the start of airgun operation will be delayed until the range to the mammals exceeds 200 m.
2) In case of absence of marine mammals within the observing range, the airguns are switched on for operation one by one within a period of 20 minutes (soft-start). The start of the next airgun follows in a regular time interval with regard to the used number of airguns in the array until the full airgun array is active after 20 minutes.
3) In case of interruption of airgun operation over more than 5 minutes, the soft-start procedure is again applied at re-start.
4) In case whales or seals are observed within the 200 m range of the ship during airgun operation, the airguns will only be shut down if the animal short signs of discomfort.
5) The soft-start procedures and any observations of whales and seals and their behaviour are documented by the watch-going nautical officer and the observing member of the scientific team.

The software procedures were documented in the seismic observer protocols. Despite our continuous observation of the ship's surrounding by the watch-going nautical officer and members of the scientific team, marine mammals were not observed in the areas of our seismic investigations.

10.2.3 Multi-channel Seismic Reflection (MCS) Recording System

(V. Damm, U. Schrader, G. Kallaus, Ü. Demir, T. Behrens, D. Pitschmann)

BGR's SERCEL SEAL System and a digital hydrophone streamer with an active length of 3,450 m were used for the MCS recording. The recording system, the DigiCOURSE System 3 data acquisition and the streamer control system are interfaced with the Master PC. The system start trigger is generated by the Master PC. Here, the data for the external header, e.g. from the DigiCOURSE System 3, navigation system, GPS-clock, pressure, etc., are received and the external header is generated, stored and sent via an interface to the SEAL system and to the navigation system (Fig. 10.4). The principal configuration of the DigiCOURSE System 3 system is shown in Fig. 10.5.

An OYO GEOSPACE GS642 thermal plotter for paper printouts of single trace plots was in use for quality control.

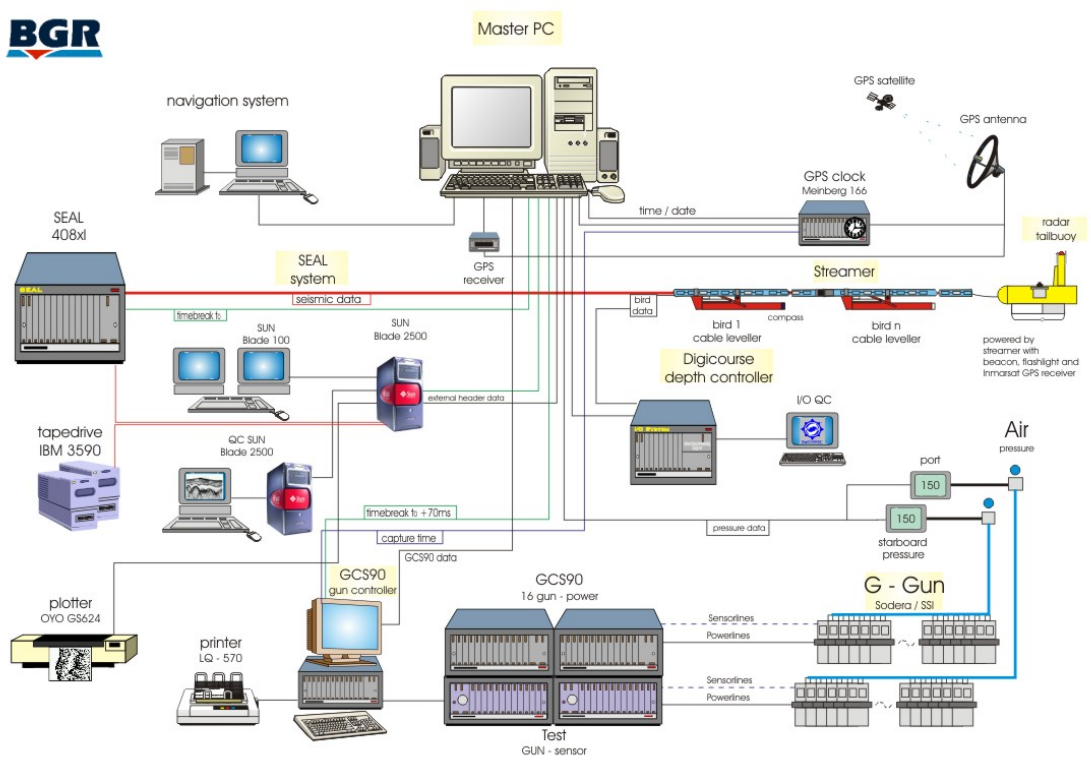

Fig. 10.4. Signal flow diagram for BGR's seismic reflection data acquisition system.

Streamer system

The used the BGR SEAL streamer during MSM09/3 consists of 23 active seismic sections (ALS) with 276 channels in total. It has a flexible architecture with redundant data transmission modes. For instance, data transmission may be reconfigured on line failure. Each channel has an individual 24 bit, Sigma Delta A/D converter. The active streamer sections have a diameter of 50 mm. The SEAL recording system was configured to handle a maximum recording capacity per streamer of 960 channels (@ 12.5 m), a maximum record length of 99s, a maximum number of seismic channels of 20.000 and 60 AUX channels. The sampling rate during the cruise was 2 ms. Record length was 14 s. We operated one SDLT tape drive during the cruise. Data format is 4byte - SEG-D revision 2, demultiplexed 32 bit IEEE, Code 8058.

In order to control the vertical streamer position (depth) and to measure the heading, the DigiCOURSE System 3 system was used. DigiCOURSE System 3 is a hardware and software package that controls and collects data from a network of acoustic sensors and streamer positioning devices. DigiCOURSE System 3 has online command, diagnostic, and performance-monitoring capabilities. A streamer recovery system (SRD-500 of Concord Technologies, Inc.) was implemented to prevent submerging of the streamer deeper than 50 m water-depth in case of emergency. DigiCOURSE System 3 employs a modular architecture which provides for a variety of configurations and levels of functionality. The minimum system equipment configuration includes two real-time processors: an Operator Interface (OI) and a Data Management Unit (DMU), a Line Interface Unit (LIU), and cable-mounted measuring devices, birds and compasses. With few exceptions, depending on the weather and sea conditions, the system stabilised the cable at a depth of 12 m ± 1 m.

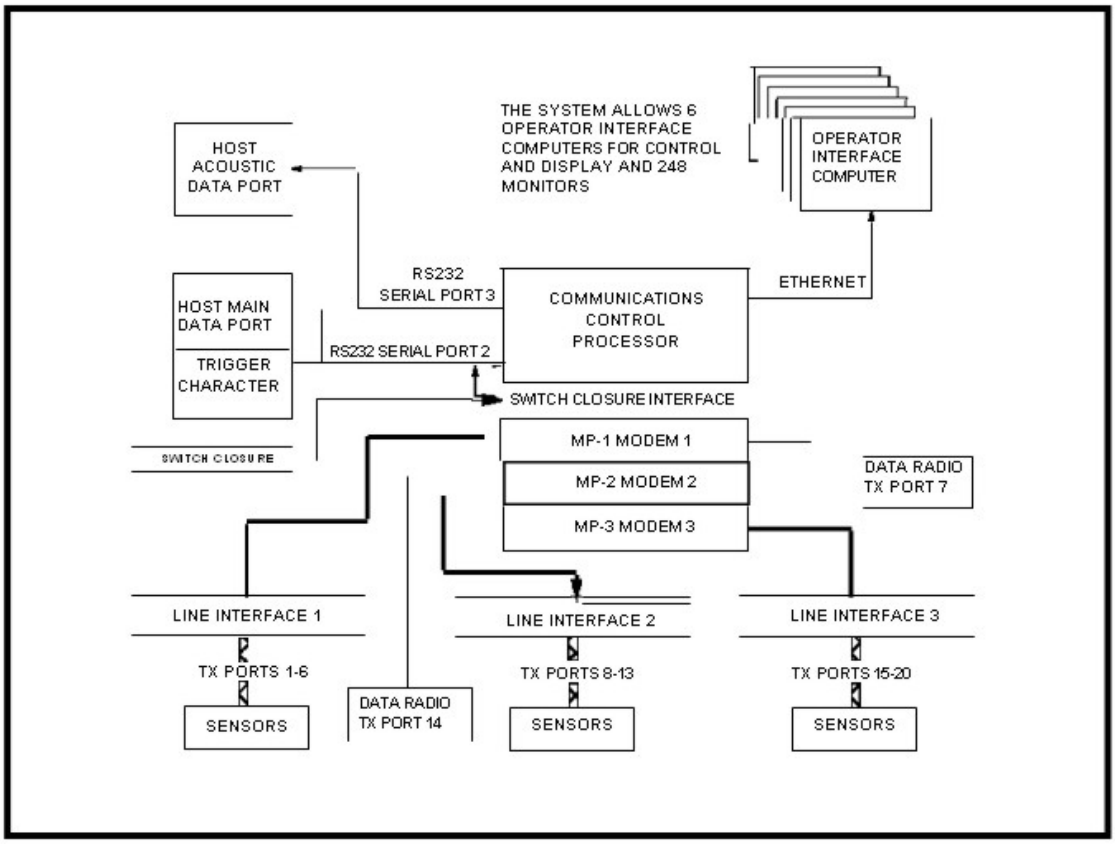

Fig. 10.5. Principal configuration of the DigiCOURSE-3 streamer depth-control System.

Tail buoy system

The radar tail buoy is powered by the streamer and equipped with a radio beacon, flashlight and an Inmarsat GPS receiver.

In-water equipment

The seismic data are amplified, filtered, and analogue-digital converted within the SEAL streamer by using the following main modules installed in the streamer consisting of 23 active line sections(ALS) and 1 LCI, 1 DCXU, 4 LAUM, 1 TAPU, 1 AXCU and 1 HAU. For explanation refer to following list and the streamer configuration overview for the individual seismic lines shown in Fig. 10.4.

ALS Acquisition Line Section

With a length of 150 m, an ALS acquires data from 12 channels with an equal spacing of 12.5 m. Each channel receives data from a group of 16 hydrophones, with a capacity of 256 nF (@ 20°C), a sensitivity of 20 V/bar open circuit, and 17.4 V/bar, with electronics included. An analogue to digital converter FDU (Field Digitizer Unit for 2 channels) with test signal generator is implemented in each Acquisition Line Section (ALS).

HAU Head Auxiliary Unit

The HAU assures power supply for the TLFOI and measures the tensile strength value between the cable and the vessel. During the cruise BGR08 the stress was about 0.9 t.

HESE/HESA Head Elastic Section Extension

2 HESE (a 50 m) and one HESA (Head Elastic Section Adapter – 10 m) were in use between the HAU and the active sections (ALS) to perform the connection between the streamer and the head section. The HESA hosts the waterbreak hydrophone. One SHS, a 6m non-elastic section, was placed between the Lead-In and the HAU.

LAUM Line Acquisition Unit – Marine

Manages data compression, data routing and power supply for the ALSs. As one LAUM covers 60 channels, 4 LAUM and 1 LAUXM were in use during the cruise.

SHS Short Head Section

A non–elastic section between the TLFOI and the HA(P)U. A head buoy can be connected to it.

TAPU Tail Acquisition and Power Unit

Situated at the end of the active streamer the TAPU is made up of one LAUM with common duties and may manage the power supply for the tail buoy. The end of the streamer is made up by a Tail elastic section (TES) and the Tail buoy (TB). The used tail buoy was equipped with satellite position monitoring via internet, radar reflector, radio beacon, and flash light.

Onboard equipment

AXCU Auxiliary Channel Unit

The AXCU box contains FCU2M (Field Digitizer Unit 2 Marine). It is used to convert analogue data coming from the airgun array and the waterbreak -section. Five auxiliary channels (AUX) are recorded (max. 6): Aux1= WB (waterbreak), Aux2=STB1 (hydrophone 1 at starboard gun array), Aux3= STB2, Aux4=BB1 and Aux5 = BB2 (hydrophone 2 at port gun array)

CM408XL Control Module Extra Large

Designed with a modular configuration, the CMXL controls the 240 acquisition channels (max. 10000). It manages via SCSI and Ethernet links the flow of acquired data between the streamer and the recording system (PRM-managed) and peripheral equipment, as tape drives, plotters, navigation and positioning and the QC system. Two CMXL may be used in parallel to increase the maximum channel capacity to 20.000. Within the CM408LX module a Line Controller Interface board (LCI) Board is situated. This interfaces with the master pc shooting system and formats the data to IEEE format

DCXU & LAUXM Deck Cable Cross Unit & Line Acquisition Unit, Cross line – Marine

Assures the connection between the streamer and the Control Module (CMXL). It also links the streamer to the necessary control modules and eventually handles the emergency stop with a warning light installed close to the winch.

PWM & PWMC Power Module & Power Module Controller

Generates a +175/-175 VDC voltage, using two separate rails – called HV1 and HV2 – to supply power to the electronics of the streamer up to 12 km long. Each PWM is linked to a Power Module Controller (PWMC). For a PWM being able to be put ON, either in REMOTE or LOCAL mode, the PWMC must be connected and powered on: an ENABLE signal is send from the PWMC to the PWM. Leakage, overload HV-alarm, emergency stop from the winch will be managed by the PWMC.

HCI Human Computer Interface

The HCI is the control unit for the operator. Script files can be saves to and/or loaded from another computer and a online help is available. A QC software running on a 'SunBlade 150' workstation enables via a permanent graphic display the control of the following functions and settings:

- Operation and function control of the different units (PWMC, PRM, QC) including initialisation and testing of individual modules
- Display of system operation
- Automatic log of observer report data
- Display of power status
- Acquisition sequence controlled by external shooting system
- On line real time signal graphic analyser
- Printout of all parameters

PRM Processing Module

The PRM is a processor software module, installed on a separate workstation 'SunBlade 2500', used for formatting the data to and from the cartridge drive, to the plotter and the SeaProQC system.

SeaProQC Sea Processing Quality Control

With a SeaProQC workstation 'SunBlade 2500' connected directly to the PRM, continuous online seismic data quality control is performed without slowing down the acquisition. Three main windows are used for quality control:

- The History display window with bar graphs shows a summary of errors and source attributes for the successive shots processed by the SeaProQC. It displays the attributes of the data from the previous shots.
- The Normal display window shows the latest incoming SEGD shot record. The traces are displayed in the time/distance range with the noise of each trace on top of the display.
- The Single Trace window shows the data of one selected channel from the streamer. With each new shot the display is updated with the new acquired trace added to the window. Four single trace windows may be opened simultaneously.

Quality control

Quality control during acquisition comprised:

- Continuous control of the airgun pressure.
- Observing the signals of the hydrophones within the arrays and adjusting the trigger delays for an optimum signal.
- Checking and recording the streamer depth and position (heading) every shot via the control screen of the DigiCOURSE System 3 system. These data are stored in the header and written to the field tapes.

- Continuous check whether all sections of the streamer are free of abnormal noise and give about the same signal amplitude. This was done for every shot via the QC Graphics display of the SeaProQC system.
- Continuous observation of the single resp. near trace records.

Fahrt **MERIAN MSM 09/3 (3450m / 276 Spuren)**
Blatt **Fahrtber.1** 23.09. bis 19.10.2008
Profile **BGR-201, 203 (60sec.),**
204 bis 206, 213(60sec.) und 215(60sec.)

													RU1	RUK2 **WB**		
												Lead In (190m)	**SHS** 6m	**HAU**	**HESE** 50m	**HESE** 50m	**HESA** 10m
													1461	193	1431	1435	1653
RUK3	RU4/R1			RUK5/R2				RU6						RUK7/R3			
ALS 1	**ALS 2**	**ALS 3**	**ALS 4**	**ALS 5**	**LAUM**	**ALS 6**	**ALS 7**	**ALS 8**	**ALS 9**	**ALS 10**	**LAUM**	**ALS 11**	**ALS 12**	**ALS 13**		
1 - 12	13 - 24	25 - 36	37 - 48	49 - 60	**1**	61 - 72	73 - 84	85 - 96	97 - 108	109 - 120	**2**	121 - 132	133 - 144	145 - 156		
7030	7029	2175	7027	8630	**451**	8629	7023	7024	7021	8633	**557**	7020	8628	8637		
RU8				RUK9/R4				RU10				RUK11/R5				
ALS 14	**ALS 15**	**LAUM**	**ALS 16**	**ALS 17**	**ALS 18**	**ALS 19**	**ALS 20**	**LAUM**	**ALS 21**	**ALS 22**	**ALS 23**	**TAPU**	**TES**	**STIC**		
157 - 168	169 - 180	**3**	181 - 192	193 - 204	205 - 216	217 - 228	229 - 240	**4**	241 - 252	253 - 264	265 - 276		50m	25m		
8617	8634	**480**	8636	7016	7012	7015	8638	**1710**	8635	8631	8627	**186**	1474	1438		

Gesamtlänge: 3730m

TS
4092

		S/N	
130m	RU1 :	36914	
180m	RUK2 :	36056	
340m	RUK3 :	36194	
490m	RU4 :	36274	Recovery
940m	RUK5 :	42778	Recovery
1390m	RU6 :	36521	
1840m	RUK7 :	36878	Recovery
2290m	RU8 :	36707	
2740m	RUK9 :	42461	Recovery
3140m	RU10 :	37821	
3640m	RUK11 :	42487	Recovery

BGR

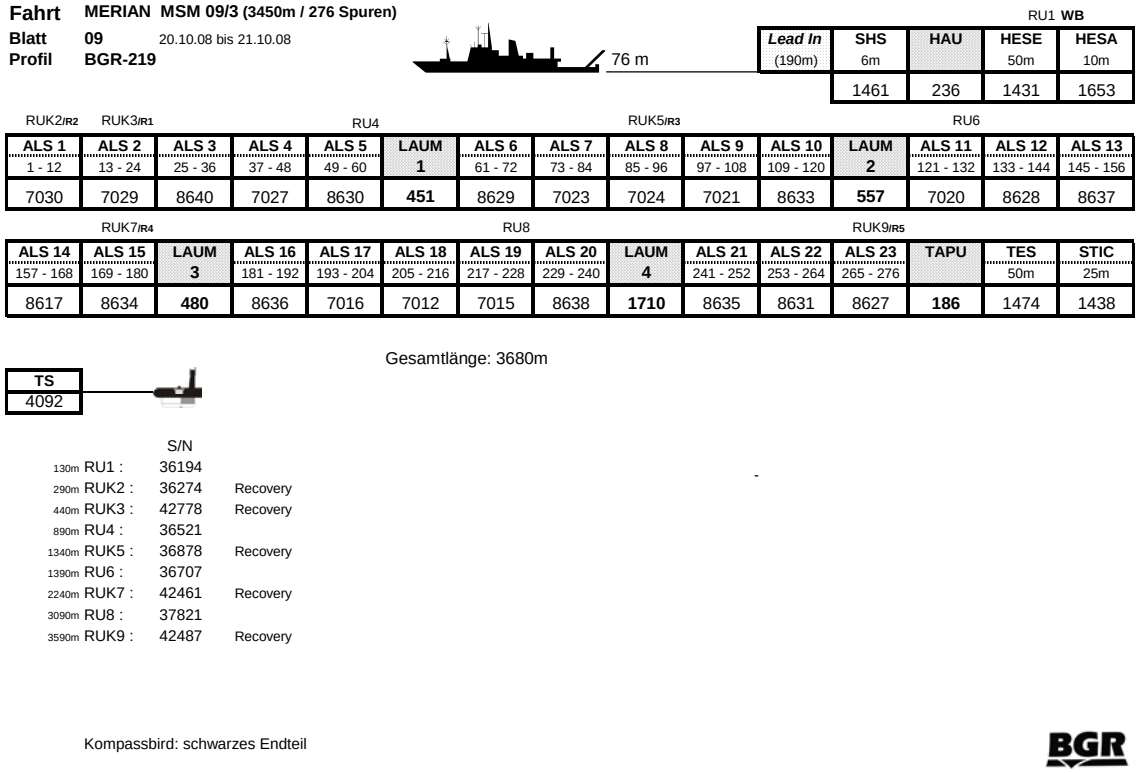

Fig. 10.6. Configurations of seismic SEAL streamer for MCS data acquisition during MSM09/3.

10.2.4 Ocean-bottom Seismometers (OBS)

(A. Schwenk, M. Fink, H. Kraft, T. Funck, A. Schlömer, M. Ruhnau, J. Gerlings, J. Sobiech, K. Gohl)

The GEOMAR-type OBS systems consist of syntactic foam floats mounted on a steel frame together with the data logger and batteries in a pressure cylinder, an acoustic release, a seismometer, a hydrophone, a radio beacon, a xenon flash light and a flag (Fig. 10.7). The system is tightly connected to an anchor frame via the acoustic releaser. The pressure cylinder contains the Marine Broadband Seismic Recorder (MBS) or a Marine Longtime Seismocorder (MLS) data logger manufactured by SEND GmbH and a pack of 48 alkali batteries. The acoustic/time release unit KUMQuat 562 is attached to the frame with the corresponding clamp and to the anchor frame hook through a hook and the releaser latch. The 3-component Mark (4.5 s natural period) seismometer is mounted to the frame. A clamp bolt is screwed tightly against the seismometer to achieve a good coupling to the anchor frame. The hydrophones are of type HighTech (HTI) or E-2PD by OAS and are attached to the steel frame. The acoustic release communicates via the K/MT 8011M deck unit.

Fig. 10.7. Deployment of OBS system.

The recording parameters are set via the Linux program SENDCOM3 which also controls the time synchronisation of the internal clock with the external GPS clock (Motorola M12 Plus Oncore). For all three profiles, the sampling frequency on all channels was set to 250 Hz for the MBS and to 200 Hz for the MLS recorders. The gain was set to 5 for the hydrophone channel and to 13 for the three seismometer channels, respectively. The data were stored on 1 or 2 GB MicroDrive PCMCIA cards of the MBS or MLS recorders.

For detailed description of the components of the OBS systems, refer to the manuals by SEND GmbH.

OBS deployments and recoveries were conducted without major problems. However, a number of xenon flashers and radio beacons did not operate when the OBS systems returned to the surface. Some of these started to operate with a delay of several minutes or even much later back in the lab. This malfunctioning may be related to the cold water temperatures (0.5-2.0°C) at the surface which prevents or delays the pressure switch to turn on.

10.3 Processing of Multi-channel Reflection Data

(V. Damm)

Seismic data processing was done using a Linux workstation with ProMAX™ 2D, Version 2003.12.1 licenses. The workstation (Fig. 10.8) has two Intel Xeon CPUs (2.8 GHz) with 512 kB cache size, an internal memory of 3.6 GB and a 120 GB internal disk. The operating system is RedHat Linux WS 3.0. A raid disk array with 2400 GB disk space is accessible from both workstations. Both workstations make use of the raid system for storage of seismic data, the database and job flows. One ½" S-DLT drive is connected for data loading and

archiving. The raid disk array was connected to workstation b3lx01 and mounted (NFS) on workstation b3lx02. Onboard processing was done for all acquired MCS data and consisted of the 4 steps geometry setup, data and geometry input, prestack processing to enhance signal quality and data stacking.

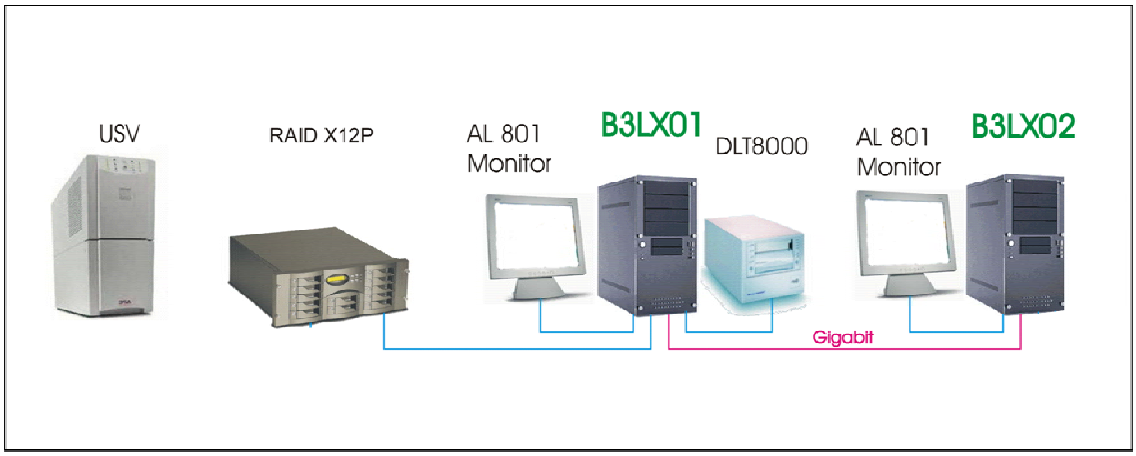

Fig. 10.8. Hardware setup scheme for seismic PROMAX processing software.

Geometry setup

The geometry of the source and the receivers was set up in relation to the GPS antenna position (Fig. 10.9). The active streamer length was set to 3437.5m / 276 channels for all lines listed in table Streamer configurations.doc (BGR08-301, BGR08-304, BGR08-305, BGR08-306, BGR08-313, BGR08-315). In ProMAX the 2D Marine Geometry Spreadsheet was used. It includes the following steps which have to be carried out in the geometry setup sequence:

File. UKOAA Import: The navigation data were transformed by the navigation group into rectangular UTM coordinates and saved in the format "STANDARD UKOOA 90 Marine 2D".

Setup: For lines BGR08-301, BGR08-304, BGR08-305, BGR08-306, and BGR08-319 the following parameters were valid: 12.5 m nominal receiver spacing, 50 m nominal station interval, 6 m nominal source depth and 12 m receiver depth. Lines BGR08-313 and BGR08-315 were acquired in combination with the seismic refraction lines AWI-20080500 and AWI-20080600 with shot intervals of 60 seconds. The nominal source station interval therefore increased to 162.5 m at about 5 kn. All units are given in meters.

Sources: The following columns in the spreadsheet have to be filled using the "Edit" option: "Source" and "Station", beginning with 1 and incrementing with 1. The streamer azimuth has to be calculated using "auto azimuth". The algorithm used for this by ProMAX is very crude. It is based only on the first and last source point, the calculated azimuth is assigned to all source positions. The column "Src Pattern" has to be filled with the number of the pattern defined in the next step. Shotpoint interval and error were checked by the QC tool.

Patterns: The streamer and source pattern has to be defined according to the spreadsheet in Fig. 10.6.

Bin: The binning consists of three steps:

1) Assign Midpoint.
2) Binning. Source station tie to CDP number: 1; CDP Number tie to source station: 10000. This tie fulfils approximately BGRs standard for CDP numbering: The first

station with full coverage is tied approximately to CDP 10000. Distance between CDPs: 6.25. This implies a nominal CDP coverage of 37 (for 276 channels) in case of a shot increment of 50 m (shot interval 18 s) and drops down to 10 in case of a shot increment of 162.5 m (shot interval 60 s during combined reflection and refraction seismic lines). Binning was done for CDP locations and receivers. In case of lines BGR08-313 and BGR08-315 acquired with shot intervals of 60 s an alternative binning with 25 m CDP spacing was done.

3) Finalize Database.

TraceQC: Quality control of the binning. Here two checks are undertaken:

a. Checking the computed offsets with the offsets given in the streamer plan by comparing the values for the last hydrophone group (channel 276) and nearest hydrophone group (channel 1).

b. Checking if the source and receiver locations (in UTM coordinates) are behind the vessel in relation to the sense of direction.

A further quality control was done by using the graphical display tools of the database application:

1. CDP fold map (View => Predefined => CDP fold map). X_COORD and Y_COORD – Axes; FOLD: Color coded and as histogram.
2. CDP fold table (Tabular => CDP): List of CDP Number, FOLD, X_COORD and Y_COORD.

Cruise: MSM 09-3
Lines: BGR08-201, BGR08-204, BGR08-205, BGR08-206, BGR08-213, BGR08-215

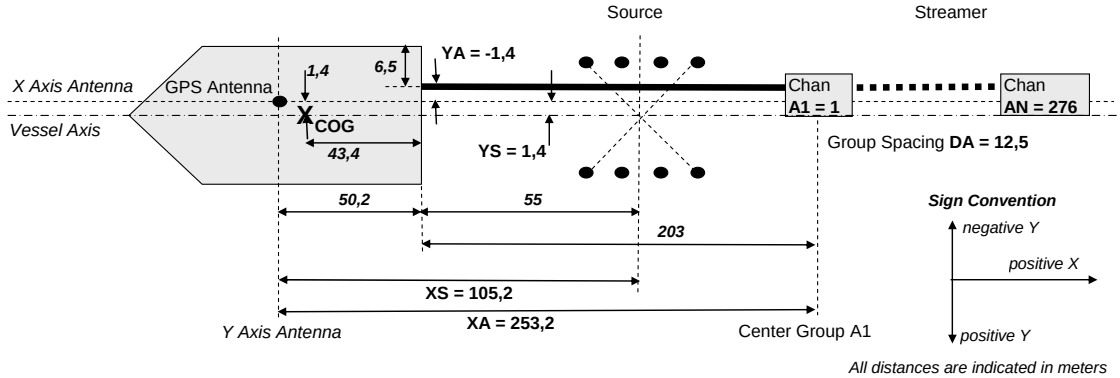

Patterns Spreadsheet for 2D Marine Geometry Assignment in ProMAX

Mark Block	Min Chan	Max Chan	Chan Inc	Src Pattern	Grp Int	X Offset	Y Offset	
1	**A1 = 1**	**AN = 276**	**1** *)		**DA = 12,5**	**XA = 253,2**	**YA = -1,4**	*Streamer Pattern*
M+1				1 **)		**XS = 105,2**	**YS = 1,4**	*Source Pattern*

*) *-1 if A1 > AN, 1 if A1 < AN* **) *The Src Pattern number was used as input in the SIN Ordered Parameter File*

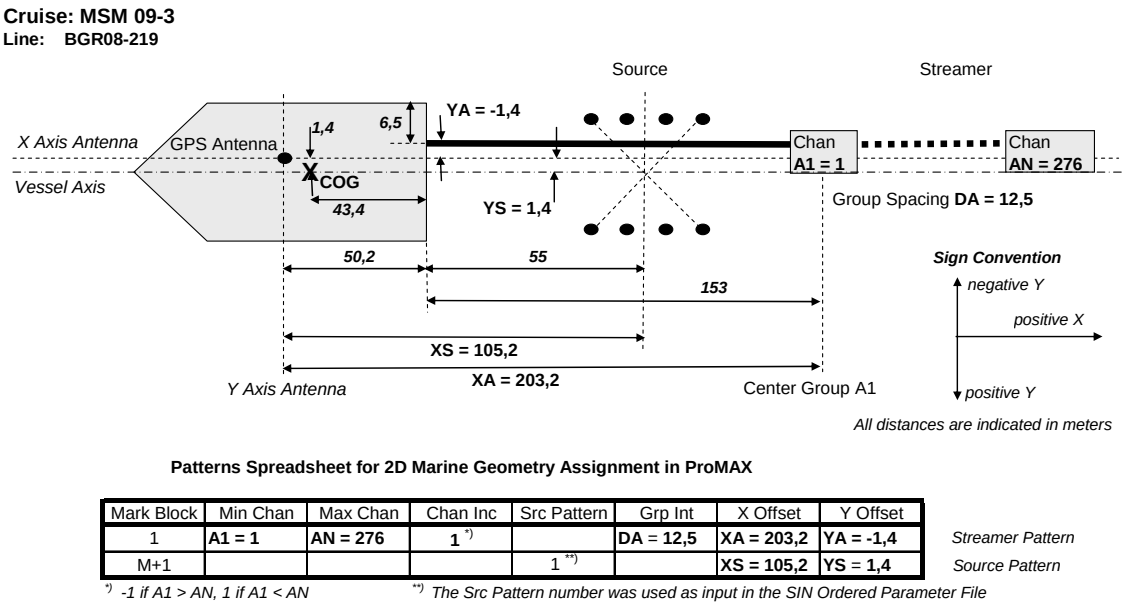

Patterns Spreadsheet for 2D Marine Geometry Assignment in ProMAX

Mark Block	Min Chan	Max Chan	Chan Inc	Src Pattern	Grp Int	X Offset	Y Offset	
1	**A1 = 1**	**AN = 276**	**1** *)		**DA = 12,5**	**XA = 203,2**	**YA = -1,4**	*Streamer Pattern*
M+1				1 **)		**XS = 105,2**	**YS = 1,4**	*Source Pattern*

*) *-1 if A1 > AN, 1 if A1 < AN* **) *The Src Pattern number was used as input in the SIN Ordered Parameter File*

Fig. 10.9. Acquisition geometries for the seismic reflection lines including ProMAX spreadsheets for definition of streamer and source pattern. Top: BGR08-301, BGR08-304, BGR08-305, BGR08-306, BGR08-313 and BGR08-315. Bottom: BGR08-319.

SEG-D input from tape and geometry application

Data were loaded from DLT tapes using the ProMAX module SEG-D Input (reading S-DLT tape). The shot-ordered data consists of 276 data channels and 5 auxiliary channels sampled at 2 ms with a recording length of 14000 ms. The auxiliary channels record data from the waterbreak hydrophone and four near field hydrophones, two inside the starboard airgun array and two inside the port side airgun array. With the "Display ensemble information" set to Yes a summary of all imported shot is written to the log-file. This is helpful in case that there are problems during acquisition and the FFID does not resemble the correct shotpoint. In case that there are FFIDs duplicated on the tape the data may be read in SOURCE order with the unwanted FFIDs excluded (e.g. 1-1249, 1251-2400).

Resampling (Resample/Desample)

The seismic data has been acquired at 2 ms sampling rate. To speed up the onboard processing, the data has been resampled to 4 ms applying a high-fidelity anti-alias filter.

SOD time correction (Header Statics)

The Sercel acquisition system starts registration 120 ms before triggering of the airguns occurs. This time delay has been verified on the auxiliary channel containing the signal from the waterbreak hydrophone at AUX CHAN -1 and on the direct water wave on the groups near to the source.

Geometry Apply (Inline Geometry Header Load)

With this ProMAX module, the geometry information from the database were written into the trace headers.

Finally, the *Trace Header Math* module inserted an entry for the line number header word.

The altered data was written to hard disk as new prestack data set (*Disk Data Output*).

Prestack processing

Bad Trace Editing

The shot gathers were checked for bad traces. If present, these can be killed and thus been excluded from further processing. Anyway, the data recorded was of very good quality with no bad traces, which had to be deleted.

Bandpass Filter

After the examination of the Interactive spectral analysis a zero-phase Ormsby bandpass filter of 5-10-95-150 Hz was applied to the data.

Prestack Deconvolution

In order to reduce ringing within the dataset and to shorten the seismic wavelet, a prestack predictive deconvolution was applied to the FFID shot records.

A deconvolution design gates was picked along the seismic section. The gate was picked within the uppermost part of the sediments, excluding the seafloor reflection.which had to be adjusted according to the seafloor and subsurface morphology.

Fig. 10.10 shows an exemplary shot gather with picked decon design gates. The deconvolution design gates were picked on shot gathers.

A predictive deconvolution with an operator length of 128ms was applied to the gates and a prediction length of 40ms, too. White noise level was 0.1.

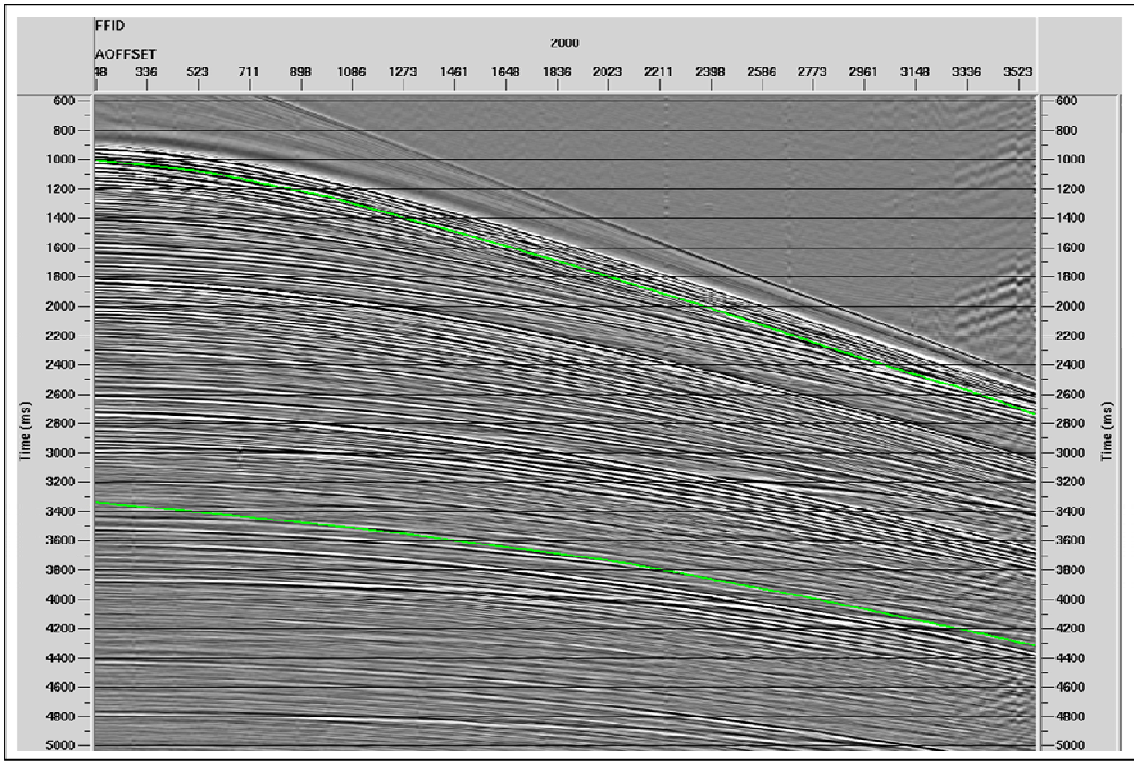

Fig. 10.10. Example for the application of a deconvolution filter to a CDP supergather showing a shot gather with picked decon design gates.

Velocity analysis

Velocities were picked at regular in intervals between 100 and 500 CDPs depending on the CDP spacing (6.25/25 m). Velocity analysis and QC were done in several work flows.

1. Picking of velocity analysis stations. The spacing between individual velocity stations was adjusted to the varying to seafloor morphology and used cdp interval.
2. Sorting into supergathers (a supergather consists of 5-7 CDPs) and calculation of semblance values and CVS panels (*Velocity Analysis Precompute*).
3. Interactive *Velocity Analysis* using semblance velocity spectrum, animated reflection hyperbolas and constant velocity stack panels (CVS).
4. QC and smoothing the velocity field with *Velocity Viewer/Point Editor*.
5. Optional QC with *Volume Viewer* in interaction with *Velocity Analysis*. The *Volume Viewer* displays a poststack section with a colour coded velocity field in the background. Velocity stations and picks are shown on the section and could interact with the *Velocity Analysis*.

The ProMAX velocity picking module included a semblance display with an interval velocity graph, a CDP supergather which could have NMO applied instantly, a series of constant velocity stack panels, and a dynamic stack panel.

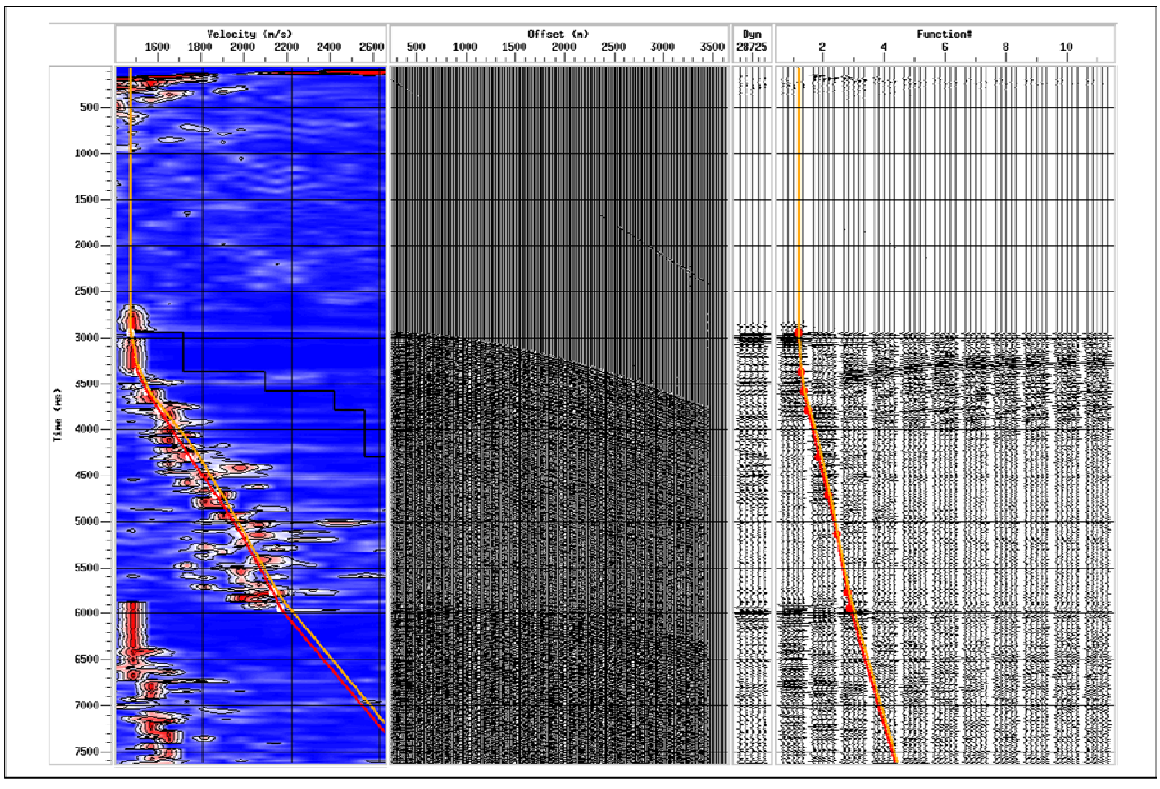

Fig. 10.11. Example of a velocity analysis applied to a CDP supergather.

Fig. 10.11 shows an exemplary velocity station. Velocities were picked by examining the information of the semblance spectrum (left panel), supergather CDP (center, left), dynamic stack (center, right) and constant velocity stacks (right panel). For improving the signal to noise ratio, supergathers were formed by combining 5-7 adjacent CDP gathers, and these

CDP gathers also made up the stack panels. Amplitudes were corrected roughly by using True Amplitude Recovery with manually given TAR velocity function (e.g. 0-1500, 9000-4000, 14000-5500).

To speed up the on screen velocity picking procedure, the velocity analysis displays were pre-computed. After velocity picking, velocities were viewed and QC'd on screen using the ProMAX velocity viewer module. This module was most useful for editing any unreasonable velocity picks and finally to smooth the velocity field for the further processing.

Water-bottom multiple suppression

Depending on water depth multiple reflections mask the primary reflections. Multiple reflection attenuation was done on all seismic sections with *Radon Velocity Filter*. The *Radon Velocity Filter* was applied to CDP gathers after NMO correction. As multiple reflections do have an approximately parabolic move-out after NMO they can be imaged in the tau-P domain. The filter will reject all data within a certain velocity bandwidth around the picked velocities (-15%, +20%). The other data will be treated as multiple energy and re-transformed into x-t domain and subtracted from the input CDP gather. Because this technique models and subtracts the multiple energy, the near offset traces should be attenuated in the same manner as far offsets. The Radon Velocity Filter partly worked well, however, it did not in the very shallow areas with less velocity discrepancy between multiple and primary

Stacking

The prestack CDP gathers have already been NMO corrected during the previous multiple suppression. A true amplitude recovery has been applied to compensate for spherical divergence ($1/(time*vel^2)$) prior to stacking. After stacking (mean stack) the traces in the CDP gathers, the stacked section was written to disk. For quality control, an unstacked single trace section was archived without multiple suppression.

Onboard processing of MSM09/3 MCS data							
Line	Shot Nos.	CDP Min/Max	UTM X	UTM Y	Length km	Processing Status	Comment
BGR08-301	6227	9713 59473	614842 308955	7266754 7322972	307.94	stack	6.25 m CDP interval
BGR08-304	9253	9713 83239	248664 362493	7551833 7997057	455.89	stack	6.25 m CDP interval
BGR08-305	2316	9713 28565	359595 417362	7997267 7894573	115.64	stack	6.25 m CDP interval
BGR08-306	3176	9713 34749	418880 274252	7895544 7955278	153.99	stack	6.25 m CDP interval
BGR08-313	1656	9928 20720	162669 377027	7793716 7629887	266.76	stack	25 m CDP interval; 60 s shot interval
BGR08-315	853	9928 15575	418211 524066	7613872 7520281	139.02	velocity analysis	25 m CDP interval; 60 s shot interval
BGR08-319	5555	9713 53553	548652 281566	7419190 7480260	271.05	stack	6.25 m CDP interval

Tab. 10.2. Summary of onboard processing of seismic reflection data.

In total 1710.3 line km of MCS data were acquired along 6 individual lines, including the 2 profiles (BGR08-313, -315) which were shot in combination with refraction seismic data acquisition based on a 60 s shot interval. Tab. 10.2 summarizes basic data of multi-channel seismic data acquired during MSM09-3 which were used during onboard processing.

An example for signal enhancement and effective multiple suppression, using the above described processing flow, is shown in Fig. 10.12.

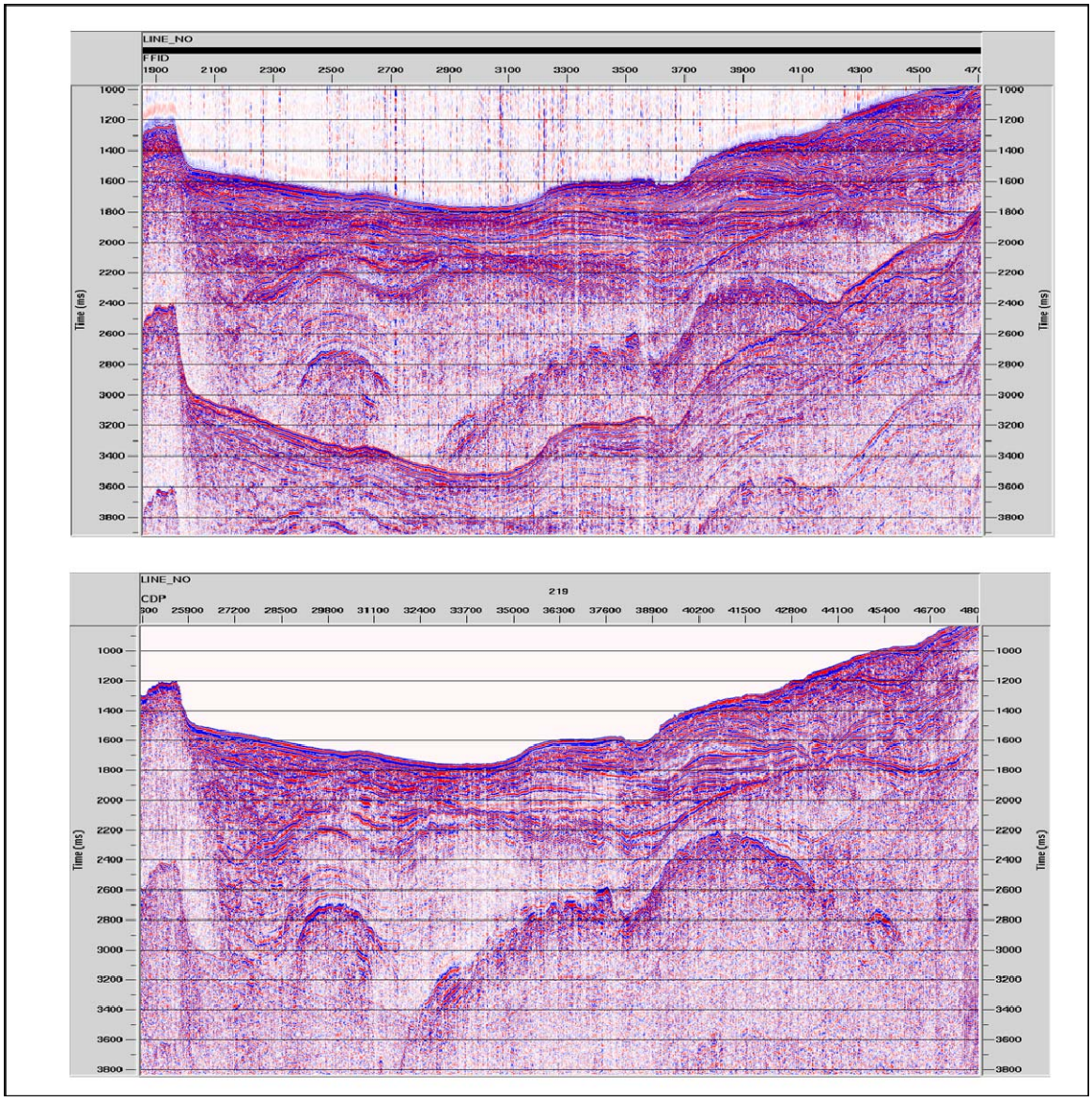

Fig. 10.12. Comparison between a brute stack (top) and a final stack after a careful velocity analysis has been applied (bottom) to the seismic reflection data of line BGR08-319.

10.4 Preliminary Results of Multi-channel Reflection Data

(V. Damm, K. Gohl)

Fig. 3.2 gives an overview of the position of all MCS lines acquired during MSM09/3. The following description of seismic profiles is based on the interpreted crustal types and distribution of volcanics and major faults in the area given by Chalmers & Pulvertraft (2001), Skaarup et al. (2006) and Oakey (2005), non-regarding the still unsolved questions of the

existence of continental or oceanic crust and their age or stratigraphy. These topics are addressed to the subsequent data processing and combined interpretation of all new geophysical data.

10.4.1 Profile BGR08-301

This line runs E-W at around parallel 66°N crossing the Davis Strait from the Greenland coast to about 30 nm off the Canadian coastline. The easternmost end of the line crosses or is close to the exploration wells Nukik-1 and Nukik-2 respectively. The total length of the line is 308 km. Stacked MCS data for the line are shown in Fig. 10.13. BGR08-301 starts at the Greenland side in relatively shallow water depth over continental basement of high reflectivity. In the central part of the line the Ungava Fault Zone is perpendicularly crossed which cuts trough a basement high, the Davis Strait High, a complex feature probably thrusted Archean continental basement and Paleogene volcanic rocks (Oakey, 2001). West of this basement high a sedimentary basin of limited extend and depth followed by volcanic layers of very strong reflectivity. Seaward dipping reflectors, which have been identified in this area by Skaarup et al. (2006) could not be imaged based on the current processing status of the line. Most prominent feature in the eastern part of the line is a 120 km wide sedimentary basin of probably Mesozoic/Cenozoic age with well stratified and undisturbed layering down to a depth of 4 s TWT. Between CDP22000 and CDP 27000 a high amplitude reflector at 3 s TWT may point to hydrocarbon accumulations (Fig. 10.13, lower panel).

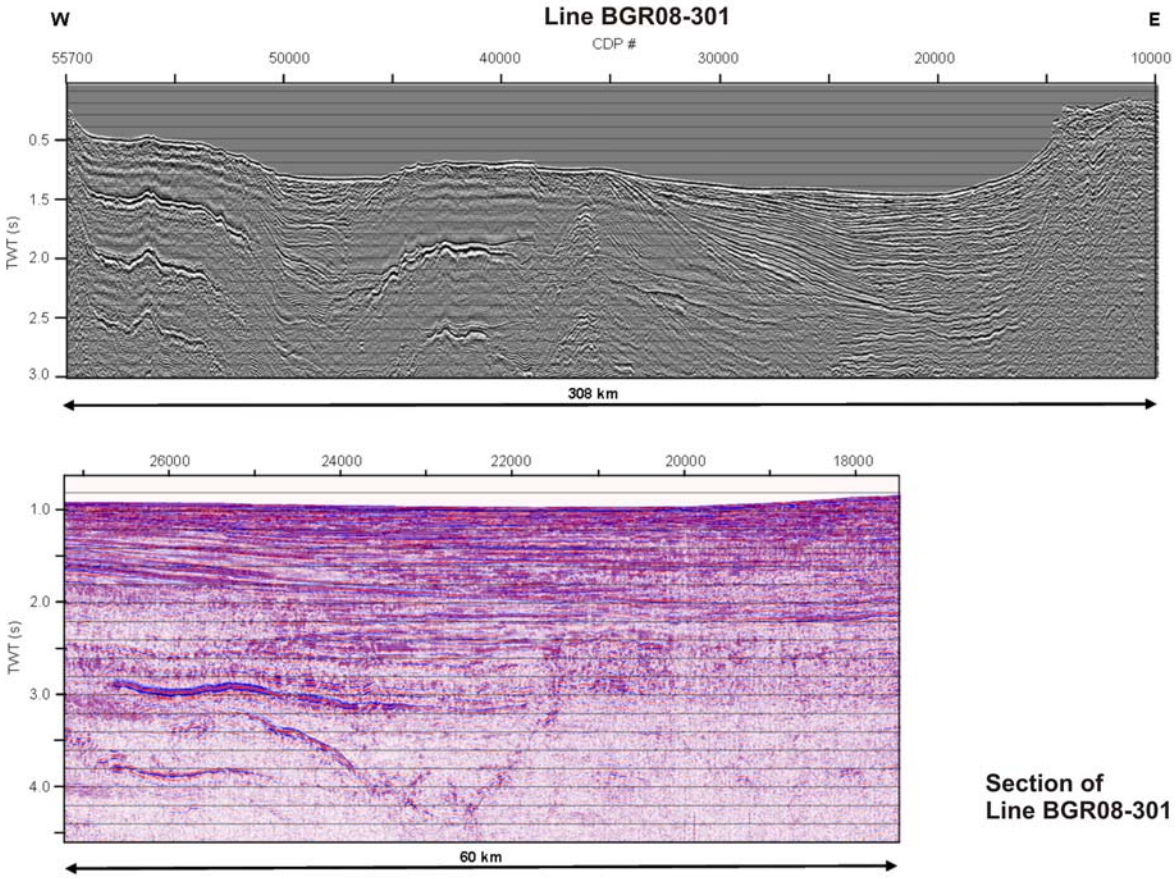

Fig. 10.13. Stacked seismic line BGR08-301. See Fig. 3.2 for location.

10.4.2 Profile BGR08-304

The location of line BGR08-304 is identical with that of the seismic refraction/wide-angle reflection line AWI-20080500 which runs from around 30 nm northwest of Cape Dyer for 456 km northwards into the centre of the Baffin Bay. The southernmost tip of the MCS line (Fig. 10.14) is characterised by highly attenuated continental crust/basement which is not well defined overlain by sediments. With increasing water depth the sedimentary layers rapidly increase and the basement structures drop down over the first 60 km to 5 s TWT. An individual basement high at 4.2 s TWT can be located at CDP 18000. As depth to basement further increases to the north the sediment thickness in the central part of the basin culminates and is at least 3 s TWT. The northernmost part of the line is characterised by two dominant features (Fig. 10.14, lower panel). The first is an overthrusting of sediments between CDP 64000 and CDP 68000 with a thrust front dipping to the south. A second dominant feature on this panel representing the northernmost part of the line is a basement high with a continuous and moderate linear slope to the south, but a sharp and steep flank to the north. This volcanic basement belongs to the Disko Volcanic Province of Cretaceous basaltic rocks, which builds up a significant part of the Greenland continental margin in this area.

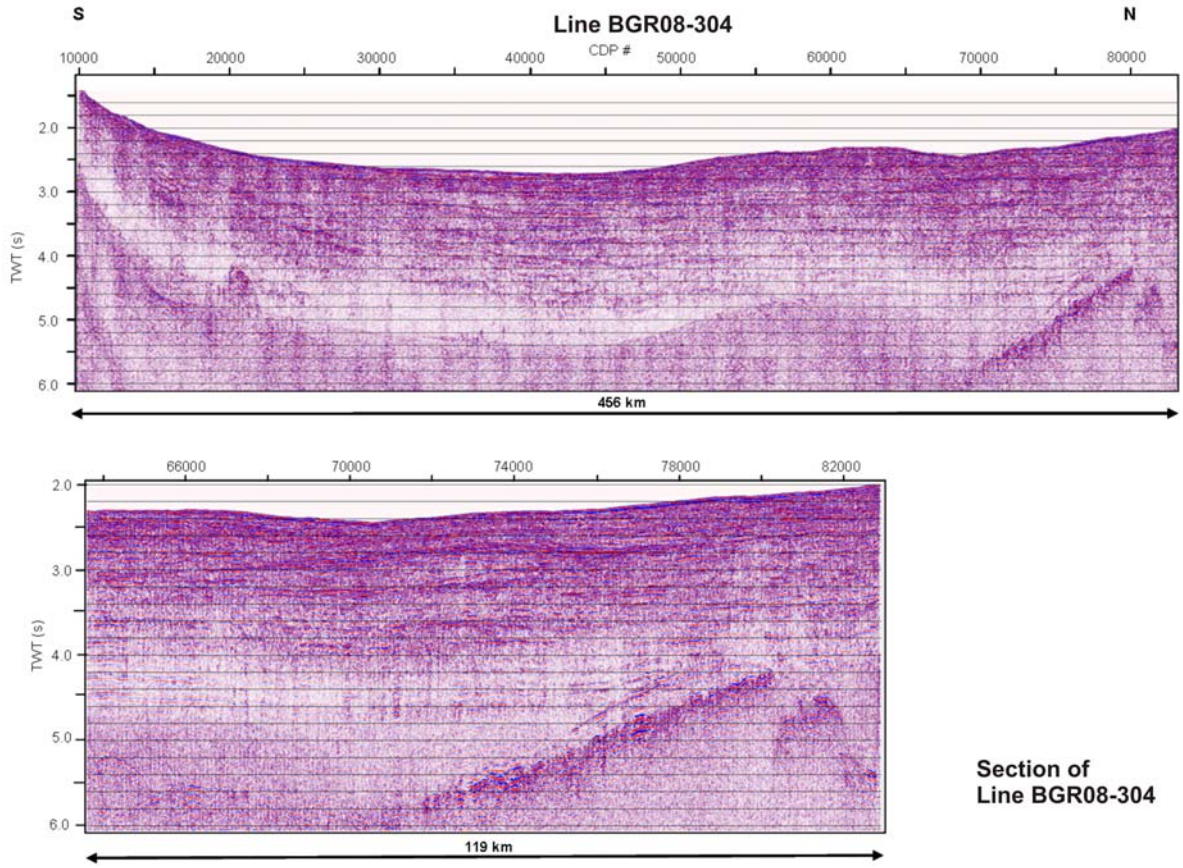

Fig. 10.14. Stacked seismic line BGR08-304. See Fig. 3.2 for location.

10.4.3 Profile BGR08-305/-306

Both lines are located in the central Baffin Bay, with BGR08-305 (Fig. 10.15, upper panel) running N-S for 116 km almost parallel to the Greenland continental margin and BGR08-306 (Fig. 10.15, lower panel) 154 km E-W and crossing line BGR08-304 in its northern part. Most prominent features on both lines are the prograding sediment structures towards the central

part of the Baffin Bay with sediment thickness of up to 3.5 s TWT. Sediments are well stratified and landward highly reflective and eroded down to 0.8 s TWT. Under this thick sediment cover the basement can be tracked to 6 s TWT. In contrary to the clear basement reflections in the seaward parts of the lines the landward side of the basement is not well defined.

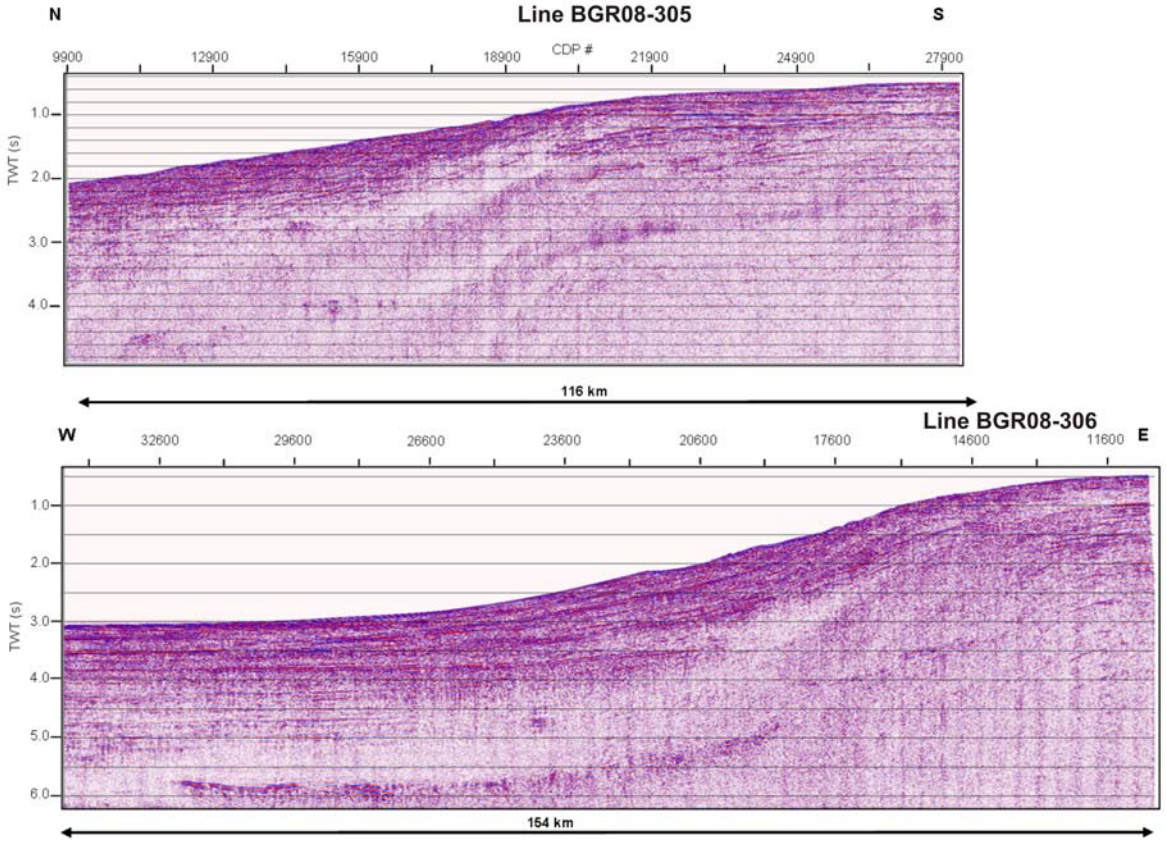

Fig. 10.15. Stacked seismic lines BGR08-306 and -305. See Fig. 3.2 for locations.

10.4.4 Profile BGR08-313/-315

Lines BGR08-313 and BGR08-315 are identical with parts of wide angle reflection/refraction line AWI-20080600 and were measured simultaneously while shooting for the OBS stations. Because of the larger shot interval (60 s) and therefore less folding the data quality of both lines is not comparable to the remaining MCS lines. CDP spacing was enlarged to 25 m. Data acquisition had to be interrupted because of fishery activity in the area. Therefore, the MCS data are split up into two parts: BGR08-313 (267 km) representing the western part (Fig. 10.16, upper panel) and BGR08-315 (139 km) at the Greenland side (Fig. 10.16, lower panel. Note: for BGR08-315 only single trace data are shown because of still ongoing processing of this line at the deadline of manuscripts for this report).

Line BGR08-313 starts on the shallow Canadian shelf with a basement high, which can be correlated with metamorphic rocks sampled by MacLean et al. (1982) just north of this position (Skaarup et al., 2006). The basement high is covered only by thin layers of sediments. In the transition to the deep water area of the Baffin Bay the basement slopes down with a steeper angle than the seabed. Interpretation of basement reflection starting from CDP 13000 gets obscure because of the strong seabed multiples. The undeformed and widely undisturbed sediment layers in the South Baffin Basin are visible for more than 3 s TWT. In the eastern part of the line a laterally limited depression is imaged by some high reflective

bended layers, which are interpreted to be volcanic interlayers/sills. Towards the east as the seabed continuously rises up to the Greenland margin the deeper parts of the sediments show increasing deformation.

Although the continuing line 215 to the east is only represented by single trace data (Fig. 10.16, lower panel) it clearly shows steep faults in the central part belonging to the transpressional Ungava Fault, which is the northern extension of the Ungava Fracture Zone. The depth penetration of this feature cannot be well imaged, since deeper layers are masked by strong multiples and high reflective basement, which belongs to the Disko Volcanic Province underlying the sediment cover. The line ends near the exploration well Hellefisk-1.

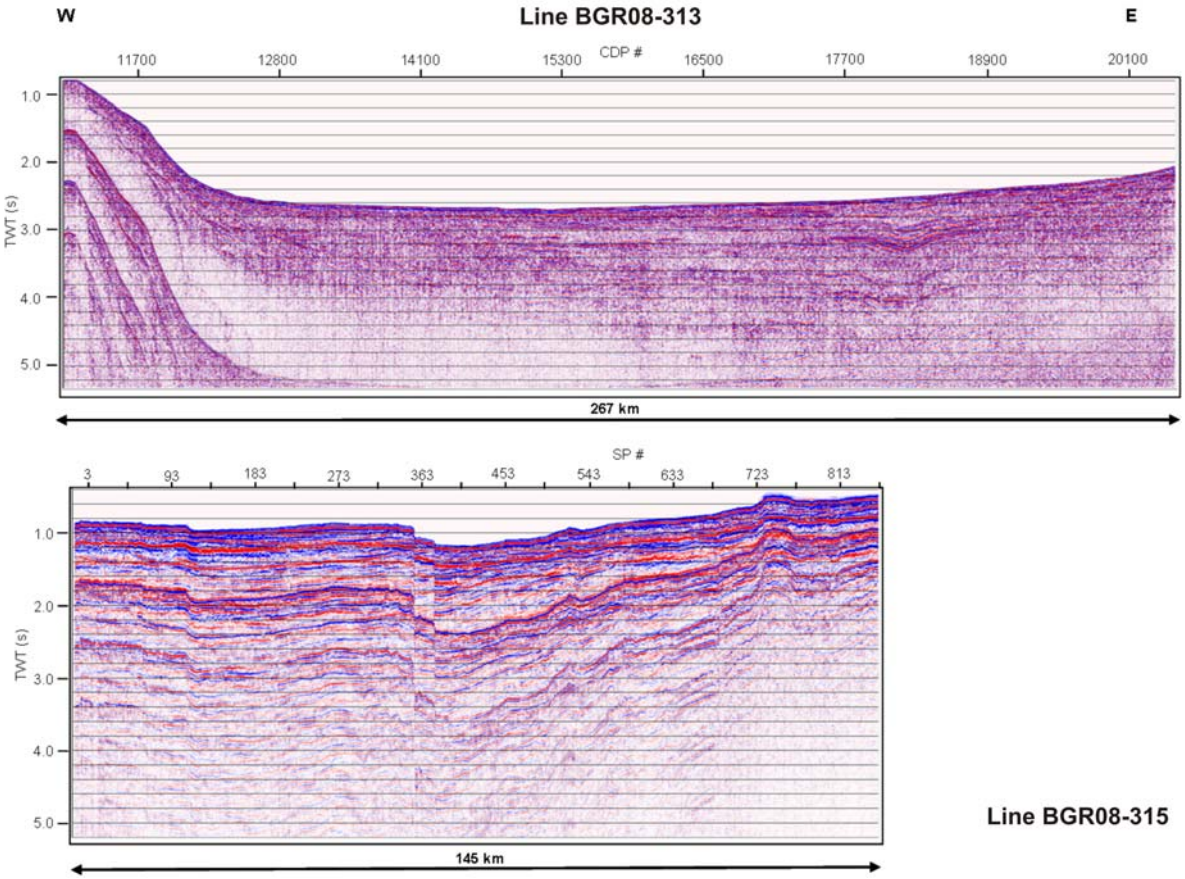

Fig. 10.16. Stacked seismic lines BGR08-313 and -315. See Fig. 3.2 for locations.

10.4.5 Profile BGR08-319

MCS line BGR08-319 runs for 271 km E-W parallel to BGR08-301/AWI-20080700, which is 320 km apart. It starts on the Greenland shelf, crosses the exploration well Ikermiut-1 and ends up north of Cape Dyer. Although line BGR08-319 (Fig. 10.17) generally crosses the same structural inventory like BGR08-301, their seismic image differs from each other in detail. The central basement high (Davis Strait High? – upper panel of Fig. 10.18) which is exposed at the seafloor is much more limited in its lateral extension than on line BGR08-301. Both end parts of the line which lie in the shallow shelf areas show high attenuating basement, which consists of volcanic rocks. Compared to line BGR08-301 sediments are accumulated in several and smaller structures at both sides of the central high layers and are of less thickness and not exceeding 0.8 s TWT. Mainly in the western part of the line

sediment layers were folded and deformed. The main difference to line BGR08-319 is the continuous presence of basement reflections which probably belong to volcanic rocks underlying the sediments. (Figs. 10.17 and 10.18). Their thickness varies along the line, but may be as thick as 1 s TWT. Underneath this horizon another prominent basement reflector is visible along the whole line with the exception of the outcropping part described above. A steep fault is developed in the easternmost part of the line between CDP 18000 and 23000, probably representing the Ungava Fault Zone (Fig. 10.18, upper panel).

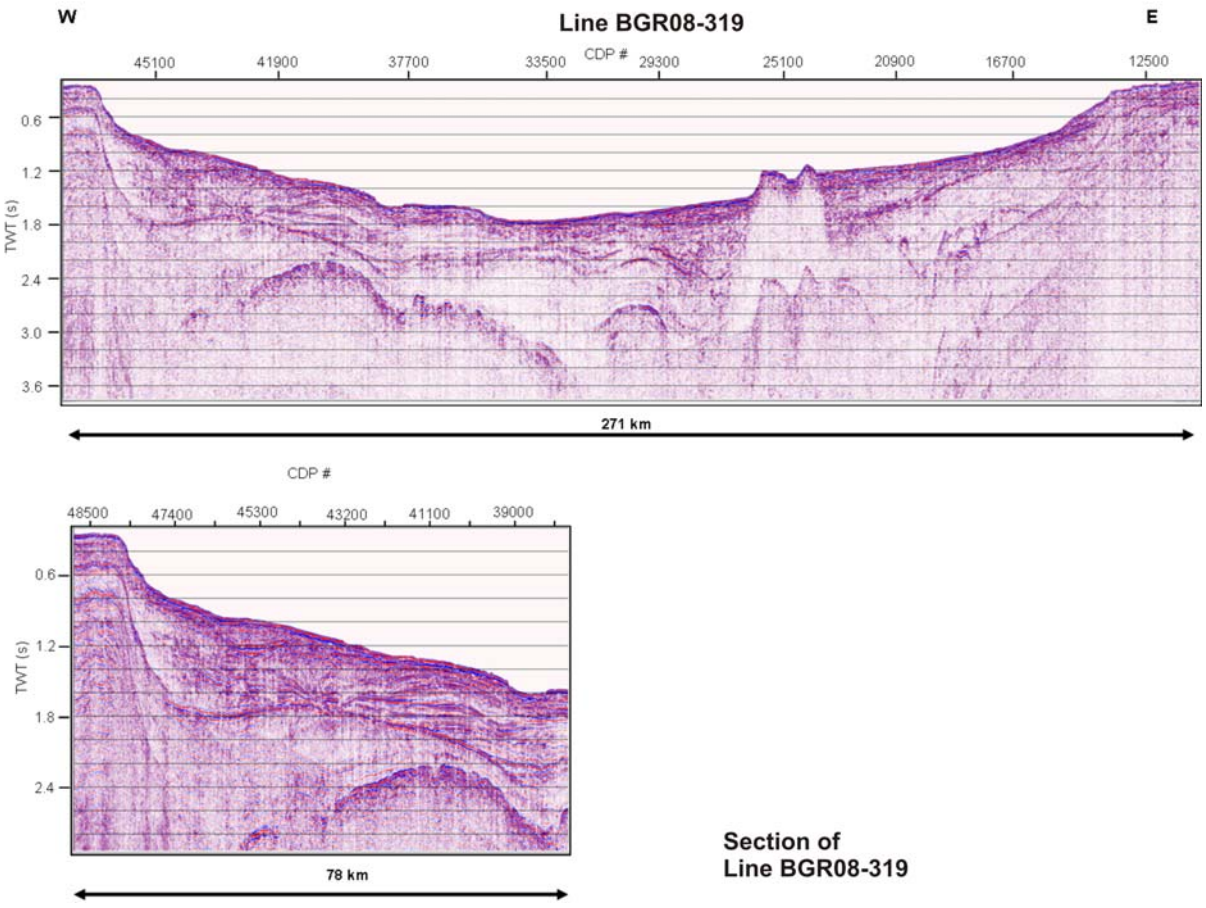

Fig. 10.17. Stacked seismic line BGR08-319. See Fig. 3.2 for location.

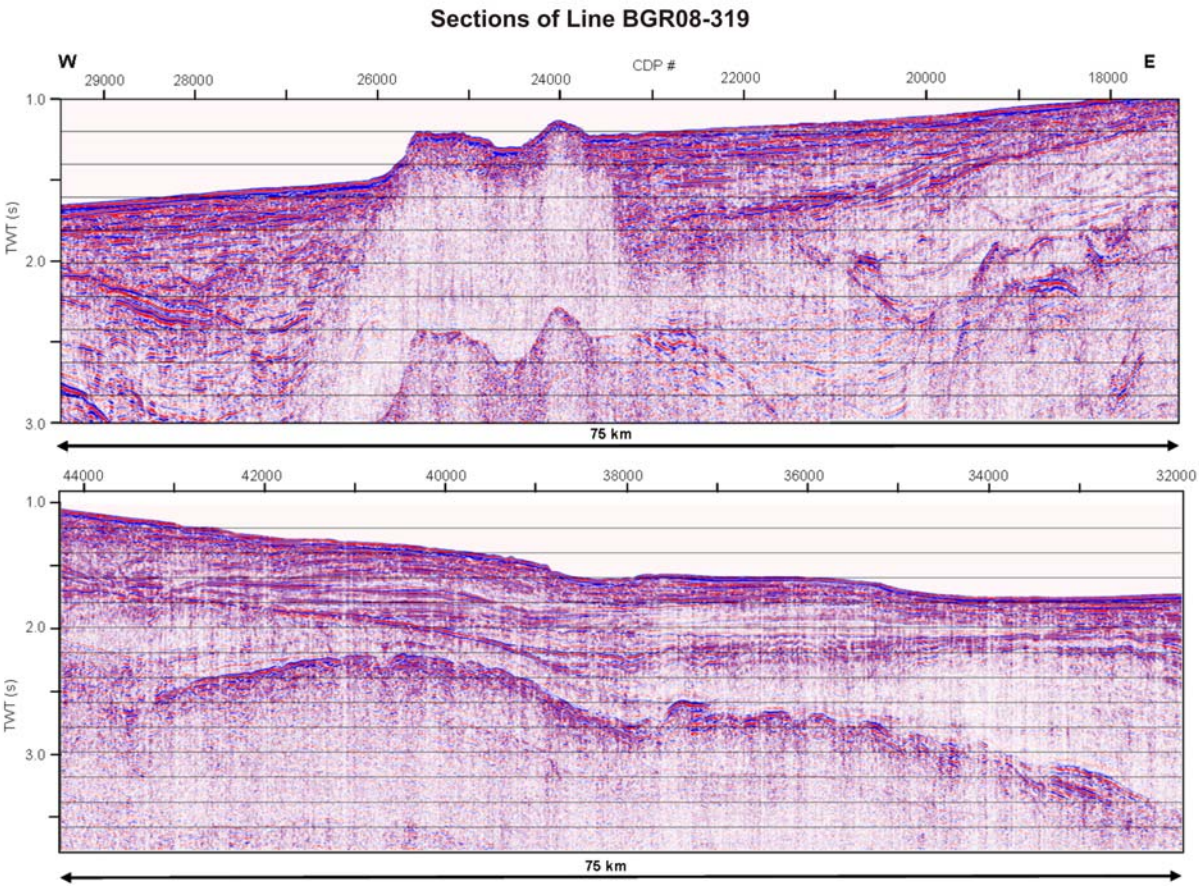

Fig. 10.18. Sections of stacked seismic line BGR08-319.

10.5 Processing of Refraction/Wide-angle OBS Data

(T. Funck, M. Finck, K. Gohl)

The refraction seismic data were processed during the cruise to detect possible problems with the OBS and to allow for an initial assessment of the geological structures encountered along the three OBS lines. Five main processing steps were carried out:

1. Compilation of navigation data (shot tables)
2. Download of the raw data
3. Conversion of the raw data to SEGY format
4. Relocalization of the OBS position
5. Data archiving

Compilation of navigation data

Initial shot tables were compiled by the BGR team that was responsible for the shooting of the airgun array. These tables (filenames bgr08-[linenumber].sp) contain the shot time (including the gun delay of 120 ms), the shot position (longitude and latitude), water depth (centre beam of the EM-120 swath bathymetric system), and the shot number. OBS line AWI-20080500 consists of shot lines BGR08-303, -303A and -303C; OBS line AWI-20080600 corresponds to shot lines BGR08-313, -314 and -315; and OBS line AWI-20080700

correlates with shot line BGR08-318 (Fig. 3.1 and App. 5). The shot tables were merged into one file for each OBS line and a manual editing was carried out during which some shot times were corrected (some times did not include the shot delay) and other shots were deleted when they were not fired at the full minute mark. The latter step was done to avoid problems with the software used for the conversion to SEGY format (program *send2x* by SEND GmbH). The SEGY files get corrupted as soon as the extracted record window for one shot includes the time of the following shot. Shots fired on a loop during maintenance of the airgun array (line AWI-20080700) were not deleted from the table. Following this editing process, shots were renumbered consecutively starting with shot number one. Figs. 10.19 through 10.21 show the final shot locations.

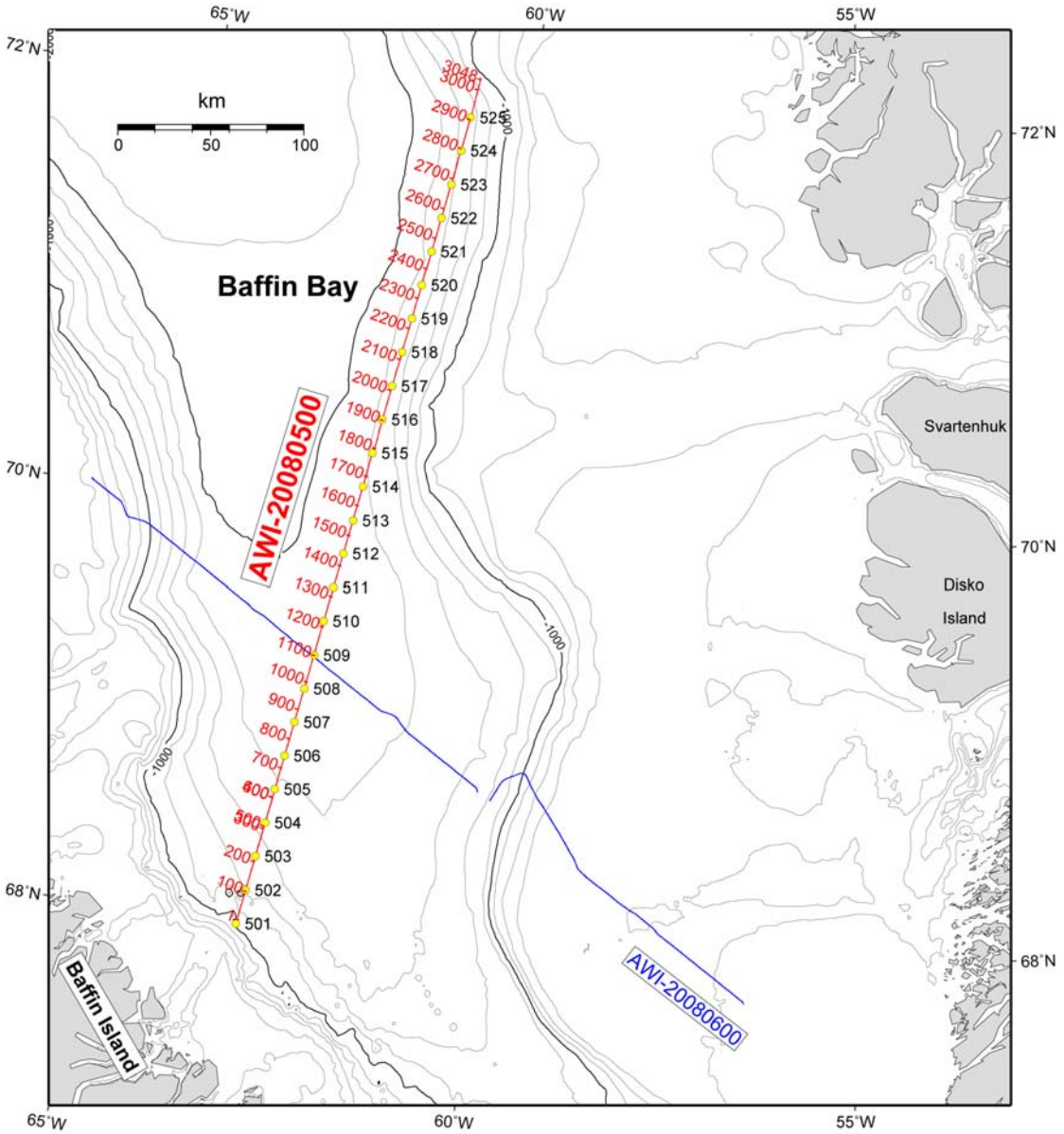

Fig. 10.19. Location map for OBS line AWI-20080500 shown together with the bathymetry (contour interval is 200 m). Every 100th shot is annotated. Circles indicate the OBS stations 501-525. This line crosses line AWI-20080600 (blue line).

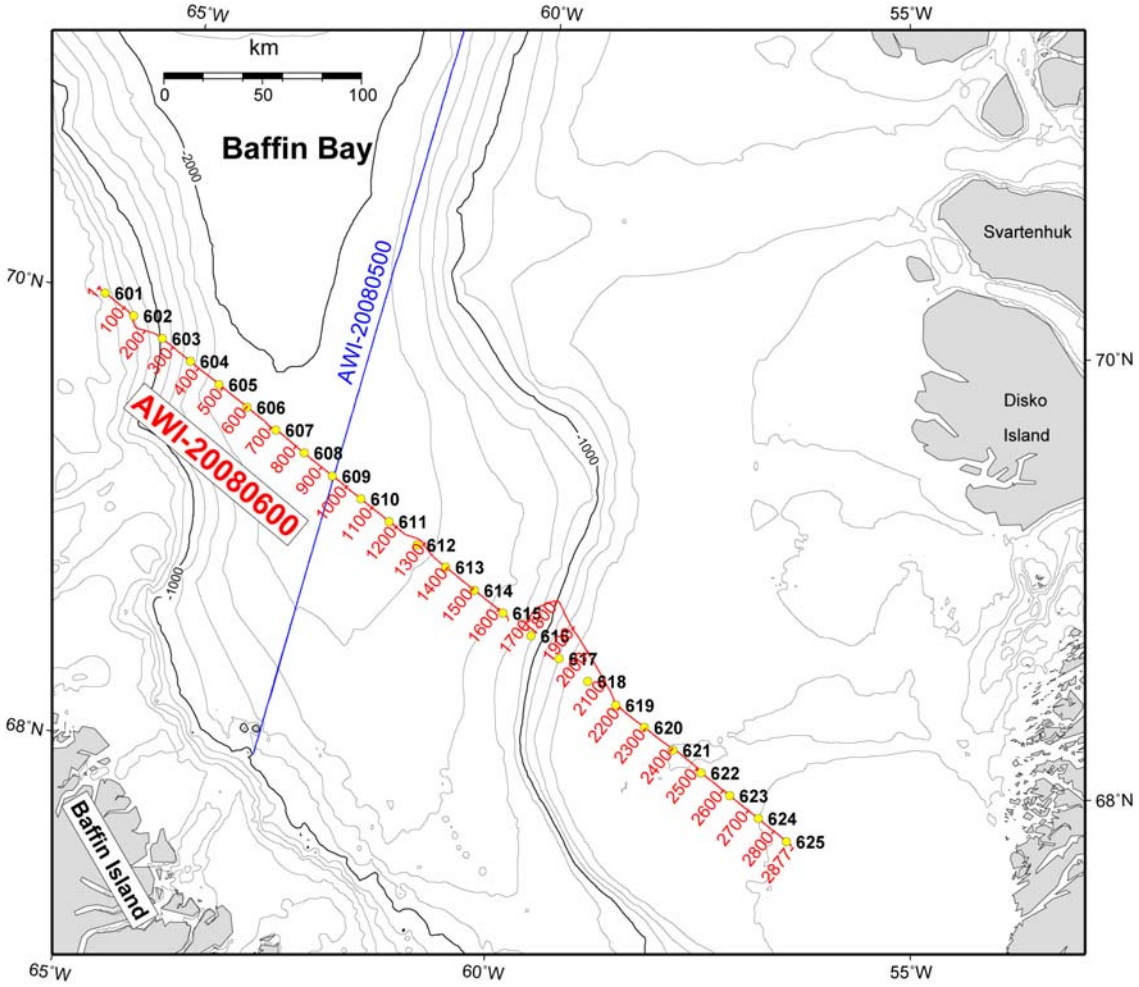

Fig. 10.20. Location map for OBS line AWI-20080600 shown together with the bathymetry (contour interval is 200 m). Every 100th shot is annotated. Circles indicate the OBS stations 601-625. This line crosses line AWI-20080500 (blue line).

The position given in the BGR shot tables is not corrected for the offset between the airgun array and the GPS antenna. Figure 10.22 shows that the centre of the airgun array was located 99.2 m behind the GPS antenna and that the antenna was shifted 1.4 m from the vessel axis towards the starboard side. To correct for this offset, the gyro heading was extracted from the ship's navigation database, using 10 s intervals that were then interpolated for the shot time. Using this heading and the given offset between the antenna and the array, the exact shot position was calculated using *GMT* (Generic Mapping Tools) software.

The water depth in the BGR shot tables was extracted from the centre beam of the EM-120 swath bathymetric system. During the MSM09/3 cruise, the echo sounder was operated with a water velocity model from the previous leg (MSM09/2) that was measured in Labrador Sea (name of profile is *SVP119_thinned.asvp,* Figure 10.23). When this sound profile was compared with other measurements from Baffin Bay, a substantial deviation was noticed resulting in errors of up to 20 m in depth. Hence, a recalculation of the water depths was necessary using the velocity profile *SVP0709* from a measurement in Baffin Bay conducted during leg MSM09/2. This velocity profile is consistent with a measurement from this leg (MSM09/3) conducted at the cross point between OBS lines AWI-20080500 and AWI-20080600.

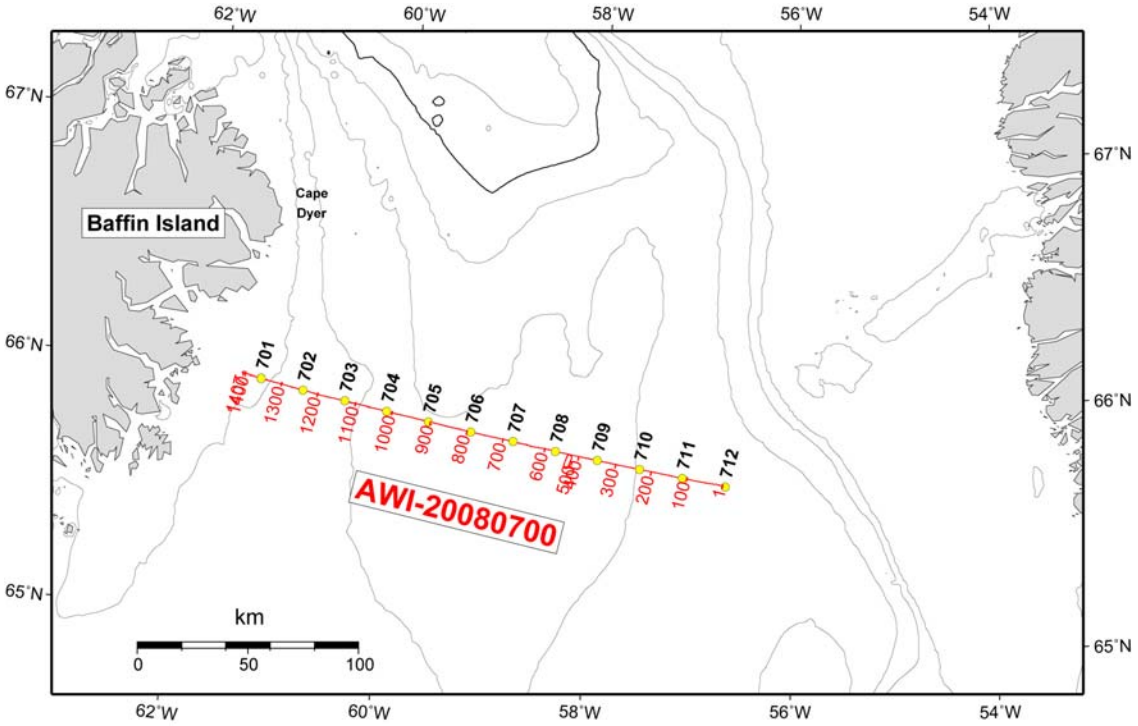

Fig. 10.21. Location map for OBS line AWI-20080700 shown together with the bathymetry (contour interval is 200 m). Every 100th shot is annotated. Circles indicate the OBS stations 701-712.

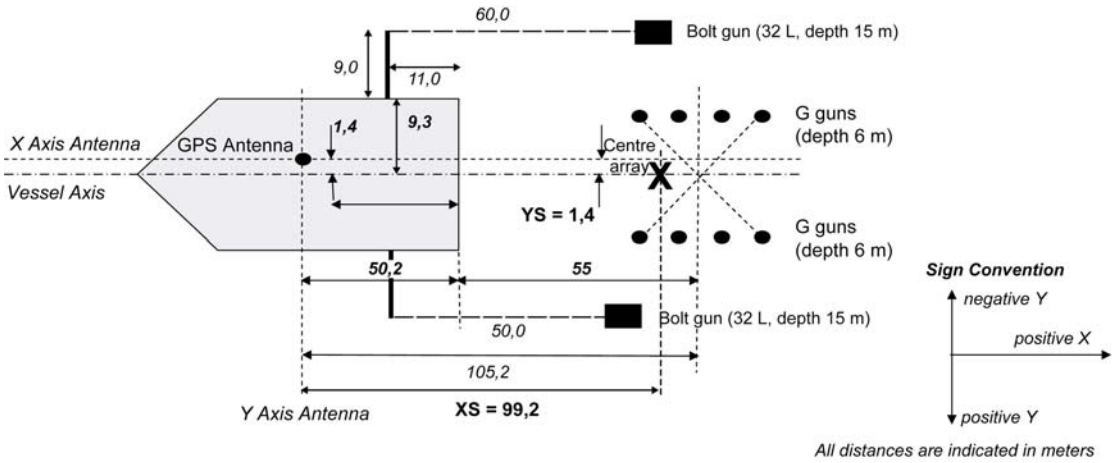

Fig. 10.22. Configuration of the airgun array with respect to the GPS antenna used for the shooting of the refraction seismic lines.

The water depth on the EM-120 system was given as depth below the echo sounder. Hence, a static correction of 6.5 m (depth of the sounder) was carried out to obtain the water depth with the sea surface as reference.

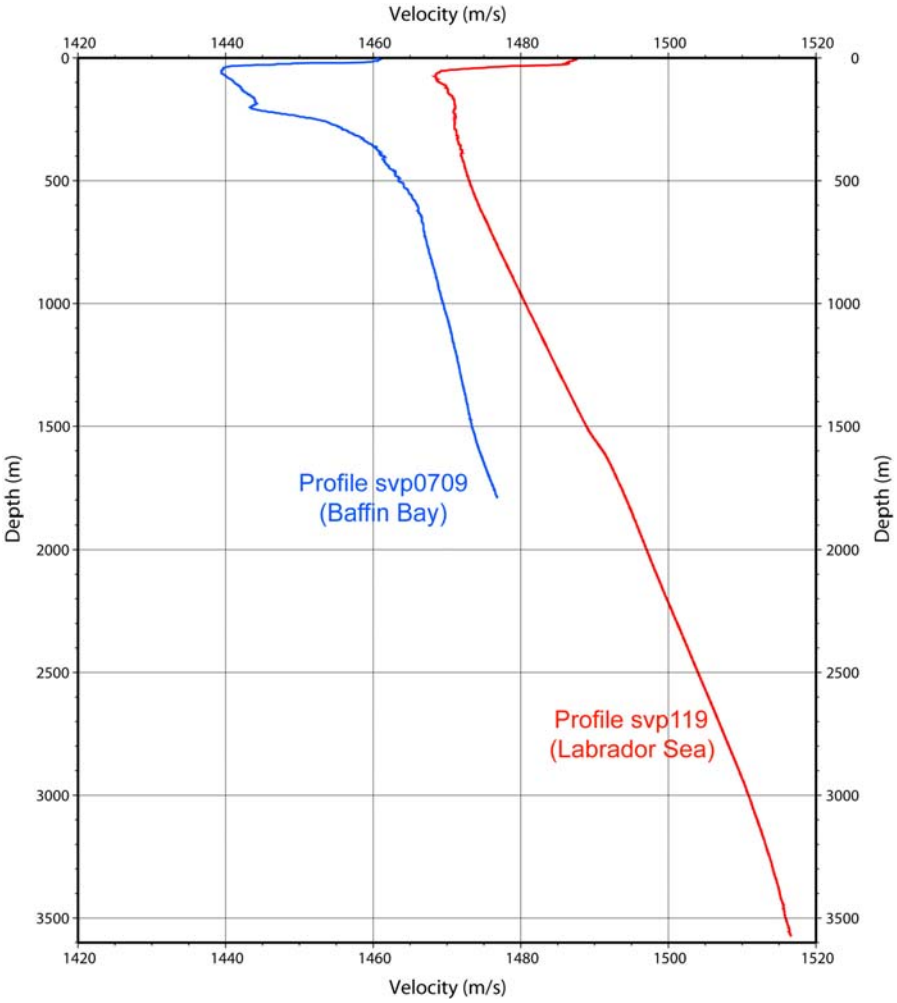

Fig. 10.23. Water velocity profiles svp0709 and svp119 obtained in Baffin Bay and Labrador Sea, respectively.

Download of the raw data

After recovery of the OBS, the cylinders with the electronics were stored in the hangar for ca. 2 hours to warm up. Then the cylinders were opened and the drift (skew) of the OBS clock was measured by comparison with the time signal of the GPS clock. A linear clock drift is assumed. The flash cards in the recorder were retrieved and transferred to a laptop computer running the LINUX operating system. Here the data on the cards (in native SEND format) were dumped to disk together with the system log files.

Conversion to SEGY format

Initial SEGY files were created on a LINUX laptop computer using the software *send2x* (SEND GmbH). The software demultiplexes the raw data and corrects for the drift of the OBS clock. Four SEGY files are obtained for each OBS. The four files correspond to the four channels on the instrument

Channel 1 - hydrophone

Channel 2 - horizontal geophone

Channel 3 - horizontal geophone

Channel 4 - vertical geophone

The output file names are generic names created by the software and contain information on the instrument, channel and recording time. Shot and station positions are recorded in the SEGY headers in arc minutes. The record length is 59.5 s and is limited by a bug in the software that does not allow for record lengths greater than the shot interval (60 s). Another bug in the software is the omission of the last shot in the shot tables when creating the SEGY files for channels 2 through 4. For lines 500 and 700, this problem was bypassed by creating an extra entry at the end of the shot table. This dummy trace was later deleted on channel 1.

For further processing, the initial SEGY files were transferred to a SUN workstation with the software package Seismic Unix installed on it. The SEGY format of the initial SEGY files could not be imported directly into Seismic Unix, presumably to some problems with the byte order although Seismic Unix normally allows for the import of SEGY data with PC byte order. To avoid this incompatibility, the initial SEGY files were transcribed by third party software to a SEGY format (EBCIDC encoded header and long integer data) readable by Seismic Unix on UNIX platforms. Initial shot-receiver offsets (calculated in GMT) were added to the SEGY headers (shots to the west of the OBS obtained a negative sign) and the long initial SEGY file names were replaced with shorter names using the nomenclature

s[station number]ch[channel number].sgy

(e.g., s622ch3.sgy for channel 3 of OBS 622).

Relocalization of OBS

The OBS position at the seafloor differs from the deployment position of the instrument, which is related to currents while the OBS is sinking to the seafloor. Hence, the initial offsets calculated from the deployment position of the OBS have to be recalculated. To obtain the instrument position at the seafloor, the arrival times of the direct water wave were picked in the program *zplot* (by Colin Zelt). These picked travel times were then compared with theoretical travel times for positions in the vicinity of the OBS deployment position. The positions are located on a regular grid around the OBS with a grid node spacing of 10 m. For the calculation of the travel times, the sound velocity profile svp0709 (Fig. 10.23) was used. The misfit between calculated and observed travel times is then calculated for each node on the grid and the minimum misfit indicates the OBS position. When the OBS is not located on the shot line, two minima are obtained (Fig. 10.24), which both have the same distance to the shot line. Even though there is an ambiguity in this case, the shot-receiver offsets are the same.

New offsets are calculated from the recalculated OBS position and written to the SEGY headers. In addition, the water depth for the shots and OBS (both corrected for the true water velocity profile) are written to the SEGY headers.

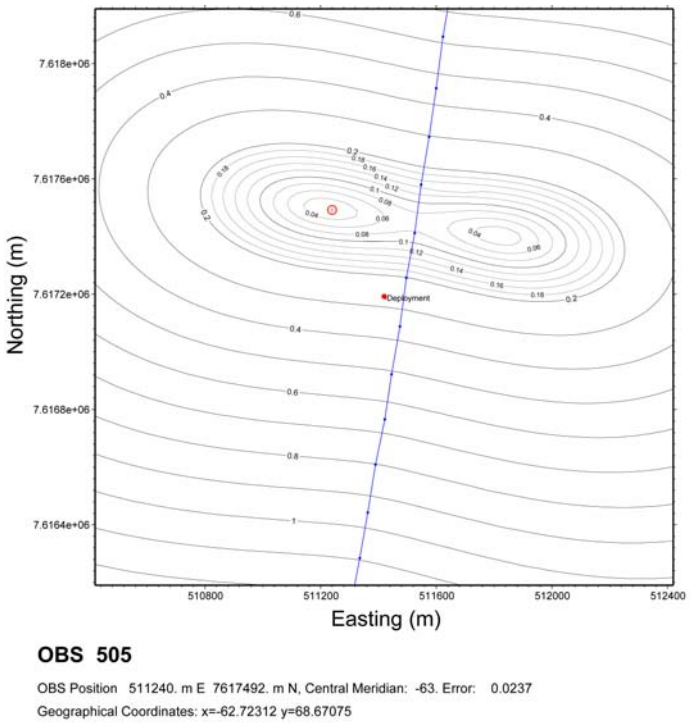

Fig. 10.24. Example showing the relocalization of OBS 505 of line AWI-20080500. The contour lines show the misfit between the observed and calculated travel times of the direct water wave within a 2 km x 2 km grid around the deployment position of the OBS. The minimum represents the OBS position at the seafloor.

Data archiving

For each OBS, four sets of the refraction seismic data are archived.

1. The raw data retrieved from the flash cards (in native SEND format).
2. The initial SEGY files obtained from the program *send2x.*
3. One set of SEGY files that can be read by Seismic Unix on a workstation (stored in the folder SEGY4UNIX). This set has the offsets added to the headers that were calculated from the OBS deployment position.
4. One set of SEGY files with the recalculated OBS position and offsets in the headers. In addition, the source and receiver water depth is written to the SEGY headers. Files are located in the folder (FINAL-RELOC).

The data are stored on an external USB hard disk with the file system mirrored on a second disk as backup. In addition to the seismic data, there are directories with the navigation files, the water velocity profiles obtained from CTD measurements, plots showing the relocalization of the OBS, and record sections for each OBS and channel (with the offsets calculated from the OBS deployment position).

10.6 Preliminary Results of Refraction/Wide-angle OBS Data

(K. Gohl, T. Funck, J. Gerlings, M. Fink)

The OBS data were displayed and plotted during the cruise mainly for data quality control. Any modelling for crustal structure and composition will be performed after the cruise in the laboratories. The following, we only show some data examples and preliminary travel-time phase identification.

10.6.1 Profile AWI-20080500

Of the 25 deployed OBS systems, one system (station 503) did not record on any channels due to malfunction of the MBS recorder. The data quality of the other systems ranges from very good to satisfying in the recording of P-wave phases up to 70 km source-receiver offsets. Most records show highly variable levels of incoherent background noise. At this stage, we explain the strong background noise either by strong bottom currents or the operation of other seismic vessels in the greater area, or a combination of both. The example record in Fig. 10.25 clearly shows refracted first-arrival phases from the upper crust (P_c) to the lower crust (P_L) as well as high-amplitude reflections from the crust-mantle boundary (P_mP). Similar observations can be made from the other records, although the data quality decreases towards both continental crustal margins in the northern and southern ends of the profile.

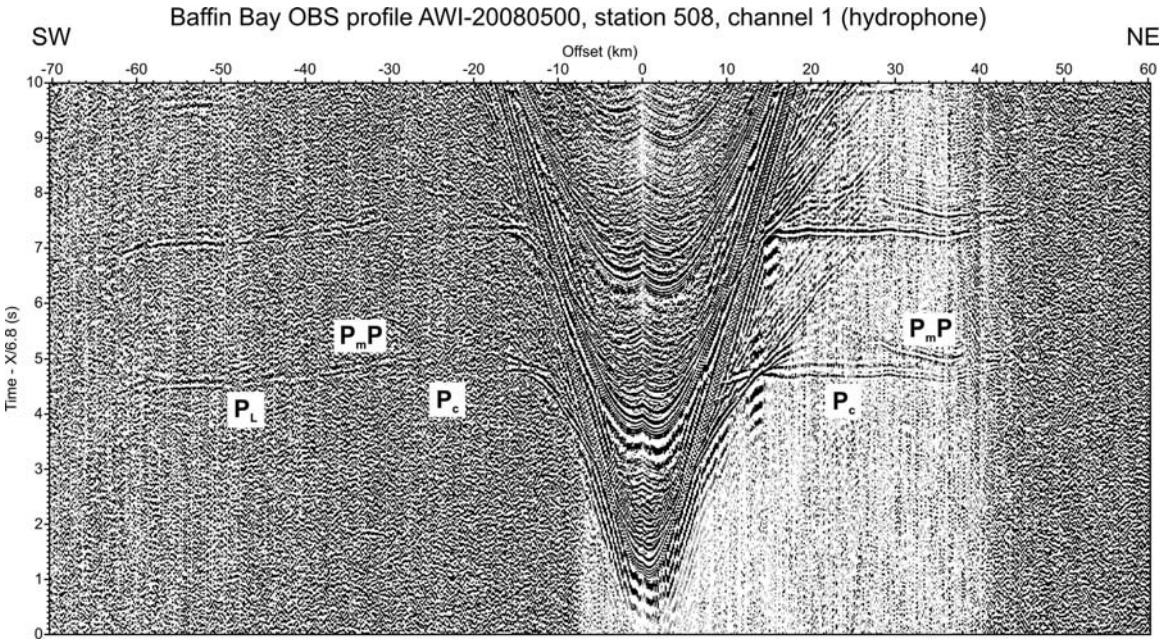

Fig. 10.25. Example of OBS record from line AWI-20080500 in Baffin Bay. Dominant travel-time phases include upper crustal refractions (P_c), lower crustal refractions (P_L) and Moho reflections (P_mP).

10.6.2 Profile AWI-20080600

Of the 25 deployed OBS systems along this profile, 8 systems suffered from technical problems. One system did not record due to human error (621), 6 systems had limited (but usable) recording lengths due to low-battery signals (605, 606, 608, 613, 614, 616), and one system (620) the clock skew could not be performed which was then adopted from previous recordings. The data quality of the other systems ranges from very good to satisfying in the recording of P-wave phases up to 100 km source-receiver offsets. Most records show highly variable levels of incoherent background noise. At this stage, we explain the strong background noise either by strong bottom currents or the operation of other seismic vessels in the greater area, or a combination of both. The example record in Fig. 10.26 shows refracted first-arrival phases from the upper crust (P_c) to the upper mantle (P_n) as well as high-amplitude reflections from the crust-mantle boundary (P_mP). Similar observations can be made from the other records.

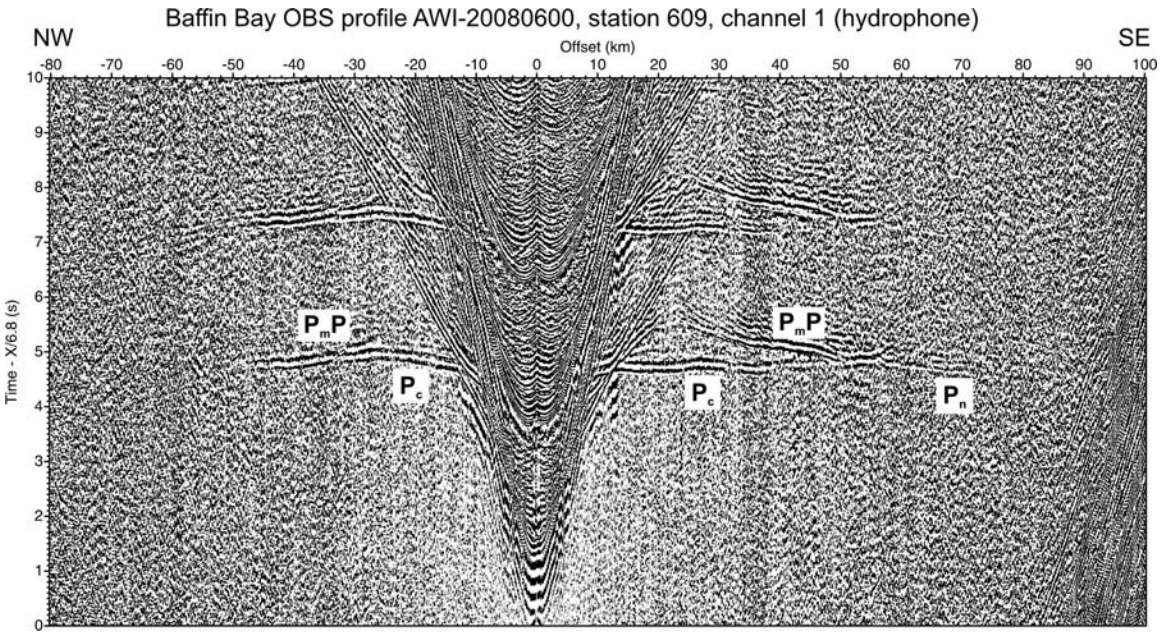

Fig. 10.26. Example of OBS record from line AWI-20080600 in Baffin Bay. Dominant travel-time phases include upper crustal refractions (P_c), Moho reflections (P_mP) and upper mantle refractions (P_n).

10.6.3 Profile AWI-20080700

All OBS systems along this profile produced useful data with phases observed at offsets up to 150 km in a few records. Most records show highly variable levels of incoherent background noise. At this stage, we explain the strong background noise either by strong bottom currents. The example record in Fig. 10.27 shows refracted first-arrival phases from the upper crust (P_c), the lower crust (P_L) and the upper mantle (P_n) as well as reflections from the crust-mantle boundary (P_mP). A peculiar observation can be made for a reflective phase from within the upper mantle ($P_{UM}P$).

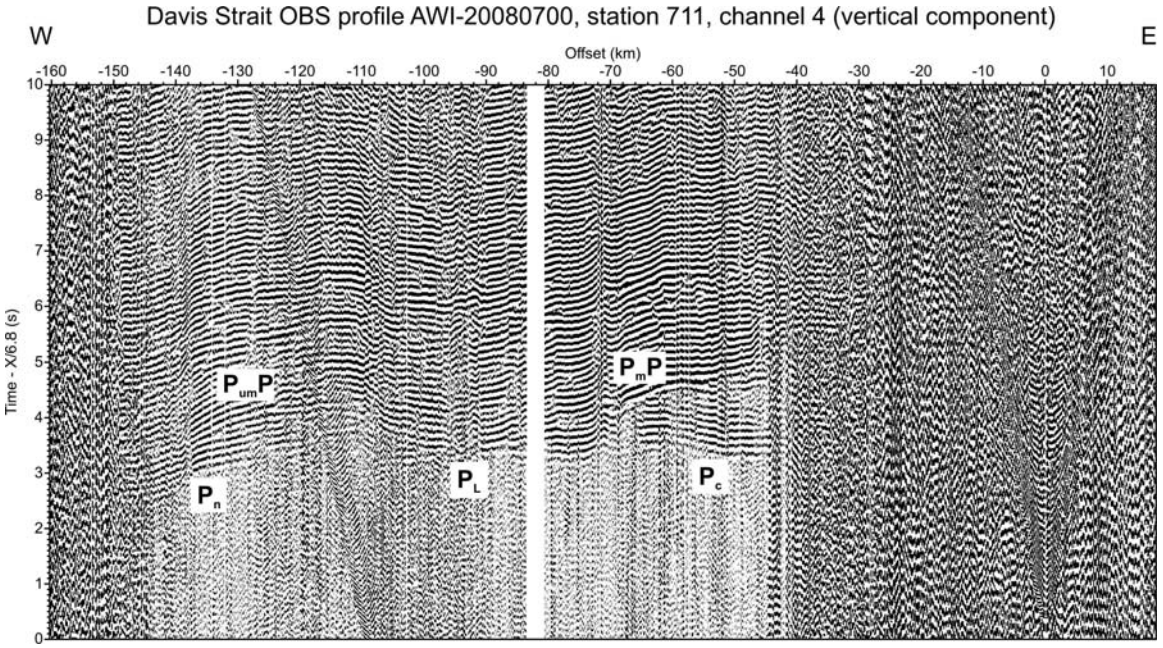

Fig. 10.27. Example of OBS record from line AWI-20080700 across Davis Strait. Dominant travel-time phases include upper crustal refractions (P_c), lower crustal refractions (P_L), Moho reflections (P_mP) as well as upper mantle refractions (P_n) and reflections ($P_{um}P$). The short-offset traces have a very low signal/noise ratio probably caused by bottom or tidal currents.

11. Acknowledgements

We wish to express our gratitude to the ship's master Karl Friedhelm von Staa, his officers and crew of RV *Merian* for their very professional and enthusiastic engagement and service to the scientific program of this leg. The IfM-GEOMAR provided the OBS systems and 3 Bolt-800CT airguns for which thank Prof. Ernst Flüh. The seismic air compressors were supplied by *Exploration Electronics Ltd* / *Airbridge Ltd* (EEL) and by the *Geological Survey of Denmark and Greenland* (GEUS). We greatly appreciate the installation and maintenance service of the compressors by Iain Miller and Richard Griffin of EEL. This cruise leg MSM09/3 was primarily funded by the *Deutsche Forschungsgemeinschaft* (DFG) and the *Bundesministerium für Bildung und Forschung* (BMBF). Substantial additional funds for the cruise were provided by the *Alfred Wegener Institute for Polar and Marine Research* (AWI), the *Bundesanstalt für Geowissenschaften und Rohstoffe* (BGR) and by GEUS.

12. References

Andersen, O.B. and Knudsen, P., Global marine gravity field from the ERS-1 and GEOSAT geodetic mission altimetry, *J. Geophys. Res., 103*, C4, 8129, 2001.

Andersen, O.B., Knudsen, P., Berry, P. and Kenyon, S., The DNSC08 ocean wide altimetry derived gravity field. Presented EGU-2008, Vienna, Austria, April, 2008.

Balkwill, H.R., Labrador Basin: structural and stratigraphic style; in: Beaumont, C. & Tankard, A.J., *Sedimentary Basins and Basin-Forming Mechanisms*; Memoir Canadian Society of Petroleum Geologists, 12, 17-43, 1987.

Bauer, K., Neben, S., Schreckenberger, B., Emmermann, R., Hinz, K., Fechner, N., Gohl, K., Schulze, A., Trumbull, R.B., and Weber, K., Deep structure of the Namibia continental margin as derived from integrated geophysical studies. *J. Geophys. Res., 105*, 25892-25853, 2000.

Chalmers, J.A., The continental margin off southern Greenland: Along-strike transition from an amagmatic to a volcanic margin, *J. Geol. Soc., 154*, 571-576, 1997.

Chalmers, J.A. & Laursen, K.H., Labrador Sea: the extent of continental and oceanic crust and the timing of the onset of seafloor spreading, *Mar. Petrol. Geol., 12*, 2005-217, 1995

Chalmers, J.A. & Oakey, G., Cretaceous-Palaeogene development of Labrador Sea and Davis Strait; presentation at Ann. Assembly European Geoscience Union, Vienna, *Geophys. Res. Abstr., 9*, 01638, 2007.

Chalmers, J.A. & Pulvertaft, T.C.R., Development of the continental margins of the Labrador Sea: a review; in: Wilson, R.C.L. et al., *Non-Volcanic Rifting of Continental Margins: A Comparison of Evidence from Land and Sea*; Geol. Soc. London Special Publ. 187, 77-105, 2001.

Chian, D. & Louden, K., The structure of Archean-Ketilidian crust along the continental shelf of southwestern Greenland from a seismic refraction profile, *Can. J. Earth Sci., 29*, 301-313, 1992.

Chian, D. & Louden, K.E., The continent-ocean crustal transition across the southwest Greenland margin, *J. Geoph. Res., 99*, 9117-9135, 1994.

Chian, D., Keen, C., Reid, I. & Louden, K.E., Evolution of nonvolcanic rifted margins: New results from the conjugate margins of the Labrador Sea, *Geology, 23*, 589– 592, 1995a

Chian, D., Louden, K.E. & Reid, I., Crustal structure of the Labrador Sea conjugate margin and implications for the formation of nonvolcanic continental margins, *J. Geoph. Res., 100*, 24239-24253, 1995b.

Courtney, R.C. and Piper, D.J.W., The gravity signature of a large Quaternary depocentre off southeast Canada. *Géographie, Physique et Quarternaire 48*, 349-360, 1992.

Engels, M., Barckhausen, U. and Gee, J.S., A new towed vector magnetometer: methods and results from a Central Pacific cruise, *Geophys. J. Int., 172*, 115-129, 2008.

Funck, T., Louden, K.E., Wardle, R.J., Hall, J., Hobro, J.W., Salisbury, M.H. & Muzzatti, A., Three-dimensional structure of the Torngat Orogen (NE Canada) from active seismic tomography, *J. Geophys. Res., 105*, 23403-23420, 2000.

Funck, T., Hopper, J.R., Larsen, H.C., Louden, K.E., Tucholke, B.E. & Holbrook, W.S., Crustal structure of the ocean-continent transition at Flemish Cap: Seismic refraction results, *J. Geophys. Res., 108*, 2531, doi:10.1029/2003JB002434, 2003.

Funck, T., Jackson, H.R., Louden, K.E., Dehler, S.A. & Wu, Y., Crustal structure of the northern Nova Scotia rifted continental margin (Eastern Canada), *J. Geophys. Res., 109*, B09102 doi:10.1029/2004JB003008, 2004.

Funck, T., Jackson, H.R, Louden, K.E. & Klingelhöfer, F., Seismic study of the transform-rifted margin in Davis Strait between Baffin Island (Canada) and Greenland: What happens when a plume meets a transform; *J. Geophys. Res., 112*, B04402, doi:10.1029/2006JB004308, 2007.

Gerlings, J., Funck, T., Jackson, R., Louden, K. & Klingelhoefer, F., Seismic evidence for plume derived volcanism during formation of the continental margin in southern Davis Strait and northern Labrador Sea, *Geophys. J. Int.*, in press.

Gohl, K. & Smithson, S.B., Structure of Archean crust and passive margin of southwest Greenland from seismic wide-angle data, *J. Geophys. Res., 98, B4*, 6623-6638, 1993.

Hall, J., Louden, K.E., Funck, T. & Deemer, S., Geophysical characteristics of the continental crust along the Lithoprobe Eastern Canadian Shield Onshore-Offshore Transect (ECSOOT): a review, *Can. J. Earth Sci., 39*, 569-587, 2002.

Hiscott, R.N. and Aksu, A.E., Submarine debris flows and continental slope evolution in front of Quaternary ice sheets, Baffin Bay, Canadian Arctic, *Am. Ass. Petrol. Geol. Bull. 78*, 445-459, 1994.

IOC, IHO, and BODC, *Centenary Edition of the GEBCO Digital Atlas*, published on CD-ROM on behalf of the Intergovernmental Oceanographic Commission and the International Hydrographic Organization as part of the General Bathymetric Chart of the Oceans, British Oceanographic Data Centre, Liverpool, 2003.

Jackson, H. R. & I. Reid, I., Crustal thickness between the Greenland and Ellesmere Island margins determined from seismic refraction, *Can. J. Earth Sci., 31*, 1407–1418, 1994.

Jackson, H.R., Funck, T., Girouard, P., Chapman, B., Klingelhöfer, F., Gerlings, J. & Jensen, A., *Cruise Report Hudson 2003-047 NUGGET (Nunavut to Greenland Geophysical Transect)*, Geol. Survey Canada, Open File 1838, 2003.

Jokat, W., Ritzmann, O., Schmidt-Aursch, M.C., Drachev, S., Gauger, S., & Snow, J., Geophysical evidence for reduced melt production on the Arctic ultraslow Gakkel mid-ocean ridge, *Nature, 426*, 962-965, doi:10.1038/nature01706, 2003.

Keen, C.E. & Barrett, D.L., Seismic refraction studies in Baffin Bay: an example of a developing ocean basin, *Geoph. J. R. astr. Soc., 30*, 253-271, 1972.

Keen, C.E., Keen, M.J. Ross, D.I. & Lack, M., Baffin Bay: small ocean basin formed by sea-floor spreading, *AAPG Bull., 58*, 1089-1108, 1974.

Kerr, J.W., A submerged continental remnant of the Labrador Sea, *Earth Planet. Sci. Lett., 2, 283-289*, doi:10.1016/0012-821X(67)90143-4, 1967.

Klose, G. W., Malterre, E., McMillan, N.J. & Zinkan, C.G., Petroleum exploration offshore southern Baffin Island, northern Labrador Sea, Canada; In Embry,, A.F. & Balkwill, H.R. (eds.), *Arctic geology and geophysics*, Memoir Canadian Society of Petroleum Geologists, 8, 233-244, 1982.

Korenaga, J., Comprehensive analysis of marine magnetic vector anomalies, *J. Geophys. Res., 100* (B1), 365-378, 1995.

LaCoste, L.J.B., Measurement of gravity at sea and in the air. *Rev. Geoph., 5*, 477-526, 1967.

Larsen, H.C. & Saunders, A.D., Tectonism and volcanism at the southeast Greenland rifted margin: A record of plume impact and later continental rupture, in Proceedings of the Ocean Drilling Program, Scientific Results, vol. 152, pp. 503–533, Ocean Drill. Program, College Station, Tex., 1998.

Ludwig, J.W., Nafe, J.E., and Drake, C.L., Seismic refraction, in: A.E. Maxwell (Eds.), *The Sea, Vol. 4*, 53-84, Wiley, New York, 1970.

MacLean, B., Srivastava, S.P., Haworth, R.T., Bedrock structures off Cumberland sound, Baffin Island Shelf: core sample and geophysical data. In: Embry, A.F., Balkwill, H.R. (Eds.), *Arctic Geology and Geophysics*. Can. Soc. Petrol. Geol. Memoir, p. 279-295, 1982.

Morelli, C., The International Standardization Net 1971. *Intern. Ass. Geodesy Spec. Public. 4*, 194, 1974.

Nielsen, T.K., Larsen, H.C., & Hopper, J.R., Contrasting rifted margin styles south of Greenland: implications for mantle plume dynamics, *Earth Planet. Sci. Lett., 200*, 271-286, doi:10.1016/S0012-821X(02)00616-7, 2002.

Oakey, G., *Cenozoic evolution and lithosphere dynamics of the Baffin Bay - Nares Strait region of Arctic Canada and Greenland*. PhD thesis, Dalhousie University, Wade Comp. Ltd., Halifax, 233 p., 2005.

Parker, R.L. and O'Brien, M.S., Spectral analysis of vector magnetic field profiles, J. *Geophys. Res., 102* (B11), 24815-24824, 1997.

Pearson, D.G., Emeleus, C.H. & Kelley, S.P., Precise $^{40}Ar/^{39}Ar$ age for the initiation of Palaeogene volcanism in the Inner Hebrides and its regional significance, *J. Geol. Soc. London, 153*, 815– 818, 1996.

Reid, I. & Jackson, H.R., Crustal structure of northern Baffin Bay, seismic refraction results and tectonic implication, *Canad. J. Earth Sci., 102*, 523-542, 1997.

Roest, W.R. & Srivastava, S.P., Sea-floor spreading in the Labrador Sea: a new Seama, N., Nogi, Y. and Isezaki, N., A new method for precise determination of the position and strike of magnetic boundaries using vector data of the geomagnetic anomaly field, *Geophys. J. Int., 113*, 155-164, 1993.

Sandwell, D.T. and Smith, W.H.F., Marine Gravity Anomaly from Geosat and ERS-1 Altimetry. *J. Geophys. Res., 102*, 10039-10054, 1997.

Skaarup, N., Jackson, H.R. & Oakey, G., Margin segmentation of Baffin Bay/Davis Strait, eastern Canada, based on seismic reflection and potential field data, *Mar. Petr. Geol., 23*, 127-144, 2006.

Sleep, N.H. and Fuyita, K., *Principles of Geophysics*, Blackwell Science, Malden, Mass., 1997.

Srivastava, S.P.,Evolution of the Labrador Sea and its bearing on the early evolution of the North Atlantic, *Geophys. J. R. astr. Soc., 52*, 313-357, 1978.

Srivastava, S.P., Falconer, R.K.H. & MacLean, B., Labrador Sea, Davis Strait, Baffin Bay: geology and geophysics – a review; in Kerr, J.W., Fergusson, A.J. & Machan, L.C. (eds.), *Geology of the North Atlantic Borderlands*, Can. Soc. Pet. Geol. Mem. 8, p. 333-398, 1981.

Srivastava, S.P. & Tapscott, C.R., Plate kinematics of the North Atlantic, in Vogt, P.R. & Tucholke, B.E. (eds.), *The Geology of North America, vol. M, The Western North Atlantic Region*, Chapter 23, pp. 379-404, Geol. Soc. Am., Boulder, CO, 1986.

Srivastava, S.P., MacLean, B., Macnab, R.F. & Jackson, H.R., Davis Strait: structure and evolution as obtained from a systematic geophysical survey ; In Embry,, A.F. & Balkwill, H.R. (eds.), *Arctic geology and geophysics*, Memoir Canadian Society of Petroleum Geologists, 8, 267-278, 1982.

Srivastava, S.P., Arthur, M.A., Clement, B., et al. (eds.), *Proc. Init. Repts. (Pt. A), ODP, 105*, College Station, TX (Ocean Drilling Program), 1987.

Storey, M., Duncan, R.A., Pedersen, A.K., Larsen, L.M. & Larsen, H.C., $^{40}Ar/^{39}Ar$ geochronology of the West Greenland Tertiary volcanic province, *Earth Planet. Sci. Lett., 160*, 569-586, doi:10.1016/S0012-821X(98)00112-5, 1998.

Verhoef, J., Roest, W.R., Macnab, R., Arkani-Hamed, J., and members of the Project team, Magnetic anomalies of the Arctic and North Atlantic oceans and adjacent land areas, *Geological Survey of Canada, Open File 3161*, CD-ROM, 1996.

Wang, Y.M., GSFC00 mean sea surface, gravity anomaly, and vertical gravity gradient from satellite altimeter data. *J. Geophys. Res., 106*, C12, 31167, 2001.

Watts, A.B., Gravity anomalies, flexure and crustal structure at the Mozambique rifted margin. *Mar. Petrol. Geol., 18*, 445-455, 2001.

Watts, A.B. and Fairhead, J.D., A process-oriented approach to modelling the gravity signature of continental margins. *Leading Edge, 17*, 258-263, 1999.

Williamson, M.-C., Villeneuve, M.E., Larsen, L.M., Jackson, H.R., Oakey, G.N. & Maclean, B., Age and petrology of offshore basalts from the Southeast Baffin Island shelf, Davis Strait, and the Western Greenland continental margin, paper presented at Joint Annual Meeting, Geol. Assoc. of Can.–Mineral. Assoc. Can., St. John's, Newfoundland and Labrador, Canada, 2001.

App. 1 Teilnehmende Institute / Participating Institutions

AWI	Alfred-Wegener-Institut für Polar- und Meeresforschung in der Helmholtz-Gemeinschaft, Am Alten Hafen 26, D-27568 Bremerhaven, Germany (www.awi.de)
BGR	Bundesanstalt für Geowissenschaften und Rohstoffe (BGR), Stilleweg 2, D-30655 Hannover, Germany (www.bgr.bund.de)
GEUS	Geological Survey of Denmark and Greenland (GEUS), Øster Voldgade 10, DK-1350 Copenhagen K, Denmark (www.geus.dk)
DAL	Dalhousie University, Dept. of Earth Sciences, Halifax NS, B3H 4JI, Canada (www.dal.ca)
GEOMAR	Leibnitz-Institut für Meereswissenschaften (IfM-GEOMAR), Wischhofstr. 1-3, D-24148 Kiel, Germany (www.ifm-geomar.de)
KUM	Umwelt- und Meerestechnik Kiel GmbH, Wischhofstr. 1-3, Geb. D5, D-24148 Kiel, Germany (www.kum-kiel.de)
EEL	Exploration Electronics Ltd. / Airbridge Ltd. Yarmouth Business Park, Suffolk Road, Great Yarmouth, Norfolk NR31 0ER, United Kingdom (www.exploration-electronics.co.uk)

App. 2 Fahrtteilnehmer / Cruise participants

Name	*Discipline*	*Institution*
Karsten Gohl	Chief Scientist	AWI
Hans-Otto Bargeloh	Gravity, Magnetics	BGR
Thomas Behrens	Multichannel Seismics	BGR
Volkmar Damm	Multichannel Seismics	BGR
Ümit Demir	Multichannel Seismics	BGR
Markus Fink	OBS Refraction Seismics	GEOMAR
Thomas Funck	OBS Refraction Seismics	GEUS
Joanna Gerlings	OBS Refraction Seismics	DAL
Richard Griffin	Seismic Compressors	EEL
Ingo Heyde	Gravity, Magnetics	BGR
Günther Kallaus	Multichannel Seismics	BGR
Helene Kraft	OBS Refraction Seismics	GEOMAR
Iain Miller	Seismic Compressors	EEL
Dirk Pitschmann	Multichannel Seismics	BGR
Marcel Ruhnau	OBS Refr. Seis., Parasound	AWI
Antje Schlömer	OBS Refraction Seismics	AWI
Uwe Schrader	Multichannel Seismics	BGR
Bernd Schreckenberger	Magnetics, Gravity	BGR
Arne Schwenk	OBS Refraction Seismics	KUM
Jennifer Sobiech	OBS Refraction Seismics	AWI

App. 3 Besatzung / Ship's Crew

Karl Friedhelm von Staa	Master
Ralf Schmidt	Chief Mate
Holm Behnisch	1st Mate
Yves-Michael Soßna	2st Mate
Gabriele Wolters	Ship’s Doctor
Thomas Ogrodnik	Chief Engineer
Benjamin Rogers	2nd Engineer
Olaf Lorenzen	3nd Engineer
Gerd Neitzel	Electrician
Frank Riedel	Electronic Engineer
Hermann Pregler	System Operator
Helmut Friesenborg	Fitter
Günther Kalis	Chief Cook
Wilfried Kluge	2nd Cook
Iris Seidel	Steward
Norbert Bosselmann	Boatswain
Karsten Peters	A. B.
Rolf Weinhold	A. B.
Frank Schrage	A. B.
Christian Roob	A. B.
Rainer Badtke	A. B.
Gerhard Müller	A. B.
Olaf Wiechert	A. B.
Eike Neunaber	Apprentice

App. 4 Stationsliste / Station List

MSM09/3 Station Book

Station	Date	Time	PositionLat	PositionLon	Depth [m]	Gear	Action	Comment
MSM9/473-1	23.09.08	12:42	65° 11.02' N	53° 55.66' W	95	Seismic reflection profile	Streamer into water	Kopfboje mit Blitzer und Sender z/W
MSM9/473-1	23.09.08	14:00	65° 14.13' N	53° 59.46' W	152	Seismic reflection profile	Remark	ca. 2000m ausgesteckt
MSM9/473-1	23.09.08	16:47	65° 20.74' N	54° 7.79' W	143	Seismic reflection profile	Remark	Streamer komplett ausgesteckt
MSM9/473-1	23.09.08	17:12	65° 22.18' N	54° 9.57' W	127	Seismic reflection profile	airguns in the water	erstes Kanonen paar des Stb. Aray zu Wasser
MSM9/473-1	23.09.08	17:46	65° 24.16' N	54° 12.04' W	117	Seismic reflection profile	Remark	Stb. arry komplett ausgebracht
MSM9/473-1	23.09.08	18:25	65° 26.35' N	54° 15.26' W	99	Seismic reflection profile	Magnetometer to water	
MSM9/473-1	23.09.08	20:14	65° 30.37' N	54° 33.36' W	113	Seismic reflection profile	profile start	
MSM9/473-1	25.09.08	03:08	65° 57.59' N	61° 10.21' W	211	Seismic reflection profile	Remark	Kursänderung nach Nord wegen Eis
MSM9/473-1	25.09.08	03:20	65° 58.07' N	61° 12.40' W	190	Seismic reflection profile	end of profile	Abbruch 12sm vor regulären Profilende
MSM9/473-1	25.09.08	04:16	66° 3.03' N	61° 14.38' W	183	Seismic reflection profile	array on deck	erstes Kanonen paar an Deck
MSM9/473-1	25.09.08	04:28	66° 4.16' N	61° 14.69' W	180	Seismic reflection profile	Remark	Stb Kanonen array komplett an Deck
MSM9/473-1	25.09.08	05:00	66° 6.26' N	61° 15.12' W	174	Seismic reflection profile	Remark	Bb. Kanonen array komplett an Deck
MSM9/473-1	25.09.08	05:17	66° 7.36' N	61° 15.12' W	176	Seismic reflection profile	Magnetometer on deck	
MSM9/473-1	25.09.08	05:21	66° 7.61' N	61° 15.10' W	174	Seismic reflection profile	Remark	Beginn Hieven des Streamers
MSM9/473-1	25.09.08	07:03	66° 11.61' N	61° 13.75' W	175	Seismic reflection profile	streamer on deck	
MSM9/474-1	25.09.08	17:03	67° 59.97' N	62° 59.95' W	1029	Ocean bottom seismometer	surface	
MSM9/475-1	25.09.08	17:54	68° 9.99' N	62° 55.73' W	1382	Ocean bottom seismometer	surface	
MSM9/476-1	25.09.08	18:45	68° 20.01' N	62° 51.52' W	1556	Ocean bottom seismometer	surface	
MSM9/477-1	25.09.08	19:35	68° 30.02' N	62° 47.41' W	1704	Ocean bottom seismometer	surface	
MSM9/478-1	25.09.08	20:25	68° 40.08' N	62° 43.13' W		Ocean bottom seismometer	surface	
MSM9/479-1	25.09.08	21:17	68° 50.08' N	62° 38.79' W	1862	Ocean bottom seismometer	surface	
MSM9/480-1	25.09.08	22:14	69° 0.12' N	62° 34.26' W		Ocean bottom seismometer	surface	
MSM9/481-1	25.09.08	23:09	69° 10.12' N	62° 29.69' W	1941	Ocean bottom seismometer	surface	
MSM9/482-1	26.09.08	00:19	69° 20.13' N	62° 25.12' W	1958	Ocean bottom seismometer	surface	
MSM9/483-1	26.09.08	01:23	69° 30.16' N	62° 20.59' W	1972	Ocean bottom seismometer	surface	
MSM9/484-1	26.09.08	02:30	69° 40.16' N	62° 15.75' W	1999	Ocean bottom seismometer	surface	
MSM9/485-1	26.09.08	03:38	69° 50.15' N	62° 10.97' W	2005	Ocean bottom seismometer	surface	
MSM9/486-1	26.09.08	04:39	70° 0.08' N	62° 6.06' W	1970	Ocean bottom seismometer	surface	
MSM9/487-1	26.09.08	05:44	70° 10.18' N	62° 0.98' W	1905	Ocean bottom seismometer	surface	
MSM9/488-1	26.09.08	06:47	70° 20.06' N	61° 56.14' W	1812	Ocean bottom seismometer	surface	
MSM9/489-1	26.09.08	07:56	70° 30.11' N	61° 51.07' W	1760	Ocean bottom seismometer	surface	
MSM9/490-1	26.09.08	09:05	70° 40.12' N	61° 45.80' W	1736	Ocean bottom seismometer	surface	
MSM9/491-1	26.09.08	10:13	70° 50.13' N	61° 40.43' W	1695	Ocean bottom	surface	

						seismometer		
MSM9/492-1	26.09.08	11:14	71° 0.15' N	61° 35.00' W	1725	Ocean bottom seismometer	surface	
MSM9/493-1	26.09.08	12:15	71° 10.15' N	61° 29.36' W		Ocean bottom seismometer	surface	
MSM9/494-1	26.09.08	13:22	71° 20.11' N	61° 24.05' W	1759	Ocean bottom seismometer	surface	
MSM9/495-1	26.09.08	14:26	71° 30.08' N	61° 18.41' W	1703	Ocean bottom seismometer	surface	
MSM9/496-1	26.09.08	15:32	71° 40.05' N	61° 12.50' W	1645	Ocean bottom seismometer	surface	
MSM9/497-1	26.09.08	16:32	71° 50.03' N	61° 6.51' W	1569	Ocean bottom seismometer	surface	
MSM9/498-1	26.09.08	17:37	71° 59.95' N	61° 0.77' W	1498	Ocean bottom seismometer	surface	
MSM9/499-1	26.09.08	18:30	72° 3.55' N	61° 7.56' W		Magnetic profile	surface	Beginn Ausstecken
MSM9/499-1	26.09.08	18:37	72° 3.27' N	61° 8.97' W	1587	Magnetic profile	information	300m ausgesteckt
MSM9/499-1	26.09.08	18:40	72° 3.12' N	61° 9.70' W	1596	Magnetic profile	Profile Start	
MSM9/499-1	26.09.08	19:07	72° 1.35' N	61° 18.71' W	1714	Magnetic profile	information	600m ausgestecht
MSM9/499-1	27.09.08	20:30	68° 2.16' N	63° 17.01' W	930	Magnetic profile	Profile End	
MSM9/499-1	27.09.08	20:47	68° 1.24' N	63° 19.41' W	838	Magnetic profile	on deck	
MSM9/500-1	27.09.08	22:51	67° 47.49' N	62° 41.96' W	797	Seismic reflection profile	Streamer into water	Kopfboje mit Sender und Blitzlicht
MSM9/500-1	27.09.08	23:36	67° 49.01' N	62° 44.75' W	839	Seismic reflection profile	airguns in the water	Bolt-Gun über Stb-Kran, 60 m ausgesteckt
MSM9/500-1	28.09.08	00:15	67° 50.33' N	62° 47.19' W	833	Seismic reflection profile	airguns in the water	Bolt-Gun über Bb-Kran, 55 m ausgesteckt
MSM9/500-1	28.09.08	01:23	67° 52.99' N	62° 50.80' W	898	Seismic reflection profile	Magnetomter to water	
MSM9/500-1	28.09.08	01:35	67° 53.73' N	62° 52.12' W	867	Seismic reflection profile	airguns in the water	Stb-Array
MSM9/500-1	28.09.08	02:25	67° 56.73' N	62° 56.64' W	869	Seismic reflection profile	airguns in the water	Bb-Array
MSM9/500-1	28.09.08	03:00	67° 58.88' N	63° 0.06' W	942	Seismic reflection profile	Remark	Alles ausgebracht - KÄ auf Profilkurs
MSM9/500-1	28.09.08	03:13	68° 0.01' N	62° 59.99' W	1028	Seismic reflection profile	profile start	
MSM9/500-1	28.09.08	10:30	68° 39.62' N	62° 43.37' W	1808	Seismic reflection profile	Remark	Profilunterbrechung, Beginn Geräte einzuholen
MSM9/500-1	28.09.08	10:53	68° 41.29' N	62° 42.54' W	1815	Seismic reflection profile	array on deck	Bb. Airgun-Arrays
MSM9/500-1	28.09.08	11:27	68° 44.33' N	62° 41.34' W	1834	Seismic reflection profile	array on deck	Stb. Airgun-Arrays
MSM9/500-1	28.09.08	12:20	68° 49.09' N	62° 39.05' W	1859	Seismic reflection profile	Remark	Beginn Einholen Streamer und Stb-Bolt - Gun
MSM9/500-1	28.09.08	12:40	68° 50.01' N	62° 38.22' W	1861	Seismic reflection profile	array on deck	Stb-Bolt - Gun
MSM9/500-1	28.09.08	13:05	68° 51.14' N	62° 37.37' W	1866	Seismic reflection profile	array on deck	Bb-Bolt - Gun
MSM9/500-1	28.09.08	13:10	68° 51.34' N	62° 37.21' W	1865	Seismic reflection profile	Magnetometer on deck	Kabel mit Streamerstrang verknotet
MSM9/500-1	28.09.08	13:20	68° 51.78' N	62° 36.86' W	1867	Seismic reflection profile	Remark	Streamerstrang wird geöffnet um Magnetometer - Wuling zu entfernen
MSM9/501-1	28.09.08	18:33	68° 14.75' N	62° 53.97' W	1481	Seismic reflection profile	Magnetomter to water	
MSM9/501-1	28.09.08	18:40	68° 15.24' N	62° 53.83' W	1490	Seismic reflection profile	airguns in the water	erste Kanone Stb. array zu Wasser
MSM9/501-1	28.09.08	18:50	68° 16.07' N	62° 53.42' W	1509	Seismic reflection profile	Remark	Magnetometer auf 600m ausgesteckt
MSM9/501-1	28.09.08	19:08	68° 17.41' N	62° 52.62' W	1536	Seismic reflection profile	Remark	Stb. Kanonen array komplett zu Wasser
MSM9/501-1	28.09.08	19:10	68° 17.55' N	62° 52.53' W	1536	Seismic reflection profile	airguns in the water	erste Kanone Bb. array zu Wasser
MSM9/501-1	28.09.08	19:23	68° 18.51' N	62° 52.06' W	1551	Seismic reflection profile	profile start	
MSM9/501-1	28.09.08	19:31	68° 19.07' N	62° 51.82' W	1553	Seismic reflection profile	Remark	Bb. Kanonen arry komplett zu Wasser

MSM9/501-1	28.09.08	19:59	68° 21.17' N	62° 51.06' W	1571	Seismic reflection profile	airguns in the water	Bolt Gun über Bb-Kran, 50m
MSM9/501-1	28.09.08	21:40	68° 30.69' N	62° 47.15' W	1715	Seismic reflection profile	airguns in the water	Stb. Boltgun zu Wasser
MSM9/501-1	30.09.08	14:30	72° 5.20' N	60° 58.05' W	1472	Seismic reflection profile	Remark	Beg. einholen Bb-Array
MSM9/501-1	30.09.08	15:03	72° 8.15' N	60° 56.57' W	1449	Seismic reflection profile	array on deck	Bb-Array eingeholt; weiter mit Stb-Array
MSM9/501-1	30.09.08	15:35	72° 10.93' N	60° 55.22' W	1357	Seismic reflection profile	array on deck	Stb-Array a/D; weiter mit Stb. Bolt-Gun
MSM9/501-1	30.09.08	15:55	72° 11.66' N	60° 54.67' W	1323	Seismic reflection profile	array on deck	Stb Bolt-Gun a/D, weiter mit Bb-Bolt
MSM9/501-1	30.09.08	15:55	72° 11.66' N	60° 54.67' W	1323	Seismic reflection profile	end of profile	
MSM9/501-1	30.09.08	16:03	72° 11.94' N	60° 54.43' W	1304	Seismic reflection profile	Magnetometer on deck	
MSM9/501-1	30.09.08	16:10	72° 12.20' N	60° 54.26' W	1288	Seismic reflection profile	array on deck	
MSM9/498-1	30.09.08	17:03	72° 2.50' N	61° 0.07' W		Ocean bottom seismometer	released	
MSM9/498-1	30.09.08	17:41	71° 59.97' N	61° 1.00' W		Ocean bottom seismometer	on deck	
MSM9/497-1	30.09.08	18:20	71° 52.62' N	61° 5.28' W		Ocean bottom seismometer	released	
MSM9/497-1	30.09.08	19:03	71° 50.13' N	61° 6.77' W		Ocean bottom seismometer	on deck	
MSM9/496-1	30.09.08	19:46	71° 42.45' N	61° 11.11' W		Ocean bottom seismometer	released	
MSM9/496-1	30.09.08	20:26	71° 39.95' N	61° 12.10' W		Ocean bottom seismometer	on deck	
MSM9/495-1	30.09.08	21:10	71° 32.78' N	61° 16.21' W		Ocean bottom seismometer	released	
MSM9/495-1	30.09.08	21:49	71° 30.04' N	61° 17.76' W		Ocean bottom seismometer	on deck	
MSM9/494-1	30.09.08	22:41	71° 22.49' N	61° 22.27' W		Ocean bottom seismometer	released	
MSM9/494-1	30.09.08	23:19	71° 20.27' N	61° 23.62' W		Ocean bottom seismometer	on deck	
MSM9/493-1	01.10.08	00:06	71° 12.90' N	61° 27.92' W		Ocean bottom seismometer	released	
MSM9/493-1	01.10.08	00:42	71° 10.29' N	61° 29.27' W		Ocean bottom seismometer	on deck	
MSM9/492-1	01.10.08	01:25	71° 2.73' N	61° 32.30' W		Ocean bottom seismometer	released	
MSM9/492-1	01.10.08	02:02	71° 0.46' N	61° 35.19' W		Ocean bottom seismometer	on deck	
MSM9/491-1	01.10.08	02:49	70° 52.74' N	61° 38.18' W		Ocean bottom seismometer	released	
MSM9/491-1	01.10.08	03:26	70° 50.46' N	61° 40.34' W		Ocean bottom seismometer	on deck	
MSM9/490-1	01.10.08	04:10	70° 42.54' N	61° 43.59' W		Ocean bottom seismometer	released	
MSM9/490-1	01.10.08	04:56	70° 40.26' N	61° 44.92' W		Ocean bottom seismometer	on deck	
MSM9/489-1	01.10.08	05:39	70° 32.74' N	61° 47.81' W		Ocean bottom seismometer	released	
MSM9/489-1	01.10.08	06:22	70° 30.07' N	61° 50.09' W		Ocean bottom seismometer	on deck	
MSM9/488-1	01.10.08	06:59	70° 23.05' N	61° 53.49' W		Ocean bottom seismometer	released	
MSM9/488-1	01.10.08	07:45	70° 19.83' N	61° 55.36' W		Ocean bottom seismometer	on deck	
MSM9/487-1	01.10.08	08:23	70° 12.85' N	61° 59.31' W		Ocean bottom seismometer	released	
MSM9/487-1	01.10.08	09:10	70° 9.76' N	62° 0.53' W		Ocean bottom seismometer	on deck	
MSM9/486-1	01.10.08	09:47	70° 2.80' N	62° 4.40' W		Ocean bottom seismometer	released	
MSM9/486-1	01.10.08	10:25	69° 59.70' N	62° 5.85' W		Ocean bottom seismometer	on deck	
MSM9/485-1	01.10.08	11:03	69° 52.88' N	62° 9.82' W		Ocean bottom seismometer	released	
MSM9/485-1	01.10.08	11:41	69° 49.99' N	62° 11.11' W		Ocean bottom	on deck	

						seismometer		
MSM9/484-1	01.10.08	12:24	69° 42.36' N	62° 13.77' W		Ocean bottom seismometer	released	
MSM9/484-1	01.10.08	13:00	69° 40.15' N	62° 15.89' W		Ocean bottom seismometer	on deck	
MSM9/483-1	01.10.08	13:46	69° 32.30' N	62° 17.83' W		Ocean bottom seismometer	released	
MSM9/483-1	01.10.08	14:23	69° 30.32' N	62° 21.04' W		Ocean bottom seismometer	on deck	
MSM9/482-1	01.10.08	15:05	69° 22.59' N	62° 22.74' W		Ocean bottom seismometer	released	
MSM9/482-1	01.10.08	15:44	69° 20.34' N	62° 25.12' W		Ocean bottom seismometer	on deck	
MSM9/481-1	01.10.08	16:28	69° 12.30' N	62° 27.03' W		Ocean bottom seismometer	released	
MSM9/481-1	01.10.08	17:10	69° 10.28' N	62° 29.76' W		Ocean bottom seismometer	on deck	
MSM9/480-1	01.10.08	17:50	69° 3.21' N	62° 32.03' W		Ocean bottom seismometer	released	
MSM9/480-1	01.10.08	18:33	69° 0.34' N	62° 34.51' W		Ocean bottom seismometer	on deck	
MSM9/479-1	01.10.08	19:15	68° 53.04' N	62° 36.80' W		Ocean bottom seismometer	released	
MSM9/479-1	01.10.08	19:53	68° 50.31' N	62° 38.94' W		Ocean bottom seismometer	on deck	
MSM9/478-1	01.10.08	20:35	68° 42.66' N	62° 40.96' W		Ocean bottom seismometer	released	
MSM9/478-1	01.10.08	21:05	68° 40.17' N	62° 43.04' W		Ocean bottom seismometer	on deck	
MSM9/477-1	01.10.08	21:42	68° 32.86' N	62° 45.48' W		Ocean bottom seismometer	released	
MSM9/477-1	01.10.08	22:21	68° 30.03' N	62° 47.31' W		Ocean bottom seismometer	on deck	
MSM9/476-1	01.10.08	22:58	68° 22.85' N	62° 50.01' W		Ocean bottom seismometer	released	
MSM9/476-1	01.10.08	23:32	68° 20.09' N	62° 51.87' W		Ocean bottom seismometer	on deck	
MSM9/475-1	02.10.08	00:12	68° 12.36' N	62° 54.69' W		Ocean bottom seismometer	released	
MSM9/475-1	02.10.08	00:44	68° 10.03' N	62° 55.51' W		Ocean bottom seismometer	on deck	
MSM9/474-1	02.10.08	01:28	68° 2.12' N	62° 58.39' W		Ocean bottom seismometer	released	
MSM9/474-1	02.10.08	01:56	67° 59.84' N	62° 59.71' W		Ocean bottom seismometer	on deck	
MSM9/502-1	02.10.08	03:17	67° 47.97' N	62° 39.07' W	843	Seismic reflection profile	Streamer into water	Kopfboje mit Blitzer und Sender (Ch. A)
MSM9/502-1	02.10.08	04:52	67° 51.50' N	62° 47.91' W	884	Seismic reflection profile	Remark	Streamer komplett ausgesteckt, 3000m
MSM9/502-1	02.10.08	04:57	67° 51.77' N	62° 48.56' W	878	Seismic reflection profile	Magnetomter to water	
MSM9/502-1	02.10.08	05:11	67° 52.60' N	62° 50.49' W	882	Seismic reflection profile	airguns in the water	erste Kanone Stb. arry zu Wasser
MSM9/502-1	02.10.08	05:25	67° 53.41' N	62° 52.31' W	847	Seismic reflection profile	Remark	Stb. Kanonen arry komplett ausgesteckt, 45m
MSM9/502-1	02.10.08	05:30	67° 53.67' N	62° 52.93' W	833	Seismic reflection profile	airguns in the water	erste kanone Bb. arry zu Wasser
MSM9/502-1	02.10.08	05:47	67° 54.57' N	62° 55.07' W	803	Seismic reflection profile	Remark	Bb. Kanonen arry komplett ausgesteckt, 45m
MSM9/502-1	02.10.08	05:47	67° 54.57' N	62° 55.07' W	803	Seismic reflection profile	Remark	Magnetometer komplett ausgesteckt, 600m
MSM9/502-1	02.10.08	06:51	67° 59.23' N	63° 0.36' W	966	Seismic reflection profile	profile start	
MSM9/502-1	02.10.08	19:24	69° 6.55' N	62° 31.47' W	1941	Seismic reflection profile	Remark	Kursänderung wegen Eis
MSM9/502-1	02.10.08	20:21	69° 11.68' N	62° 29.18' W	1939	Seismic reflection profile	Remark	wieder auf Kurs
MSM9/502-1	03.10.08	12:40	70° 36.83' N	61° 47.54' W	1749	Seismic reflection profile	Remark	Kursänderung wegen Eis
MSM9/502-1	03.10.08	14:10	70° 44.96' N	61° 43.51' W	1705	Seismic reflection profile	Remark	wieder auf Kurs

MSM9/502-1	03.10.08	16:06	70° 54.97' N	61° 37.87' W	1702	Seismic reflection profile	Remark	Kursänderung wegen Eis
MSM9/502-1	03.10.08	18:06	71° 4.95' N	61° 32.44' W	1750	Seismic reflection profile	Remark	wieder auf Kurs
MSM9/502-1	04.10.08	05:06	72° 1.93' N	60° 59.75' W	1471	Seismic reflection profile	end of profile	Beginn drehmanöver über Stb.
MSM9/502-1	04.10.08	05:19	72° 2.99' N	60° 58.13' W	1448	Seismic reflection profile	Remark	Beginn drehen über Bb.
MSM9/502-1	04.10.08	06:39	72° 2.93' N	61° 6.67' W	1562	Seismic reflection profile	Remark	Beendigung des Drehmanövers, auf Sollkurs 148°
MSM9/502-1	04.10.08	07:03	72° 1.09' N	61° 3.09' W	1518	Seismic reflection profile	profile start	
MSM9/502-1	04.10.08	18:37	71° 8.37' N	59° 17.43' W	351	Seismic reflection profile	end of profile	Beginn drehen über Stb.
MSM9/502-1	04.10.08	18:52	71° 7.09' N	59° 16.58' W	355	Seismic reflection profile	Remark	Beginn drehen über Bb.
MSM9/502-1	04.10.08	20:23	71° 9.11' N	59° 13.53' W	345	Seismic reflection profile	Remark	Drehen über Stb.
MSM9/502-1	04.10.08	20:41	71° 9.30' N	59° 17.97' W	346	Seismic reflection profile	profile start	
MSM9/502-1	05.10.08	12:33	71° 35.45' N	63° 25.09' W	2273	Seismic reflection profile	end of profile	
MSM9/502-1	05.10.08	12:35	71° 35.51' N	63° 25.60' W	2272	Seismic reflection profile	Remark	Beginn Einholen
MSM9/502-1	05.10.08	12:50	71° 35.97' N	63° 29.56' W	2274	Seismic reflection profile	Magnetometer on deck	
MSM9/502-1	05.10.08	13:13	71° 36.30' N	63° 35.80' W	2276	Seismic reflection profile	array on deck	Bb-Array a/D
MSM9/502-1	05.10.08	13:35	71° 36.18' N	63° 41.94' W	2274	Seismic reflection profile	array on deck	Stb.-Array a/D
MSM9/502-1	05.10.08	15:47	71° 42.05' N	63° 53.89' W	2286	Seismic reflection profile	streamer on deck	
MSM9/503-1	05.10.08	16:18	71° 43.84' N	63° 47.35' W	2290	Magnetic profile	surface	
MSM9/503-1	05.10.08	16:29	71° 44.25' N	63° 44.62' W	2289	Magnetic profile	information	Magnetometer komplett ausgesteckt, 750m
MSM9/503-1	05.10.08	16:37	71° 44.58' N	63° 42.66' W	2288	Magnetic profile	Profile Start	
MSM9/503-1	05.10.08	18:37	71° 51.38' N	62° 44.81' W	2240	Magnetic profile	information	Beginn Drehfahrt über Bb., Kalibrierung
MSM9/503-1	05.10.08	19:07	71° 51.64' N	62° 43.89' W	2241	Magnetic profile	information	Beendigung Drehfahrt
MSM9/503-1	05.10.08	21:00	71° 57.33' N	61° 47.92' W	1988	Magnetic profile	Profile End	
MSM9/504-1	05.10.08	21:24	71° 56.26' N	61° 39.61' W	1924	Magnetic profile	Profile Start	
MSM9/504-1	05.10.08	23:00	71° 39.43' N	61° 48.05' W	1962	Magnetic profile	information	Kusänderung auf 175°, Eisberg auf Kurslinie
MSM9/504-1	06.10.08	01:30	71° 14.31' N	62° 0.85' W	2035	Magnetic profile	information	zurück auf Track
MSM9/504-1	06.10.08	19:41	68° 14.76' N	63° 28.26' W	1291	Magnetic profile	Profile End	
MSM9/504-1	06.10.08	19:54	68° 13.96' N	63° 29.11' W	1275	Magnetic profile	on deck	
MSM9/505-1	07.10.08	17:20	69° 18.85' N	62° 22.92' W	1954	Magnetic profile	surface	
MSM9/505-1	07.10.08	17:33	69° 18.32' N	62° 20.17' W	1952	Magnetic profile	information	Magnetometer komplett ausgesteckt, 750m
MSM9/505-1	07.10.08	17:37	69° 18.14' N	62° 19.22' W	1947	Magnetic profile	Profile Start	
MSM9/505-1	08.10.08	09:23	67° 49.23' N	56° 29.13' W	169	Magnetic profile	Profile End	
MSM9/505-1	08.10.08	09:48	67° 47.92' N	56° 23.66' W	155	Magnetic profile	on deck	
MSM9/506-1	10.10.08	08:30	67° 49.25' N	56° 29.33' W	175	Ocean bottom seismometer	surface	
MSM9/507-1	10.10.08	09:22	67° 55.27' N	56° 50.26' W	224	Ocean bottom seismometer	surface	
MSM9/508-1	10.10.08	10:19	68° 1.27' N	57° 11.41' W	294	Ocean bottom seismometer	surface	
MSM9/509-1	10.10.08	11:17	68° 7.19' N	57° 32.69' W	384	Ocean bottom seismometer	surface	
MSM9/510-1	10.10.08	12:16	68° 13.10' N	57° 54.07' W	425	Ocean bottom seismometer	surface	
MSM9/511-1	10.10.08	13:15	68° 18.88' N	58° 15.89' W	312	Ocean bottom seismometer	surface	
MSM9/512-1	10.10.08	14:16	68° 24.46' N	58° 37.85' W	344	Ocean bottom seismometer	surface	
MSM9/513-1	10.10.08	15:14	68° 30.46' N	58° 59.84' W	315	Ocean bottom seismometer	surface	
MSM9/514-1	10.10.08	16:07	68° 36.15' N	59° 22.04' W	578	Ocean bottom seismometer	surface	
MSM9/515-1	10.10.08	17:02	68° 41.77' N	59° 44.37' W	1268	Ocean bottom	surface	

						seismometer		
MSM9/516-1	10.10.08	18:32	68° 47.30' N	60° 6.96' W	1575	Ocean bottom seismometer	surface	
MSM9/517-1	10.10.08	19:26	68° 52.86' N	60° 29.80' W	1703	Ocean bottom seismometer	surface	
MSM9/518-1	10.10.08	20:19	68° 58.38' N	60° 52.71' W	1776	Ocean bottom seismometer	surface	
MSM9/519-1	10.10.08	21:12	69° 3.75' N	61° 16.10' W	1865	Ocean bottom seismometer	surface	
MSM9/520-1	10.10.08	22:02	69° 9.16' N	61° 39.41' W	1907	Ocean bottom seismometer	surface	
MSM9/521-1	10.10.08	22:55	69° 14.46' N	62° 2.86' W	1931	Ocean bottom seismometer	surface	
MSM9/522-1	10.10.08	23:52	69° 19.78' N	62° 26.44' W	1956	Ocean bottom seismometer	surface	
MSM9/523-1	11.10.08	00:57	69° 25.05' N	62° 50.46' W	1986	Ocean bottom seismometer	surface	
MSM9/524-1	11.10.08	01:59	69° 30.14' N	63° 14.55' W	2032	Ocean bottom seismometer	surface	
MSM9/525-1	11.10.08	03:05	69° 35.29' N	63° 39.05' E	1959	Ocean bottom seismometer	surface	
MSM9/526-1	11.10.08	04:31	69° 40.34' N	64° 3.47' W	1938	Ocean bottom seismometer	surface	
MSM9/527-1	11.10.08	05:47	69° 45.37' N	64° 28.15' W	1800	Ocean bottom seismometer	surface	
MSM9/528-1	11.10.08	07:01	69° 50.29' N	64° 53.11' W	1046	Ocean bottom seismometer	surface	
MSM9/529-1	11.10.08	08:20	69° 55.16' N	65° 18.22' W	600	Ocean bottom seismometer	surface	
MSM9/530-1	11.10.08	09:38	69° 59.95' N	65° 43.60' W	243	Ocean bottom seismometer	surface	
MSM9/531-1	11.10.08	11:46	70° 2.57' N	65° 52.05' W	185	Magnetic profile	surface	Magnetometer
MSM9/531-1	11.10.08	12:06	70° 4.06' N	65° 54.59' W	168	Magnetic profile	information	600m ausgesteckt
MSM9/531-1	11.10.08	13:09	70° 0.04' N	65° 44.56' W	231	Magnetic profile	Profile Start	
MSM9/531-1	11.10.08	14:35	69° 52.88' N	65° 6.80' W	759	Magnetic profile	information	Ausweichen Eisberg
MSM9/531-1	11.10.08	16:15	69° 44.68' N	64° 25.87' W	1843	Magnetic profile	information	zurück auf Track
MSM9/531-1	11.10.08	22:06	69° 14.84' N	62° 4.26' W	1932	Magnetic profile	Profile End	
MSM9/532-1	11.10.08	22:07	69° 14.75' N	62° 3.84' W	1986	Magnetic profile	Profile Start	
MSM9/532-1	12.10.08	02:06	68° 35.69' N	62° 22.00' W	1805	Magnetic profile	information	Kursänderung auf 117°
MSM9/532-1	12.10.08	03:45	68° 29.28' N	61° 45.32' W	1785	Magnetic profile	information	Kursänderung auf 009°
MSM9/532-1	12.10.08	11:03	69° 40.49' N	61° 12.92' W	1829	Magnetic profile	Profile End	
MSM9/532-1	12.10.08	11:31	69° 42.69' N	61° 17.20' W	1825	Magnetic profile	on deck	
MSM9/533-1	12.10.08	21:09	70° 10.26' N	66° 12.99' W	142	Seismic reflection profile	Streamer into water	Kopfboje mit Blitzer zu Wasser
MSM9/533-1	12.10.08	23:02	70° 4.61' N	66° 0.66' W	172	Seismic reflection profile	airguns in the water	Stb. Bolt Gun z/W
MSM9/533-1	12.10.08	23:28	70° 3.33' N	65° 56.82' W	191	Seismic reflection profile	Remark	Streamer komplett ausgesteckt, 3700m
MSM9/533-1	12.10.08	23:43	70° 2.42' N	65° 53.82' W	198	Seismic reflection profile	airguns in the water	Bb. erste Airgun Array z/W
MSM9/533-1	13.10.08	00:02	70° 1.30' N	65° 50.19' W	191	Seismic reflection profile	airguns in the water	Bb. Airgun Arrays komplett z/W
MSM9/533-1	13.10.08	00:03	70° 1.24' N	65° 49.99' W	191	Seismic reflection profile	profile start	Beginn Softstart
MSM9/533-1	13.10.08	00:15	70° 0.65' N	65° 47.51' W	201	Seismic reflection profile	airguns in the water	Stb. erste Airgun Array z/W
MSM9/533-1	13.10.08	00:35	69° 59.84' N	65° 43.09' W	250	Seismic reflection profile	airguns in the water	Stb. Airgun Arrays komplett z/W
MSM9/533-1	13.10.08	02:06	69° 55.95' N	65° 22.38' W	564	Seismic reflection profile	Remark	KÄ nach Stb wegen Eisberg
MSM9/533-1	13.10.08	03:40	69° 51.52' N	65° 3.79' W	807	Seismic reflection profile	airguns in the water	Bb Bolt-Gun nach Auftauen z/W, 50m ausgesteckt
MSM9/533-1	13.10.08	04:00	69° 51.26' N	64° 58.92' W	922	Seismic reflection profile	Remark	zurück auf Track
MSM9/533-1	13.10.08	13:13	69° 27.26' N	63° 0.35' W	1983	Seismic reflection profile	Remark	Bb. Bolt Gun a/D
MSM9/533-1	13.10.08	16:00	69° 19.46' N	62° 25.00' W	1954	Seismic reflection profile	airguns in the water	Bb. Bolt Gun nach auftauen wieder z/W, 50 m ausgesteckt
MSM9/533-1	13.10.08	20:42	69° 6.23' N	61° 26.07' W	1891	Seismic reflection profile	Remark	Ausweichen wegen Eis

MSM9/533-1	13.10.08	22:34	69° 0.84' N	61° 2.84' W	1814	Seismic reflection profile	Remark	zurück auf Track
MSM9/533-1	14.10.08	03:35	68° 45.40' N	60° 2.37' W	1520	Seismic reflection profile	Remark	Wegen Annäherung von Gebiet mit vielen Langleinen wird der Streamer geborgen.
MSM9/533-1	14.10.08	03:40	68° 44.96' N	60° 2.28' W	1511	Seismic reflection profile	Remark	Unterbrechung schießen
MSM9/533-1	14.10.08	05:22	68° 38.64' N	60° 5.59' W	1486	Seismic reflection profile	streamer on deck	Drehen auf KüG 030°
MSM9/533-1	14.10.08	07:00	68° 43.14' N	59° 51.89' W	1407	Seismic reflection profile	Remark	Fortsetzung Profil
MSM9/533-1	14.10.08	11:12	68° 44.19' N	59° 13.08' W	531	Seismic reflection profile	Streamer into water	Kopfboje z/W
MSM9/533-1	14.10.08	12:30	68° 39.48' N	59° 3.37' W	337	Seismic reflection profile	Remark	Leckage im Streamer, Aussetzen wird unterbrochen
MSM9/533-1	14.10.08	12:37	68° 39.05' N	59° 2.54' W	313	Seismic reflection profile	Remark	Leckage abgedichtet, Aussetzen wir fortgesetzt
MSM9/533-1	14.10.08	13:03	68° 37.39' N	58° 59.43' W	307	Seismic reflection profile	Streamer into water	3700m z/W
MSM9/533-1	14.10.08	13:06	68° 37.18' N	58° 59.01' W	304	Seismic reflection profile	end of profile	
MSM9/534-1	14.10.08	13:09	68° 36.95' N	58° 58.58' W	307	Seismic reflection profile	profile start	Neustart
MSM9/534-1	14.10.08	15:45	68° 25.58' N	58° 39.22' W	346	Seismic reflection profile	alter course	Schwenken ein auf ursprünglichen Track
MSM9/534-1	14.10.08	19:15	68° 14.13' N	57° 57.47' W	387	Seismic reflection profile	Remark	Kursänderung wegen Eis
MSM9/534-1	14.10.08	21:28	68° 7.07' N	57° 32.67' W	383	Seismic reflection profile	Remark	Zurück auf Track
MSM9/534-1	15.10.08	02:56	67° 49.38' N	56° 29.75' W	172	Seismic reflection profile	Remark	Überfahren Profil-Endpunkt
MSM9/534-1	15.10.08	03:22	67° 47.72' N	56° 25.55' W	163	Seismic reflection profile	end of profile	
MSM9/534-1	15.10.08	03:55	67° 45.07' N	56° 23.10' W	151	Seismic reflection profile	array on deck	Stb-Array
MSM9/534-1	15.10.08	04:10	67° 43.82' N	56° 21.99' W	141	Seismic reflection profile	array on deck	Bb-Array
MSM9/534-1	15.10.08	04:40	67° 42.58' N	56° 20.78' W	158	Seismic reflection profile	array on deck	Bb Bolt-Gun
MSM9/534-1	15.10.08	05:05	67° 41.40' N	56° 19.75' W	143	Seismic reflection profile	array on deck	Stb Bolt-Gun
MSM9/534-1	15.10.08	07:14	67° 34.94' N	56° 14.52' W	133	Seismic reflection profile	streamer on deck	
MSM9/506-1	15.10.08	08:44	67° 49.13' N	56° 29.38' W	172	Ocean bottom seismometer	released	
MSM9/506-1	15.10.08	08:58	67° 49.18' N	56° 29.10' W		Ocean bottom seismometer	on deck	
MSM9/507-1	15.10.08	09:51	67° 54.92' N	56° 49.40' W		Ocean bottom seismometer	released	
MSM9/507-1	15.10.08	10:03	67° 55.35' N	56° 50.10' W		Ocean bottom seismometer	on deck	
MSM9/508-1	15.10.08	10:55	68° 1.09' N	57° 11.00' W		Ocean bottom seismometer	released	
MSM9/508-1	15.10.08	11:03	68° 1.34' N	57° 11.28' W		Ocean bottom seismometer	on deck	
MSM9/509-1	15.10.08	11:53	68° 6.70' N	57° 31.65' W		Ocean bottom seismometer	released	
MSM9/509-1	15.10.08	12:16	68° 7.16' N	57° 32.43' W		Ocean bottom seismometer	on deck	
MSM9/510-1	15.10.08	13:06	68° 12.72' N	57° 53.29' W		Ocean bottom seismometer	released	
MSM9/510-1	15.10.08	13:19	68° 13.21' N	57° 54.24' W		Ocean bottom seismometer	on deck	
MSM9/511-1	15.10.08	14:07	68° 18.66' N	58° 15.24' W		Ocean bottom seismometer	released	
MSM9/511-1	15.10.08	14:22	68° 19.01' N	58° 16.03' W		Ocean bottom seismometer	on deck	
MSM9/512-1	15.10.08	15:09	68° 23.69' N	58° 36.08' W		Ocean bottom seismometer	released	
MSM9/512-1	15.10.08	15:23	68° 24.43' N	58° 37.69' W		Ocean bottom	on deck	

						seismometer		
MSM9/513-1	15.10.08	16:15	68° 29.65' N	58° 57.87' W		Ocean bottom seismometer	released	
MSM9/513-1	15.10.08	16:30	68° 30.47' N	58° 59.82' W		Ocean bottom seismometer	on deck	
MSM9/514-1	15.10.08	17:19	68° 35.40' N	59° 19.63' W		Ocean bottom seismometer	released	
MSM9/514-1	15.10.08	17:31	68° 36.13' N	59° 21.90' W		Ocean bottom seismometer	on deck	
MSM9/515-1	15.10.08	18:21	68° 40.97' N	59° 39.20' W		Ocean bottom seismometer	released	
MSM9/515-1	15.10.08	18:49	68° 41.60' N	59° 43.61' W		Ocean bottom seismometer	on deck	
MSM9/516-1	15.10.08	19:37	68° 46.23' N	60° 2.82' W		Ocean bottom seismometer	released	
MSM9/516-1	15.10.08	20:10	68° 47.15' N	60° 6.60' W		Ocean bottom seismometer	on deck	
MSM9/517-1	15.10.08	20:55	68° 51.16' N	60° 23.25' W		Ocean bottom seismometer	released	
MSM9/517-1	15.10.08	21:33	68° 52.70' N	60° 29.58' W		Ocean bottom seismometer	on deck	
MSM9/518-1	15.10.08	22:13	68° 56.62' N	60° 45.78' W		Ocean bottom seismometer	released	
MSM9/518-1	15.10.08	22:55	68° 58.34' N	60° 52.69' W		Ocean bottom seismometer	on deck	
MSM9/519-1	15.10.08	23:33	69° 2.03' N	61° 8.86' W		Ocean bottom seismometer	released	
MSM9/519-1	16.10.08	00:17	69° 3.86' N	61° 16.44' W		Ocean bottom seismometer	on deck	
MSM9/520-1	16.10.08	00:57	69° 7.66' N	61° 32.57' W		Ocean bottom seismometer	released	
MSM9/520-1	16.10.08	01:45	69° 9.25' N	61° 39.76' W		Ocean bottom seismometer	on deck	
MSM9/521-1	16.10.08	02:24	69° 12.97' N	61° 57.05' W		Ocean bottom seismometer	released	
MSM9/521-1	16.10.08	03:05	69° 14.50' N	62° 3.70' W		Ocean bottom seismometer	on deck	
MSM9/522-1	16.10.08	03:45	69° 18.15' N	62° 20.50' W		Ocean bottom seismometer	released	
MSM9/522-1	16.10.08	04:15	69° 19.83' N	62° 26.54' W		Ocean bottom seismometer	on deck	
MSM9/523-1	16.10.08	04:54	69° 23.30' N	62° 43.90' W		Ocean bottom seismometer	released	
MSM9/523-1	16.10.08	05:31	69° 24.96' N	62° 50.40' W		Ocean bottom seismometer	on deck	
MSM9/524-1	16.10.08	06:11	69° 28.55' N	63° 7.78' W		Ocean bottom seismometer	released	
MSM9/524-1	16.10.08	06:45	69° 29.98' N	63° 14.19' W		Ocean bottom seismometer	on deck	
MSM9/525-1	16.10.08	07:27	69° 33.69' N	63° 32.21' W		Ocean bottom seismometer	released	
MSM9/525-1	16.10.08	08:02	69° 35.19' N	63° 38.13' W		Ocean bottom seismometer	on deck	
MSM9/526-1	16.10.08	08:42	69° 38.94' N	63° 56.55' W		Ocean bottom seismometer	released	
MSM9/526-1	16.10.08	09:14	69° 40.17' N	64° 2.98' W		Ocean bottom seismometer	on deck	
MSM9/527-1	16.10.08	09:55	69° 43.95' N	64° 21.92' W		Ocean bottom seismometer	released	
MSM9/527-1	16.10.08	10:35	69° 45.18' N	64° 27.92' W		Ocean bottom seismometer	on deck	
MSM9/528-1	16.10.08	11:19	69° 49.27' N	64° 48.27' W		Ocean bottom seismometer	released	
MSM9/528-1	16.10.08	11:41	69° 50.17' N	64° 52.94' W		Ocean bottom seismometer	on deck	
MSM9/529-1	16.10.08	12:26	69° 54.58' N	65° 15.71' W		Ocean bottom seismometer	released	
MSM9/529-1	16.10.08	12:41	69° 55.05' N	65° 18.00' W		Ocean bottom seismometer	on deck	
MSM9/530-1	16.10.08	13:31	69° 59.66' N	65° 41.95' W		Ocean bottom seismometer	released	
MSM9/530-1	16.10.08	13:46	69° 59.89' N	65° 43.90' W		Ocean bottom seismometer	on deck	

MSM9/535-1	16.10.08	21:35	70° 10.13' N	60° 43.11' W	658	Magnetic profile	surface	
MSM9/535-1	16.10.08	22:19	70° 9.54' N	60° 39.21' W	626	Magnetic profile	information	volle Länge ausgesteckt (750m)
MSM9/535-1	16.10.08	22:22	70° 9.31' N	60° 39.22' W	621	Magnetic profile	Profile Start	
MSM9/535-1	17.10.08	09:23	68° 20.19' N	61° 24.54' W	1732	Magnetic profile	information	Kursänderung auf 172°
MSM9/535-1	17.10.08	19:17	66° 41.79' N	60° 51.13' W	424	Magnetic profile	information	Kursänderung auf 195°
MSM9/535-1	17.10.08	20:30	66° 29.33' N	60° 59.28' W	326	Magnetic profile	Profile End	
MSM9/535-1	17.10.08	20:55	66° 26.24' N	61° 1.40' W	284	Magnetic profile	on deck	
MSM9/536-1	17.10.08	23:05	65° 58.22' N	61° 19.59' W	187	Ocean bottom seismometer	surface	
MSM9/537-1	18.10.08	00:01	65° 56.46' N	60° 54.24' W	361	Ocean bottom seismometer	surface	
MSM9/538-1	18.10.08	00:56	65° 54.75' N	60° 28.88' W	416	Ocean bottom seismometer	surface	
MSM9/539-1	18.10.08	01:52	65° 52.99' N	60° 3.42' W	500	Ocean bottom seismometer	surface	
MSM9/540-1	18.10.08	02:47	65° 51.27' N	59° 37.95' W	599	Ocean bottom seismometer	surface	
MSM9/541-1	18.10.08	03:40	65° 49.52' N	59° 12.69' W	570	Ocean bottom seismometer	surface	
MSM9/542-1	18.10.08	04:32	65° 47.80' N	58° 47.18' W	498	Ocean bottom seismometer	surface	
MSM9/543-1	18.10.08	05:23	65° 46.02' N	58° 21.75' W	517	Ocean bottom seismometer	surface	
MSM9/544-1	18.10.08	06:18	65° 44.31' N	57° 56.61' W	540	Ocean bottom seismometer	surface	
MSM9/545-1	18.10.08	07:14	65° 42.58' N	57° 31.24' W	609	Ocean bottom seismometer	surface	
MSM9/546-1	18.10.08	08:08	65° 40.77' N	57° 5.65' W	654	Ocean bottom seismometer	surface	
MSM9/547-1	18.10.08	09:03	65° 39.05' N	56° 40.46' W	661	Ocean bottom seismometer	surface	
MSM9/548-1	18.10.08	10:24	65° 41.52' N	56° 30.96' W	667	Seismic reflection profile	airguns in the water	Stb. Bolt Gun z/W
MSM9/548-1	18.10.08	10:44	65° 40.68' N	56° 32.72' W	667	Seismic reflection profile	airguns in the water	Bb. Bolt Gun z/W
MSM9/548-1	18.10.08	10:55	65° 40.26' N	56° 33.67' W	664	Seismic reflection profile	profile start	Beginn Soft Start
MSM9/548-1	18.10.08	11:00	65° 40.00' N	56° 34.34' W	660	Seismic reflection profile	airguns in the water	1. Airgun-Array Stb. z/W
MSM9/548-1	18.10.08	11:16	65° 39.04' N	56° 36.95' W	663	Seismic reflection profile	airguns in the water	Airgun-Arrays Stb. komplett ausgesteckt
MSM9/548-1	18.10.08	11:18	65° 38.93' N	56° 37.28' W	665	Seismic reflection profile	airguns in the water	1. Airgun-Array Bb. z/W
MSM9/548-1	18.10.08	11:32	65° 38.79' N	56° 40.12' W	663	Seismic reflection profile	airguns in the water	Airgun-Arrays Bb. komplett ausgesteckt
MSM9/548-1	18.10.08	11:45	65° 39.26' N	56° 42.74' W	664	Seismic reflection profile	profile start	
MSM9/548-1	18.10.08	18:52	65° 45.41' N	58° 13.56' W	539	Seismic reflection profile	Remark	Beginn einholen Stb. arry, vertörnt
MSM9/548-1	18.10.08	19:24	65° 43.73' N	58° 15.50' W	533	Seismic reflection profile	array on deck	
MSM9/548-1	18.10.08	19:24	65° 43.73' N	58° 15.50' W	533	Seismic reflection profile	Remark	Neuausbringen Stb. arry
MSM9/548-1	18.10.08	19:39	65° 42.85' N	58° 16.24' W	540	Seismic reflection profile	Remark	Stb. arry komplett ausgesteckt
MSM9/548-1	18.10.08	20:42	65° 45.50' N	58° 13.67' W	540	Seismic reflection profile	Remark	Zurück auf Track
MSM9/548-1	19.10.08	11:42	65° 59.12' N	61° 31.82' W	176	Seismic reflection profile	end of profile	
MSM9/548-1	19.10.08	12:14	66° 0.61' N	61° 29.25' W	168	Seismic reflection profile	array on deck	Bb. Airgun-Arrays a/D
MSM9/548-1	19.10.08	12:36	66° 1.51' N	61° 24.79' W	170	Seismic reflection profile	array on deck	Stb. Airgun-Arrays a/D
MSM9/548-1	19.10.08	12:54	66° 2.16' N	61° 21.96' W	175	Seismic reflection profile	array on deck	Stb. Bolt Gun a/D
MSM9/548-1	19.10.08	13:06	66° 2.60' N	61° 20.00' W	174	Seismic reflection profile	array on deck	Bb. Bolt Gun a/D
MSM9/536-1	19.10.08	13:28	65° 59.39' N	61° 20.14' W	179	Ocean bottom seismometer	released	
MSM9/536-1	19.10.08	13:41	65° 58.26' N	61° 19.40' W	183	Ocean bottom seismometer	on deck	

MSM9/537-1	19.10.08	14:34	65° 56.53' N	60° 54.71' W	360	Ocean bottom seismometer	released	
MSM9/537-1	19.10.08	14:48	65° 56.58' N	60° 54.11' W	360	Ocean bottom seismometer	on deck	
MSM9/538-1	19.10.08	15:41	65° 54.87' N	60° 29.81' W	375	Ocean bottom seismometer	released	
MSM9/538-1	19.10.08	15:54	65° 55.04' N	60° 28.53' W	379	Ocean bottom seismometer	on deck	
MSM9/539-1	19.10.08	16:41	65° 53.40' N	60° 6.73' W	473	Ocean bottom seismometer	released	
MSM9/539-1	19.10.08	16:57	65° 53.21' N	60° 3.20' W	504	Ocean bottom seismometer	on deck	
MSM9/540-1	19.10.08	17:48	65° 51.74' N	59° 40.69' W		Ocean bottom seismometer	released	
MSM9/540-1	19.10.08	18:09	65° 51.53' N	59° 37.50' W		Ocean bottom seismometer	on deck	
MSM9/541-1	19.10.08	19:00	65° 49.81' N	59° 15.00' W		Ocean bottom seismometer	released	
MSM9/541-1	19.10.08	19:18	65° 49.64' N	59° 12.41' W		Ocean bottom seismometer	on deck	
MSM9/542-1	19.10.08	20:07	65° 48.06' N	58° 49.30' W		Ocean bottom seismometer	released	
MSM9/542-1	19.10.08	20:27	65° 47.87' N	58° 46.75' W		Ocean bottom seismometer	on deck	
MSM9/543-1	19.10.08	21:18	65° 46.31' N	58° 23.69' W		Ocean bottom seismometer	released	
MSM9/543-1	19.10.08	21:37	65° 45.83' N	58° 21.37' W		Ocean bottom seismometer	on deck	
MSM9/544-1	19.10.08	22:30	65° 44.53' N	57° 58.98' W		Ocean bottom seismometer	released	
MSM9/544-1	19.10.08	22:51	65° 44.01' N	57° 56.29' W		Ocean bottom seismometer	on deck	
MSM9/545-1	19.10.08	23:44	65° 42.79' N	57° 34.03' W		Ocean bottom seismometer	released	
MSM9/545-1	20.10.08	00:07	65° 42.23' N	57° 30.94' W		Ocean bottom seismometer	on deck	
MSM9/546-1	20.10.08	00:59	65° 40.97' N	57° 8.42' W		Ocean bottom seismometer	released	
MSM9/546-1	20.10.08	01:23	65° 40.56' N	57° 5.50' W		Ocean bottom seismometer	on deck	
MSM9/547-1	20.10.08	02:12	65° 39.42' N	56° 42.65' W		Ocean bottom seismometer	released	
MSM9/547-1	20.10.08	02:28	65° 39.04' N	56° 40.77' W		Ocean bottom seismometer	on deck	
MSM9/549-1	20.10.08	10:11	66° 40.45' N	55° 39.46' W	151	Seismic reflection profile	Streamer into water	Kopfboje mit Blinklicht und Sender z/W
MSM9/549-1	20.10.08	12:07	66° 47.14' N	55° 41.74' W	126	Seismic reflection profile	Remark	Streamer 3760m komplett z/W
MSM9/549-1	20.10.08	12:12	66° 47.52' N	55° 41.99' W	124	Seismic reflection profile	Magnetomter to water	
MSM9/549-1	20.10.08	13:04	66° 51.46' N	55° 45.10' W	113	Seismic reflection profile	Remark	Einholen des Magnetometers wegen techn. Problemen
MSM9/549-1	20.10.08	13:11	66° 51.93' N	55° 46.08' W	114	Seismic reflection profile	Remark	Einholen Streamer wegen techn. Problemen
MSM9/549-1	20.10.08	13:17	66° 52.26' N	55° 47.13' W	123	Seismic reflection profile	Magnetometer on deck	
MSM9/549-1	20.10.08	16:52	66° 53.28' N	55° 37.09' W	102	Seismic reflection profile	Remark	Weiterhin Reparatur am ausgesteckten Streamer; Schiffskurs zum Profilstart
MSM9/549-1	20.10.08	18:02	66° 52.99' N	55° 48.11' W	116	Seismic reflection profile	Magnetomter to water	
MSM9/549-1	20.10.08	18:04	66° 53.00' N	55° 48.57' W	115	Seismic reflection profile	Remark	Streamer komplett ausgesteckt, 3700m
MSM9/549-1	20.10.08	18:22	66° 53.07' N	55° 52.87' W	127	Seismic reflection profile	airguns in the water	erste Kanone Stb. array zu Wasser
MSM9/549-1	20.10.08	18:24	66° 53.11' N	55° 53.31' W	124	Seismic reflection profile	Remark	Magnetometer komplett ausgesteckt, 600m
MSM9/549-1	20.10.08	18:36	66° 53.44' N	55° 55.76' W	128	Seismic reflection profile	profile start	

MSM9/549-1	20.10.08	18:36	66° 53.44' N	55° 55.76' W	128	Seismic reflection profile	Remark	Stb. Kanonen array komplett zu Wasser
MSM9/549-1	20.10.08	18:38	66° 53.49' N	55° 56.17' W	129	Seismic reflection profile	airguns in the water	erste Kanone Bb. array zu Wasser
MSM9/549-1	20.10.08	18:53	66° 53.88' N	55° 59.16' W	150	Seismic reflection profile	Remark	Bb. Kanonen arry komplett ausgesteckt
MSM9/549-1	21.10.08	22:22	67° 21.48' N	62° 5.51' W	286	Seismic reflection profile	end of profile	
MSM9/549-1	21.10.08	22:28	67° 21.84' N	62° 6.54' W	260	Seismic reflection profile	Remark	Beginn Einholen Bb. Airgun-Arrays
MSM9/549-1	21.10.08	22:46	67° 23.07' N	62° 9.31' W	235	Seismic reflection profile	array on deck	Bb. Airgun-Arrays komplett a/D
MSM9/549-1	21.10.08	22:48	67° 23.21' N	62° 9.60' W	235	Seismic reflection profile	Remark	Beginn Einholen Stb. Airgun-Arrays
MSM9/549-1	21.10.08	23:07	67° 24.59' N	62° 12.61' W	185	Seismic reflection profile	array on deck	Stb. Airgun-Arrays komplett a/D
MSM9/549-1	21.10.08	23:19	67° 25.41' N	62° 14.50' W	126	Seismic reflection profile	Magnetometer on deck	
MSM9/549-1	21.10.08	23:22	67° 25.55' N	62° 14.79' W	120	Seismic reflection profile	Remark	Beginn Einholen Steamer
MSM9/549-1	22.10.08	01:08	67° 29.54' N	62° 25.02' W	165	Seismic reflection profile	streamer on deck	

App. 5 Geophysikalische Profilliste / Geophysical Profile List

profile number	corresp. station no. MSM9/…	shot point start/ end	date	time UTC	latitude	longitude	course	S = seis. reflect. OBS=seis. refr. M = magnetics G = gravity B = bathymetry P = Parasound	length (km)
BGR08-301	473-1	1	23.09.08	20:14:29	65° 30.379 N	54° 33.419 W		S,M,G,B,P	
		6227	25.09.08	03:22:04	65° 58.202 N	61° 12.639 W	283°		307.94
BGR08-302	499-1		26.09.08	19:00	72° 01.940 N	61° 17.606 W		M,G,B,P	
			27.09.08	20:27	68° 02.649 N	63° 16.842 W	191°		449.40
AWI-20080500 /	500-1	1	28.09.08	03:34:00	68° 01.821 N	62° 59.230 W		OBS,S,M,G,B,P	
BGR08-303		416	28.09.08	10:29:00	68° 39.531 N	62° 43.416 W	9°		70.66
AWI-20080500 /	500-1	1	28.09.08	19:23:00	68° 18.507 N	62° 52.059 W		OBS,S,M,G,B,P	
BGR08-303A		79	28.09.08	20:40:00	68° 25.099 N	62° 49.529 W	8°		12.33
AWI-20080500 /	500-1	1	28.09.08	21:09:00	68° 27.776 N	62° 48.529 W		OBS,M,G,B,P	
BGR08-303C		2568	30.09.08	15:56:00	72° 11.697 N	60° 54.639 W	9°		420.59
BGR08-304	502-1	1	02.10.08	06:51:18	67° 59.223 N	63° 00.367 W		S,M,G,B,P	
		9353	04.10.08	05:06:58	72° 01.983 N	60° 59.732 W	9°		455.89
BGR08-305	502-1	1	04.10.08	07:03:19	72° 01.090 N	61° 03.096 W		S,M,G,B,P	
		2316	04.10.08	18:37:49	71° 08.328 N	59° 17.330 W	147°		115.64
BGR08-306	502-1	1	04.10.08	20:41:01	71° 09.297 N	59° 17.961 W		S,M,G,B,P	
		3176	05.10.08	12:33:32	71° 35.457 N	63° 25.166 W	290°		153.99
BGR08-307	503-1		05.10.08	16:53	71° 45.425 N	63° 36.549 W		M,G,B,P	
			05.10.08	21:00	71° 57.329 N	61° 47.948 W	70°		66.38
BGR08-308	504-1		05.10.08	21:24	71° 56.272 N	61° 39.608 W		M,G,B,P	
			06.10.08	19:43	68° 14.453 N	63° 28.400 W	190°		416.38
BGR08-309	505-1		07.10.08	17:32	69° 18.334 N	62° 20.256 W		M,G,B,P	
			08.10.08	09:21	67° 49.408 N	56° 29.782 W	122°		288.54
BGR08-310	531-1		11.10.08	13:10	69° 59.941 N	65° 44.013 W		M,G,B,P	
			11.10.08	22:07	69° 14.752 N	62° 03.851 W	119°		164.74
BGR08-311	532-1		11.10.08	22:25	69° 12.344 N	62° 03.926 W		M,G,B,P	
			12.10.08	02:07	68° 35.563 N	62° 21.882 W	190°		69.15
BGR08-312	532-1		12.10.08	03:45	68° 29.279 N	61° 45.318 W		M,G,B,P	
			12.10.08	11:08	69° 41.298 N	61° 13.328 W	9°		135.02
AWI-20080600 /	533-1	1	13.10.08	00:03:00	70° 01.246 N	65° 50.002 W		OBS,S,G,B,P	
BGR08-313		1656	14.10.08	03:38:00	68° 45.137 N	60° 02.282 W	119°		266.76
AWI-20080600 /	533-1	1	14.10.08	06:59:00	68° 43.057 N	59° 52.017 W		OBS,G,B,P	
BGR08-314		368	14.10.08	13:06:00	68° 37.180 N	58° 59.017 W	107°		37.32
AWI-20080600 /	534-1	1	14.10.08	13:10:00	68° 36.878 N	58° 58.442 W	150°/	OBS,S,G,B,P	
BGR08-315		853	15.10.08	03:22:00	67° 47.723 N	56° 25.556 W	119°		139.02
BGR08-316	535-1		16.10.08	22:17	70° 09.664 N	60° 39.207 W		M,G,B,P	
			17.10.08	09:23	68° 20.243 N	61° 24.526 W	189°		204.78
BGR08-317	535-1		17.10.08	09:23	68° 20.191 N	61° 24.537 W		M,G,B,P	
			17.10.08	20:29	66° 29.566 N	60° 59.106 W	171°		205.64
AWI-20080700 /	548-1	19	18.10.08	11:45:00	65° 39.258 N	56° 42.735 W		OBS,G,B,P	
BGR08-318		1429	19.10.08	11:42:00	65° 59.117 N	61° 31.806 W	282°		222.25
BGR08-319	549-1	1	20.10.08	18:36:27	66° 53.446 N	55° 55.821 W		S,M,G,B,P	
		5555	21.10.08	22:22:19	67° 21.497 N	62° 05.571 W	284°		271.05
BGR08-Cal			22.10.08	18:22	64° 17.189 N	56° 46.305 W		M,G,B,P	
			22.10.08	18:57	64° 16.536 N	56° 45.499 W			

App. 6 OBS Stationsliste / OBS Station List, Profile AWI-20080500

	Deployment				Recovery		
Station	Lat	Lon	Depth	Date/Time	Lat	Lon	Date/Time
OBS 525	71° 59,963' N	61° 00,787' W	1492 m	26.09.08 / 17:37	71° 59,968' N	61° 01,001' W	30.09.08 / 17:41
OBS 524	71° 50,070' N	61° 06,608' W	1571 m	26.09.08 / 16:34	71° 50,128' N	61° 06,781' W	30.09.08 / 19:03
OBS 523	71° 40,070' N	61° 12,628' W	1647 m	26.09.08 / 15:32	71° 39,966' N	61° 12,064' W	30.09.08 / 20:26
OBS 522	71° 30,081' N	61° 18,409' W	1703 m	26.09.08 / 14:25	71° 30,053' N	61° 17,666' W	30.09.08 / 21:10
OBS 521	71° 20,119' N	61° 24,099' W	1754 m	26.09.08 / 13:22	71° 20,269' N	61° 23,593' W	30.09.08 / 22:42
OBS 520	71° 10,149' N	61° 29,381' W	1793 m	26.09.08 / 12:15	71° 10,290' N	61° 29,280' W	01.10.08 / 00:06
OBS 519	71° 00,155' N	61° 35,010' W	1723 m	26.09.08 / 11:14	71° 00,482' N	61° 35,388' W	01.10.08 / 02:03
OBS 518	70° 50,135' N	61° 40,434' W	1691 m	26.09.08 / 10:13	70° 50,467' N	61° 40,348' W	01.10.08 / 03:25
OBS 517	70° 40,124' N	61° 45,812' W	1735 m	26.09.08 / 09:05	70° 40,252' N	61° 44,971' W	01.10.08 / 04:55
OBS 516	70° 30,105' N	61° 51,074' W	1769 m	26.09.08 / 07:56	70° 30,064' N	61° 50,108' W	01.10.08 / 06:21
OBS 515	70° 20,145' N	61° 56,221' W	1812 m	26.09.08 / 06:49	70° 19,828' N	61° 55,333' W	01.10.08 / 07:45
OBS 514	70° 10,182' N	62° 01,030' W	1901 m	26.09.08 / 05:45	70° 09,730' N	62° 00,478' W	01.10.08 / 09:11
OBS 513	70° 00,071' N	62° 06,037' W	1970 m	26.09.08 / 04:38	69° 59,689' N	62° 05,822' W	01.10.08 / 10:26
OBS 512	69° 50,165' N	62° 11,046' W	2002 m	26.09.08 / 03:38	69° 49,982' N	62° 11,099' W	01.10.08 / 11:42
OBS 511	69° 40,151' N	62° 15,737' W	1998 m	26.09.08 / 02:29	69° 40,160' N	62° 15,865' W	01.10.08 / 13:00
OBS 510	69° 30,183' N	62° 20,757' W	1973 m	26.09.08 / 01:23	69° 30,355' N	62° 21,177' W	01.10.08 / 14:24
OBS 509	69° 20,133' N	62° 25,134' W	1958 m	26.09.08 / 00:19	69° 20,342' N	62° 25,112' W	01.10.08 / 15:44
OBS 508	69° 10,106' N	62° 29,695' W	1940 m	25.09.08 / 23:08	69° 10,282' N	62° 29,762' W	01.10.08 / 17:09
OBS 507	69° 00,129' N	62° 34,272' W	1909 m	25.09.08 / 22:14	69° 00,340' N	62° 34,510' W	01.10.08 / 18:33
OBS 506	68° 50,082' N	62° 38.779' W	1861 m	25.09.08 / 21:17	68° 50,311' N	62° 38,928' W	01.10.08 / 19:53
OBS 505	68° 40,082' N	62° 43,123' W	1800 m	25.09.08 / 20:24	68° 40,090' N	62° 43,110' W	01.10.08 / 21:06
OBS 504	68° 30,056' N	62° 47,399' W	1702 m	25.09.08 / 19:35	68° 30,029' N	62° 47,289' W	01.10.08 / 22:21
OBS 503	68° 20,087' N	62° 51,511' W	1561 m	25.09.08 / 18:47	68° 20,087' N	62° 51,920' W	02.10.08 / 23:32
OBS 502	68° 10,038' N	62° 55,749' W	1385 m	25.09.08 / 17:55	68° 10,035' N	62° 55,527' W	02.10.08 / 00:43
OBS 501	67° 59,972' N	62° 59,953' W	1033 m	25.09.08 / 17:03	67° 59,842' N	62° 59,710' W	02.10.08 / 01:55

App. 7 OBS Stationsliste / OBS Station List, Profile AWI-20080600

	Deployment				Recovery		
Station	Lat	Lon	Depth	Date/Time	Lat	Lon	Date/Time
OBS 601	69°59,952' N	65°43,606' W	243 m	11.10.08//09:38	69°59,890' N	65°43,881' W	16.10.08//13:45
OBS 602	69°55,155' N	65°18,253' W	600 m	11.10.08//08:20	69°55,054' N	65°17,996' W	16.10.08//12:40
OBS 603	69°50,290' N	64°53,111' W	1044 m	11.10.08//07:00	69°50,167' N	64°52,941' W	16.10.08//11:41
OBS 604	69°45,361' N	64°28,313' W	1799 m	11.10.08//05:48	69°45,183' N	64°28,313' W	16.10.08//10:35
OBS 605	69°40,329' N	64°03,458' W	1939 m	11.10.08//04:32	69°40,179' N	64°02,949' W	16.10.08//09:15
OBS 606	69°35,297' N	63°39,078' W	1958 m	11.10.08//03:06	69°35.187 N	63°38.125' W	16.10.08//08:02
OBS 607	69°30,145' N	63°14,564' W	1973 m	11.10.08//01:59	69°29.979' N	63°14.182' W	16.10.08//06:45
OBS 608	69°25,062' N	62°50,466' W	1987 m	11.10.08//00:56	69°24.980' N	62°50.239' W	16.10.08//05:33
OBS 609	69°19,782' N	62°26,453' W	1954 m	10.10.08//23:51	69°19.782' N	62°26.481' W	16.10.08//04:17
OBS 610	69°14,455' N	62°02,862' W	1930 m	10.10.08//22:56	69°14,545' N	62°93,645' W	16.10.08//03:07
OBS 611	69°09,161' N	61°39,408' W	1906 m	10.10.08//22:02	69°09,285' N	61°39,678' W	16.10.08//01:44
OBS 612	69°03,749' N	61°16.102' W	1863 m	10.10.08//21:11	69°03,886' N	60°16,441' W	16.10.08//00:15
OBS 613	68°58,384' N	60°52,703' W	1777 m	10.10.08//20:18	68°58,340' N	60°52,693' W	15.10.08//22:54
OBS 614	68°52,860' N	60°29,812' W	1703 m	10.10.08//19:26	68°52,696' N	60°29,602' W	15.10.08//21:33
OBS 615	68°47,297' N	60°06,958' W	1571 m	10.10.08//18:32	68°47,149' N	60°06,600' W	15.10.08//20:10
OBS 616	68°41.787' N	59°44.416' W	1271 m	10.10.08//17:02	68°41.604' N	59°43.655' W	15.10.08//18:48
OBS 617	68°36.146' N	59°22.070' W	575 m	10.10.08//16:07	68°36.128' N	59°21.735' W	15.10.08//17:33
OBS 618	68°30.457' N	58°59.862' W	315 m	10.10.08//15:14	68°30.464' N	58°59.800' W	15.10.08//16:30
OBS 619	68°24.448' N	58°37.907' W	343 m	10.10.08//14:16	68°24.432' N	58°37.678' W	15.10.08//15:23
OBS 620	68°18,875' N	58°15,877' W	313 m	10.10.08//13:15	68°19,008' N	58°16,059' W	15.10.08//14:20
OBS 621	68°13,100' N	57°54,078' W	425 m	10.10.08//12:16	68°13,205' N	57°54,237' W	15.10.08//13:18
OBS 622	68°07,193' N	57°32,686' W	383 m	10.10.08//11:17	68°07,196' N	57°32,429' W	15.10.08//12:12
OBS 623	68°01,271' N	57°11,410' W	293 m	10.10.08//10:19	68°01,350' N	57°11,232' W	15.10.08//11:03
OBS 624	67°55,267' N	56°50,295' W	220 m	10.10.08//09:22	67°55,338' N	56°50,259' W	15.10.08//10:02
OBS 625	67°49,253' N	56°29,324' W	173 m	10.10.08//08:29	67°49,253' N	56°29,324' W	15.10.08//08:58

App. 8 OBS Stationsliste / OBS Station List, Profile AWI-20080700

	Deployment				Recovery		
Station	Lat	Lon	Depth	Date/Time	Lat	Lon	Date/Time
OBS 701	65°58,223' N	61°19,575' W	187 m	17.10.08//23:06	65°58.264' N	61°19.396' W	19.10.08//13:41
OBS 702	65°56,463' N	60°54,234' W	360 m	18.10.08//00:01	65°56.578' N	60°54.114' W	19.10.08//14:47
OBS 703	65°54,757' N	60°28,866' W	375 m	18.10.08//00:55	65°55.051' N	60°28.504' W	19.10.08//15:53
OBS 704	65°52,989' N	60°03,420' W	500 m	18.10.08//01:52	65°53.214' N	60°03.181' W	19.10.08//16:57
OBS 705	65°51.271' N	59°37.958' W	597 m	18.10.08//02:47	65°51.534' N	59°37.497' W	19.10.08//18:08
OBS 706	65°49.522' N	59°12.650' W	570 m	18.10.08//03:40	65°49.647' N	59°12.401 W	19.10.08//19:18
OBS 707	65°47.821' N	58°47.182' W	198 m	18.10.08//04:31	65°47.866' N	58°46.763' W	19.10.08//20:26
OBS 708	65°46.027' N	58°21.670' W	518 m	18.10.08//05:23	65°45.831' N	58°21.388' W	19.10.08//21:36
OBS 709	65°44,311' N	57°56,618' W	539 m	18.10.08//06:17	65°44,008' N	57°56,281' W	19.10.08//22:51
OBS 710	65°42,581' N	57°31,239' W	608 m	18.10.08//07:13	65°42,227' N	57°30,932' W	20.10.08//00:07
OBS 711	65°40,772' N	57°05,640' W	653 m	18.10.08//08:08	65°40,578' N	57°05,523' W	20.10.08//01:21
OBS 712	65°39,051' N	56°40,446' W	661 m	18.10.08//09:03	65°39,044' N	56°40,766' W	20.10.08//02:27

Die "Berichte zur Polar- und Meeresforschung" (ISSN 1866-3192) werden beginnend mit dem Heft Nr. 569 (2008) ausschließlich elektronisch als Open-Access-Publikation herausgegeben. Ein Verzeichnis aller Hefte einschließlich der Druckausgaben (Heft 377-568) sowie der früheren **"Berichte zur Polarforschung** (Heft 1-376, von 1982 bis 2000) befindet sich im Internet in der Ablage des electronic Information Center des AWI (**ePIC**) unter der URL http://epic.awi.de. Durch Auswahl "Reports on Polar- and Marine Research" auf der rechten Seite des Fensters wird eine Liste der Publikationen in alphabetischer Reihenfolge (nach Autoren) innerhalb der absteigenden chronologischen Reihenfolge der Jahrgänge erzeugt.

To generate a list of all Reports past issues, use the following URL: http://epic.awi.de and select the right frame to browse "Reports on Polar and Marine Research". A chronological list in declining order, author names alphabetical, will be produced, and pdf-icons shown for open access download.

Verzeichnis der zuletzt erschienenen Hefte:

Heft-Nr. 574/2008 — "The South Atlantic Expedition ANT-XXIII/5 of the Research Vessel 'Polarstern' in 2006", edited by Wilfried Jokat

Heft-Nr. 575/2008 — "The Expedition ANTARKTIS-XXIII/10 of the Research Vessel 'Polarstern' in 2007", edited by Andreas Macke

Heft-Nr. 576/2008 — "The 6th Annual Arctic Coastal Dynamics (ACD) Workshop, October 22-26, 2006, Groningen, Netherlands", edited by Pier Paul Overduin and Nicole Couture

Heft-Nr. 577/2008 — "Korrelation von Gravimetrie und Bathymetrie zur geologischen Interpretation der Eltanin-Impaktstruktur im Südpazifik", von Ralf Krocker

Heft-Nr. 578/2008 — "Benthic organic carbon fluxes in the Southern Ocean: regional differences and links to surface primary production and carbon export", by Oliver Sachs

Heft-Nr. 579/2008 — "The Expedition ARKTIS-XXII/2 of the Research Vessel 'Polarstern' in 2007", edited by Ursula Schauer.

Heft-Nr. 580/2008 — "The Expedition ANTARKTIS-XXIII/6 of the Research Vessel 'Polarstern' in 2006", edited by Ulrich Bathmann

Heft-Nr. 581/2008 — "The Expedition of the Research Vessel 'Polarstern' to the Antarctic in 2003 (ANT-XX/3)", edited by Otto Schrems

Heft-Nr. 582/2008 — "Automated passive acoustic detection, localization and identification of leopard seals: from hydro-acoustic technology to leopard seal ecology", by Holger Klinck

Heft-Nr. 583/2008 — "The Expedition of the Research Vessel 'Polarstern' to the Antarctic in 2007 (ANT-XXIII/9)", edited by Hans-Wolfgang Hubberten

Heft-Nr. 584/2008 — "Russian-German Cooperation SYSTEM LAPTEV SEA: The Expedition Lena - New Siberian Islands 2007 during the International Polar Year 2007/2008", edited by Julia Boike, Dmitry Yu. Bolshiyanov, Lutz Schirrmeister and Sebastian Wetterich

Heft-Nr. 585/2009 — "Population dynamics of the surf clams *Donax hanleyanus* and *Mesodesma mactroides* from open-Atlantic beaches off Argentina", by Marko Herrmann

Heft-Nr. 586/2009 — "The Expedition of the Research Vessel 'Polarstern' to the Antarctic in 2006 (ANT-XXIII/7)", edited by Peter Lemke

Heft-Nr. 587/2009 — "The Expedition of the Research Vessel 'Maria S. Merian' to the Davis Strait and Baffin Bay in 2008 (MSM09/3), edited by Karsten Gohl, Bernd Schreckenberger, and Thomas Funck